

Louisiana Tech University

Louisiana Tech Digital Commons

Doctoral Dissertations

Graduate School

Summer 8-2021

Novel Methods for Determining Polymer Content and Polymer Degradation in Asphalt Binder

Roksana Hossain

Louisiana Tech University

Follow this and additional works at: <https://digitalcommons.latech.edu/dissertations>

Recommended Citation

Hossain, Roksana, "" (2021). *Dissertation*. 944.

<https://digitalcommons.latech.edu/dissertations/944>

This Dissertation is brought to you for free and open access by the Graduate School at Louisiana Tech Digital Commons. It has been accepted for inclusion in Doctoral Dissertations by an authorized administrator of Louisiana Tech Digital Commons. For more information, please contact digitalcommons@latech.edu.

**NOVEL METHODS FOR DETERMINING POLYMER
CONTENT AND POLYMER DEGRADATION
IN ASPHALT BINDER**

By

Roksana Hossain, B. S., M. S.

A Dissertation Presented in Partial Fulfillment
of the Requirements of the Degree
Doctor of Philosophy

COLLEGE OF ENGINEERING AND SCIENCE
LOUISIANA TECH UNIVERSITY

August 2021

LOUISIANA TECH UNIVERSITY

GRADUATE SCHOOL

June 28, 2021

Date of dissertation defense

We hereby recommend that the dissertation prepared by

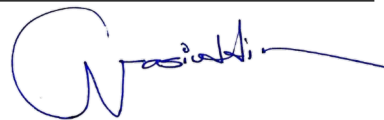
Roksana Hossain, B.S., M.S.

entitled **Novel Methods for Determining Polymer Content and Polymer**

Degradation in Asphalt Binder

be accepted in partial fulfillment of the requirements for the degree of

Doctor of Philosophy in Engineering, Materials & Infrastructure Systems Conc.



Nazimuddin M. Wasiuddin
Supervisor of Dissertation Research



Jay Xingran Wang
Head of Engineering

Doctoral Committee Members:

Nazimuddin M. Wasiuddin

C. Shawn Sun

Sven Eklund

Jay Xingran Wang

Elizabeth Matthews

Approved:



Hisham Hegab
Dean of Engineering & Science

Approved:



Ramu Ramachandran
Dean of the Graduate School

ABSTRACT

Styrene-butadiene-styrene (SBS) is the most common modifier used in asphalt binder modification because of its superior performance compared to some others that are used. SBS modified asphalt binder increases the rutting resistance and decreases the fatigue and thermal cracking susceptibility of asphalt pavement. However, SBS modified asphalt binder tends to separate and is subjected to thermal degradation during construction and aging degradation during its service life. As a result, quality control of SBS modified asphalt binder is needed, although no standard test method is available to quantify SBS degradation due to aging.

In this study, two methods for quantifying SBS polymer in asphalt binder were investigated: by mechanical and by chemical analysis. For mechanical analysis, a novel dynamic shear rheometer (DSR)-based extensional deformation test was developed using Sentmanat extensional rheometer (SER). From the second peak elongation force parameter, different polymers can be identified as elastomeric and plastomeric. Finally, the second peak elongation force was proposed as a parameter to quantify elastomeric polymer in asphalt binder with a calibration curve.

For chemical analysis, the Fourier transform infrared (FT-IR) spectrometer with attenuated total reflectance (ATR) was used to collect the absorbance intensity of the SBS modified asphalt binder. No significant effect of the difference in PG binders, the types of SBS polymer, and the presence of crosslinking agent were observed on polybutadiene (PB)

and polystyrene (PS) functional groups. Therefore, PB and PS end blocks were analyzed to establish a universal regression model for SBS polymer quantification in asphalt binder. The PS model was found to be the best fit model ($R^2 = 0.97$) for SBS quantification after verifying with refinery supplied SBS modified binders with initially unknown SBS contents.

The extensional deformation test parameters were investigated to determine SBS degradation due to aging during construction and service life. Laboratory aging such as rolling thin film oven (RTFO) and pressure aging vessel (PAV) were performed for SBS modified asphalt binder and mixture. Two parameters (F_2 and F_2/F_1) were proposed to evaluate the SBS degradation directly after oxidative aging. Both values reduced after RTFO aging and further reduced after PAV aging, which indicated SBS polymer degradation.

Finally, the FT-IR spectrometer was used to understand the change in different functional groups of the unmodified and modified asphalt binder after oxidative aging. SBS content in the asphalt binder decreased after RTFO and PAV aging.

Based on the findings of this study, an extensional deformation test was recommended to be used for SBS polymer content determination and aging related SBS degradation. The FT-IR based universal calibration curve developed in this study can predict SBS content in about 30-min using ten samples in the asphalt plant. Therefore, the findings of this study will contribute significantly to the quality control of the asphalt binders.

APPROVAL FOR SCHOLARLY DISSEMINATION

The author grants to the Prescott Memorial Library of Louisiana Tech University the right to reproduce, by appropriate methods, upon request, any or all portions of this Dissertation. It is understood that “proper request” consists of the agreement, on the part of the requesting party, that said reproduction is for his personal use and that subsequent reproduction will not occur without written approval of the author of this Dissertation. Further, any portions of the Dissertation used in books, papers, and other works must be appropriately referenced to this Dissertation.

Finally, the author of this Dissertation reserves the right to publish freely, in the literature, at any time, any or all portions of this Dissertation.

Author Roksana Hossain

Date 08/02/2021

DEDICATION

To my Mother

TABLE OF CONTENTS

ABSTRACT.....	iii
APPROVAL FOR SCHOLARLY DISSEMINATION	v
DEDICATION	vi
LIST OF FIGURES	xiv
LIST OF TABLES	xix
ACKNOWLEDGMENT.....	xxi
CHAPTER 1 INTRODUCTION	1
1.1 Modification of Asphalt Binder	1
1.2 SBS Modified Asphalt Binder	2
1.3 Research Need	3
1.3.1 Polymer Identification and Polymer Content Determination through Mechanical Analysis using Sentmanat Extensional Rheometer (SER) (Task 1).....	3
1.3.2 Polymer Content Determination through Chemical Analysis using a FT-IR Spectrometer (Tasks 2 & 3)	4
1.3.3 Determination of SBS Polymer Degradation in Asphalt Binder and Asphalt Mixture due to Oxidative Aging (Tasks 4, 5 & 6)	6
1.4 Research Hypothesis and Objectives	6
1.5 Outline of the Dissertation	7
CHAPTER 2 A NOVEL EXTENSIONAL DEFORMATION TEST FOR IDENTIFICATION AND DETERMINATION OF ELASTOMERIC POLYMER.....	12
2.1 Introduction.....	12
2.1.1 Objective	15

2.2	Materials and Experimental Plan.....	15
2.2.1	Materials and Preparation of Modified Asphalt Binder.....	17
2.2.1.1	SBS Mixing.....	17
2.2.1.2	SBR Latex Mixing.....	17
2.2.1.3	PPA Mixing.....	17
2.2.1.4	CR Mixing.....	18
2.2.1.5	HDPE Mixing.....	18
2.2.2	Principle of DSR-based Extensional Deformation Test.....	18
2.2.3	Sample Preparation.....	19
2.2.3.1	Preparing the Binder.....	19
2.2.3.2	Controlling the Sample Thickness.....	19
2.2.3.3	Cutting the Sample to the Desired Dimensions.....	22
2.2.4	Test Procedure.....	22
2.3	Results and Discussions.....	24
2.3.1	Elongation Force.....	24
2.3.2	Elongation Force vs. Step Time Curve Characterization.....	24
2.3.3	Stiffness of Different Types of Modified Asphalt Binders.....	26
2.3.4	Second Peak Elongation Force, F_2 , at Similar Stiffness.....	28
2.3.5	Polymer Content Determination.....	29
2.3.5.1	Polymer (latex) Modified Asphalt Emulsion (PMAE).....	30
2.3.5.2	Latex Modified Asphalt Binder (PMAB).....	31
2.3.6	Temperature Sweep (DSR) Test Results.....	33
2.3.7	Multiple Stress Creep Recovery (MSCR) Test Results.....	34
2.4	Conclusion.....	36
	CHAPTER 3 SBS CONTENT DETERMINATION BY EVALUATING POLYBUTADIENE FUNCTIONAL GROUP.....	38

3.1	Introduction.....	38
3.1.1	Objective.....	41
3.2	Materials and Experimental Plan.....	41
3.2.1	Materials.....	41
3.2.2	Preparation of SBS Modified Binders in Laboratory.....	42
3.2.3	FT-IR Spectroscopy.....	44
3.2.4	Data Collection from Laboratory Prepared SBS Modified Binders.....	45
3.2.5	In-Situ Data Collection from Plant Modified Binders.....	46
3.2.6	Data Collection from Refinery Supplied SBS Modified Binders.....	47
3.3	Results and Discussion.....	48
3.3.1	Qualitative Analysis of FT-IR Spectrum.....	48
3.3.2	Quantitative Analysis of FT-IR Spectrum.....	49
3.3.3	Effect of Binder's Performance Grades and Sources on Peak Absorbance Height.....	51
3.3.4	Effect of Cross-linking Agent on Peak Absorbance Height.....	53
3.3.5	Effect of SBS Polymer Sources and Structures on Peak Absorbance Height.....	54
3.3.6	Evaluation of Variability.....	55
3.3.7	Linear Regression Analysis Considering Peak Height and Peak Area.....	56
3.3.8	Prediction of SBS Content in Laboratory Prepared Binders.....	58
3.3.9	Model Implementation on Plant Modified Binders.....	59
3.3.10	Model Validation from Refinery Supplied SBS Modified Binders.....	60
3.4	Conclusion.....	61
CHAPTER 4 SBS CONTENT DETERMINATION BY EVALUATING POLYSTYRENE FUNCTIONAL GROUP.....		63
4.1	Introduction.....	63

4.1.1	Objectives	66
4.2	Materials and Methods.....	66
4.2.1	Materials	66
4.2.2	Experimental Plan.....	67
4.2.3	Principle of FT-IR Spectroscopy	67
4.2.4	Preparation of SBS Modified Asphalt Binder in the Laboratory.....	68
4.2.5	Data Collection from Laboratory Prepared Binders	69
4.2.6	FT-IR Spectrometer Data collection form Refinery Supplied Binders	71
4.2.7	Spectral Analysis	71
4.3	Results and Discussion	73
4.3.1	Qualitative Analysis of FT-IR Spectrum	73
4.3.2	Quantitative Analysis for Linear Regression.....	74
4.3.3	Peak Absorbance Area and Height Analysis	75
4.3.4	Developments of the Model.....	77
4.3.5	Accuracy of the Models	78
4.3.6	Application in Refinery Supplied Binders.....	79
4.3.7	Selection of the Final Model.....	80
4.3.8	KS-test.....	81
4.3.9	Effects of SBS Polymer Sources, Binder Grades and Sources, and Cross-linking Agents.....	82
4.3.10	Model Validation with New Laboratory Modified Binders	82
4.4	Conclusion	84
CHAPTER 5 A NOVEL EXTENSIONAL DEFORMATION TEST FOR EVALUATING SBS DEGRADATION DUE TO AGING OF ASPHALT BINDER... 86		
5.1	Introduction.....	86
5.1.1	Objectives	89

5.2	Methodology	89
5.2.1	Extensional Rheology Tests in DSR Platform Using SER Fixture	89
5.2.2	Materials and Preparation of PMAB.....	90
5.2.2.1	SBS Mixing	90
5.2.2.2	PPA Mixing.....	91
5.2.2.3	SBS and PPA Mixing	91
5.2.2.4	UV Aging	91
5.2.3	Experimental Plan.....	92
5.2.3.1	Sample Preparation.....	93
5.2.3.2	Test Procedure	95
5.3	Result and Discussion.....	95
5.3.1	Effect of Temperature and Speed on Mixing.....	95
5.3.2	DSR-based Extensional Test Parameter	96
5.3.3	Effectiveness of Different Types of Modifiers (SBS, PPA-SBS and PPA) .	97
5.3.4	Polymer Degradation Due to Aging	98
5.3.4.1	Reduction of F_2 Value after RTFO and PAV Aging.....	98
5.3.4.2	Reduction of F_2/F_1 after RTFO and PAV Aging.....	100
5.3.4.3	Understanding the F_2 Value of Stiffer Binder due to Aging by Increasing the Testing Temperature until Stiffness (F_1) of Aged Binder becomes the same as Unaged State.....	102
5.3.4.4	Degradation due to UV Aging.....	104
5.4	Conclusions.....	105
CHAPTER 6 A NOVEL EXTENSIONAL DEFORMATION TEST FOR EVALUATING SBS DEGRADATION DUE TO AGING OF ASPHALT MIXTURE		107
6.1	Introduction.....	107
6.1.1	Objectives	109

6.2	Materials and Experimental Plan	110
6.2.1	SBS Modified Asphalt Binder	110
6.2.2	Laboratory Aged Asphalt Mixture.....	110
6.2.3	Experimental Plan.....	111
6.2.4	Sample Preparation	111
6.2.5	Test Procedure	113
6.3	Result and Discussion.....	114
6.3.1	Effect of Temperature on Elongation Force	114
6.3.2	Reduction in F ₂ Value after Laboratory Aging at 85°C.....	116
6.3.3	Reduction in F ₂ Value after Extreme Aging at 135°C.....	118
6.3.4	Statistical Analysis.....	121
6.4	Conclusion	122
CHAPTER 7 UNDERSTANDING OF OXIDATIVE AGING AND EVALUATION OF SBS DEGRADATION USING FT-IR SPECTRA.....		124
7.1	Introduction.....	124
7.1.1	Objectives	127
7.2	Methodology.....	127
7.2.1	Asphalt Binder	127
7.2.2	UV and oven aging simulation test in the laboratory	127
7.2.3	Materials and Experimental Plan	128
7.2.4	FT-IR Spectrometer Data Collection	129
7.2.5	FT-IR Spectrometer Data Analysis.....	130
7.3	Result and Discussion.....	131
7.3.1	Analysis of Carbonyl and Sulfoxide Content	131
7.3.2	Carbonyl and Sulfoxide Indices of Aged Asphalt Binder at Similar Stiffness	133

7.3.3	Prediction of SBS Content in Asphalt Binder before and after Aging	135
7.3.4	Carbonyl and Sulfoxide Indices of Aged SBS Modified Asphalt Binders.	137
7.4	Conclusions.....	139
CHAPTER 8 CONCLUSIONS AND RECOMMENDATIONS		141
8.1	Conclusions.....	141
8.1.1	SBS Polymer Quantification by Mechanical Analysis	141
8.1.2	SBS Polymer Quantification by Chemical Analysis	142
8.1.3	Evaluation of SBS Polymer Degradation by Mechanical Analysis.....	143
8.1.4	Evaluation of SBS Polymer Degradation by Chemical Analysis	144
8.2	Recommendations for Future Work	145
REFERENCES		147

LIST OF FIGURES

Figure 1-1: Molecular structure of SBS polymer.	2
Figure 1-2: Research objectives and outline.	8
Figure 2-1: Mixing of polymer with asphalt binder by the high shear mixer at a fixed temperature and a fixed speed.	16
Figure 2-2: (a) Binder placed in a small can, (b) Binder poured in the silicon mold, (c) Binder's shape after being removed from the silicone mold, (d) Binder placed between two stainless steel plates, (e) Silicone mat placed above the binder, (f) A thick glass placed over the silicon mat, (g) The loads placed over the thick glass, (h) Binder's shape after removing the loads, (i) Cracked during the cutting process due to a long cooling period, (j) Sticking to the metal edge due to a short cooling period, (k) Cutting the sample to the desired length, (l) Specimen with desired dimensions.	20
Figure 2-3: (a) The SER fixture before loading the specimen, (b) SER fixture after loading the specimen, (c) Clamps kicked out due to the high stresses, (d) Double-sided adhesion tape fixed to the drums, (e) Loading the sample post to the double-side adhesion tape, (f) Software screenshot shows the test Parameter, (g) Software screenshot shows the DSR control panel, (h) Sample during the extensional deformation test, (i) Sample after the end of the test.	23
Figure 2-4: Elongation Force vs Step Time at 4°C (a) for PMAE and (b) for PMAB.	25
Figure 2-5: Elongation force (F_1 and F_2) of different types of binders at (a) 4°C, (b) 12°C, and (c) 16°C.	27
Figure 2-6: F_2 at similar stiffness for different types of modified binder at (a) 4°C, (b) 12°C, and (c) 16°C.	29
Figure 2-7: (a) First peak elongation force vs. the percent of polymer for PMAE at 4°C, and (b) Second peak elongation force vs. the percent of polymer for PMAE at 4°C.	31
Figure 2-8: (a) First peak elongation force vs. percent of polymer at 4°C, and (b) Second peak elongation force vs. percent of polymer at 4°C.	32
Figure 2-9: $G^*/\sin\delta$ at different temperatures of (a) PMAE and (b) PMAB.	33

Figure 2-10: Multiple stress creep recovery at 3.2 kPa stress of (a) PMAE and (b) PMAB.	35
Figure 2-11: Non-recoverable creep compliance (J_{nr}) at 3.2 kPa stress of (a) PMAE and (b) PMAB.	36
Figure 3-1: (a) Heating samples in a quart can in the melting pot, (b) Adding powder SBS in the liquid asphalt binder, (c) Mixing in the high shear mixer for 2.5 hours, (d) Sample collection using a spatula, (e) Placing sample on diamond ATR sensor of FT-IR spectrometer.	43
Figure 3-2: (a) Collecting the hot sample from the asphalt tank, (b) Storing samples in gallon cans in the plant, (c) Placing the sample on the ATR sensor by a spatula, (d) Ensuring a good connection between sensor and sample, (e) Collecting FT-IR spectra and (f) Repeating the same procedure for other samples.	47
Figure 3-3: Typical FT-IR spectrum of unmodified and SBS modified asphalt binder. .	48
Figure 3-4: Effect of different percentages of SBS content in asphalt binder on the absorbance intensity at wavenumber 965 cm^{-1}	50
Figure 3-5: SBS quantification in peak height and peak area method.	51
Figure 3-6: Relation between peak absorbance height and SBS content considering (a) different PG binders and (b) different sources of same PG binder.	52
Figure 3-7: Relation between peak absorbance height and SBS content considering the effect of cross-linking agent.	53
Figure 3-8: Relation between absorbance height and SBS content considering (a) three different SBS polymer structure, (b) two different SBS polymer sources.	54
Figure 3-9: Correlation between SBS content and (a) peak height at 965 cm^{-1} with outlier data points, (b) peak height at 965 cm^{-1} without outlier data points, (c) peak area at 965 cm^{-1} with outlier data points, and (d) peak area at 965 cm^{-1} without outlier data points.	57
Figure 4-1: Materials and experimental plan.	68
Figure 4-2: (a) Heating binder can inside a melting pot, (b) Adding powdered SBS in the liquid asphalt binder, (c) Mixing of SBS using high shear mixer for 2.5 hours, (d) Collecting sample with a spatula for FT-IR spectroscopy, and (e) Placing sample on the diamond ATR sensor of the handheld FT-IR spectrometer.	70
Figure 4-3: Measurement of peak absorbance area and peak absorbance height.	72
Figure 4-4: Typical FT-IR spectrum of unmodified and SBS modified binder.	74

Figure 4-5: Effect of SBS content (%) on (a) wavenumber 965 cm^{-1} and (b) wavenumber 699 cm^{-1}	75
Figure 4-6: Relationship between peak absorbance height and area at the wavenumber 699 cm^{-1} and 965 cm^{-1} , and SBS content (%) considering (a) SBS modified PG 64-22, (b) SBS modified PG 52-34, (c) SBS modified PG 58-28, and (d) addition of sulfur in SBS modified PG 64-22 binder.	76
Figure 4-7: Correlation among SBS content (%) and (a) peak area at 965 cm^{-1} with all the data points, (b) peak area at 965 cm^{-1} without outlier data points, (c) peak height at 699 cm^{-1} with all the data points, and (d) peak height at 699 cm^{-1} without outlier data points.....	78
Figure 4-8: Relation between the actual and predicted SBS content considering all the models.	81
Figure 4-9: Effect on peak absorbance height due to (a) addition of sulfur as a cross-linking agent, (b) difference in base binder, (c) difference in SBS polymer sources, and (d) difference in base binder sources.	83
Figure 5-1: (a) Sample over the circular PAV plate inside the UV aging chamber, (b) Sample in the silicon mold, (c) Sample preparation inside the oven, (d) Specimen with desired dimensions, (e) SER fixture before loading the sample, (f) SER fixture after loading the sample, (g) Software screenshot shows test parameters, (h) Software screenshot shows the DSR control panel, and (i) Sample after the end of the test.....	94
Figure 5-2: High shear mixer speed-temperature curve for original PG 67-22 binder (a) original curve, and (b) Y-axis being dimensionless.	96
Figure 5-3: Second peak elongation force vs. percent of polymer at 4°C for different types of polymers.....	97
Figure 5-4: Second peak elongation force of different percent of polymer at (a) 12°C and (b) 16°C	99
Figure 5-5: Second peak elongation force over first peak elongation force- (a) temperature curve for PG 76-22, (b) different percent of polymer at 12°C and (c) different percent of polymer at 16°C	100
Figure 5-6: Elongation force-step time curve for (a) 4% SBS modified PG 64-22 (original, RTFO and PAV aged), (b) 4% SBS modified PG 64-22 (PAV aged), (c) 6% SBS modified PG 64-22 (original, RTFO and PAV aged), and (d) 6% SBS modified PG 64-22 (PAV aged).....	103
Figure 5-7: Second peak elongation force of different types of UV and oven aged binder.	105

Figure 6-1: (a) Collection of mixture in a bowl before aging started, (b) Laboratory mixture aging at 85°C and 135°C, and (c) Asphalt binder extraction from loose mixture.	111
Figure 6-2: (a) Binder placed between two stainless steel plates, (b) A silicone mat and a glass plate over the sample, (c) Sample preparation in the oven, (d) Binder size after removing the loads, (e) SER inserted in DSR host system, (f) Sample shape before the test, and (g) Sample shape after the end of the test.....	113
Figure 6-3: Elongation force and step time curve of mixture extracted binder (a) 1-Day aged, (b) 3-Days aged, and (c) 5-Days aged (aged at 85°C).	114
Figure 6-4: Elongation force and step time curve of mixture extracted binder (a) 4-Hours aged, (b) 8-Hour aged, and (c) 12-Hour aged (aged at 135°C).....	116
Figure 6-5: Relation between temperature and stiffness of the mixture extracted binder (aged at 85°C).	117
Figure 6-6: Reduction in F_2 value of the laboratory aged mixture extracted binder at equal stiffness (aged at 85°C).	119
Figure 6-7: Relation between temperature and stiffness of the mixture extracted binder (aged at 135°C).	120
Figure 6-8: Reduction in F_2 value at similar stiffness of the SBS modified mixture extracted binder (aged at 135°C).	121
Figure 7-1: (a) UV aging of PG 64-22 binder, (b) Oven aging of PG 64-22 binder, (c) Sample placed over the FT-IRS for data collection, (d) Data collection using Microlab PC software, and (e) Spectrum after data collection.	128
Figure 7-2: Experimental flowchart.....	129
Figure 7-3: C=O peak height index ($1695\text{ cm}^{-1}/1456\text{ cm}^{-1}$) for PG 64-22 original and aged binder.....	132
Figure 7-4: S=O peak height index ($1031\text{ cm}^{-1}/1456\text{ cm}^{-1}$) for PG 64-22 original and aged binder.....	132
Figure 7-5: Relation between RTFO and PAV aged (W/O RTFO) PG 64-22 binder considering (a) Stiffness (b) Phase angle.....	133
Figure 7-6: Comparison of C=O index of RTFO and PAV aged PG 64-22 binder at similar stiffness.	134
Figure 7-7: Comparison of S=O index of RTFO and PAV aged PG 64-22 binder at similar stiffness.	134

Figure 7-8: PB content of different types of modified binders from different sources after RTFO and PAV aging. 136

Figure 7-9: Carbonyl content of different modified binders from different sources before and after RTFO and PAV aging. 138

Figure 7-10: Sulfoxide content of different modified binders from different sources before and after RTFO and PAV aging. 139

LIST OF TABLES

Table 2-1: Materials and experimental plan.	16
Table 2-2: Similar Stiffness (F_1) Value of Different Types of Modified Binders.	28
Table 3-1: Polymer content determination by FT-IR spectrometer in previous studies..	40
Table 3-2: Materials and test matrix.	44
Table 3-3: Statistical hypothesis analysis result.	56
Table 3-4: Statistical analysis of peak height or peak area vs. SBS content at 965 cm^{-1}	58
Table 3-5: SBS content prediction of the laboratory-prepared binders.	59
Table 3-6: Field trial results of SBS quantification model.	60
Table 3-7: Validation of the prediction model with refinery supplied binders.....	61
Table 4-1: Previous studies on the quantification of SBS in Asphalt Binder.....	67
Table 4-2: Statistical analysis of SBS content and peak height at 965 cm^{-1} and 699 cm^{-1}	79
Table 4-3: Actual and predicted SBS content (%) of the refinery supplied binders.....	80
Table 4-4: KS-test result of all the prediction models.	82
Table 4-5: Actual and predicted SBS content of the laboratory prepared SBS modified binders.	84
Table 5-1: Literature review on mixing technique of PPA and SBS with base binder and on UV aging procedure.	92
Table 5-2: Summary of materials and experimental plan.	93
Table 5-3: Percent reduction of F_2/F_1 values of different types of binder at different temperature after RTFO and PAV aging.	101

Table 5-4: Percent reduction of F_2 value due to aging of different types of samples at similar stiffness, F_1	104
Table 6-1: Summary of Materials and Experimental Plan.....	112
Table 6-2: Statistical Analysis of Laboratory aged Mixture Extracted Binder.....	122
Table 7-1: Literature on aging determination of SBS modified asphalt binders.	130
Table 7-2: Reduction in SBS content (%) after RTFO and PAV aging.	137

ACKNOWLEDGMENT

To begin, I want to express my gratitude to ALLAH, The Almighty, for giving me the opportunity and ability to complete this work: “So, which of the favors of your Lord would you deny?”

I would like to thank my doctoral committee chairman Dr. Nazimuddin M. Wasiuddin for his continuous support, relentless appreciation, guidance, and supervision throughout my doctoral study and every aspect of my life. The continuous consulting and encouragement of my supervisor encouraged me to finish this study after going through the most challenging time of my life. I would like to acknowledge Dr. Jay Wang, Dr. Elizabeth Matthews, Dr. Shawn Sun, and Dr. Sven Eklund for serving on my doctoral committee.

Many thanks to my colleagues Dr. Shams Arafat, Lamiya Noor, Waleed M. Omer, S M Rahat Rahman, and undergraduate students who helped me in the lab. Lastly, I would like to express my gratitude to my mother, father, grandparents, and uncle (Sawkat Hossain) for their continuous support, encouragement, and prayers. This acknowledgment will be incomplete without mentioning my husband (Abdullah Al Arafat), and my daughter (Anita Arafat). Without your love and support, this journey would be the toughest.

And finally, last but by no means the least, I want to acknowledge all my teachers and the sisters who helped me continue my study during pregnancy and after childbirth.

CHAPTER 1

INTRODUCTION

1.1 Modification of Asphalt Binder

The USA roadway system consists of 2.6 million miles of paved areas, among which 94% are paved with asphalt [2]. Most of the asphalt pavement laid is hot mix construction (HMA) in which 15% of the content is an asphalt binder (volumetrically) [3]. Although the asphalt binder content is not much, it has a significant effect on asphalt pavement performance. However, due to significant changes in asphalt cement, rapid increasing of traffic volumes over the years, and deferred maintenance and construction of thinner pavements, the asphalt binder necessitated the inclusion of modifiers for better sustainability and performance [4]. Modification of asphalt binder has been going on since the mid-20th century. It is assumed that 10% of the asphalt pavement is modified with different modifiers [2].

Commonly used modifiers are styrene-butadiene-styrene (SBS), styrene-butadiene-rubber (SBR) latex, ground tire rubber (GTR), polyphosphoric acid (PPA), and Ethylene vinyl acetate (EVA). The use of modified asphalt binder reduces the common pavement distresses such as rutting, fatigue cracking, thermal cracking, and stripping [5]. Among all

the modifiers, SBS is the most used polymer in asphalt binder modification due to its excellent contribution to superior pavement [6].

1.2 SBS Modified Asphalt Binder

SBS is an elastomeric block copolymer that increases the elastic property of the asphalt binder. The chemical structure of SBS contains three chains: polystyrene, polybutadiene, and polystyrene (**Figure 1-1**). Polystyrene is a hard plastic that gives durability and stiffness, and polybutadiene is a synthetic rubber that provides elastic properties [7]. The addition of SBS polymer improves the physical and rheological properties of the base binder [8]. SBS modified asphalt binder resists the low temperature cracking better than the unmodified binder [7]. In addition, it enhances the complex modulus of the base binder, resulting in high temperature rutting resistance, fatigue, and thermal cracking resistance of the pavement [9], [10].

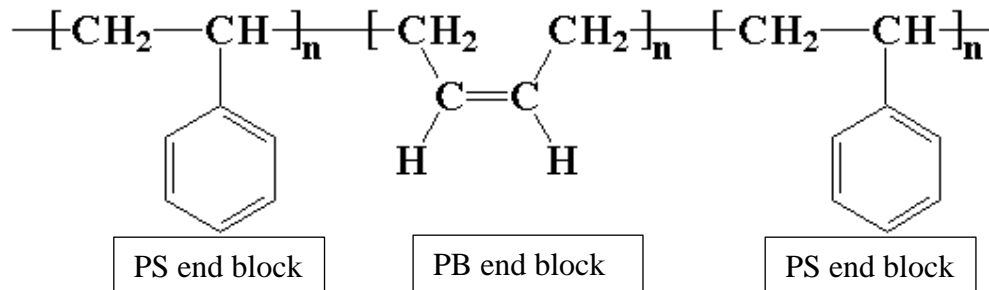


Figure 1-1: Molecular structure of SBS polymer.

At high temperatures, the SBS modified asphalt binder shows the highest recovery on the strain with non-recoverable creep compliance [11]. Furthermore, SBS polymer improves the asphalt aggregate bonding, which leads to durable pavement [12]. The use of SBS modified asphalt binder reduces pavement distress and increases the service life.

However, the main concern of using SBS modified asphalt binders in pavement construction is the degradation of SBS polymer due to aging [13], [14]. Physical and rheological properties of aged SBS modified asphalt binder are different from the unaged binder because of the oxidation of base binder and the degradation of SBS polymer [15]. Due to aging, the temperature susceptibility of SBS modified asphalt binder increases, resulting in reduced low temperature cracking resistance of asphalt pavement [16].

1.3 Research Need

1.3.1 Polymer Identification and Polymer Content Determination through Mechanical Analysis using Sentmanat Extensional Rheometer (SER) (Task 1)

The current Superpave (superior performing pavements) performance grade (PG) tests were developed based on the engineering properties of the asphalt binder and performed on the linear viscoelastic region. However, the polymer does not react at the linear viscoelastic region [17]. Therefore, characterization of polymer modified asphalt binder is not possible with the current Superpave tests.

Some state Department of Transportation (DOTs) have added PG+ (supplemental specifications) test specifications to address the shortcomings of PG test specifications considering the elasticity, ductility, fracture energy, and failure energy. Currently, there are four PG+ tests specifications in some state DOTs: phase angle, elastic recovery, force ductility, and toughness and tenacity. However, the main drawback of these tests is that they are empirical and inconsistent across the states. Also, these test results do not relate well to pavement performance. Later, another new PG+ test named multiple stress creep recovery (MSCR) was developed to provide a more comprehensive behavior of polymer modified asphalt binder. MSCR test characterizes the binder in the non-linear and failure

region, but the failure mechanism in the field is not always in shear mode. Therefore, no changes were performed in low temperature binder grading in the MSCR based PG system.

On the other hand, the polymer can be broadly characterized at various temperature by SER, an extensional flow rheometer. The recently introduced SER can be used inside a host system like dynamic shear rheometer (DSR), which is detachable and can provide the extensional rheological characteristics in a controlled environment. SER fixture was developed to eradicate the flaws of the previously used extensional rheometer in the case of extensional flow control and uniformity. For applying high strain, SER has a dual wind-up extensional rheometer system. Extensional rheology of natural rubber and linear LDPE (low-density polyethylene) was determined at different strain rates in previous studies. Along with extensional rheology, tensile testing, tear testing, adhesion testing, high speed cut growth testing, and dynamic friction testing can also be performed using the SER fixture [17]. Therefore, a new test method is required to use the SER fixture for characterizing polymer modified asphalt binder.

1.3.2 Polymer Content Determination through Chemical Analysis using a FT-IR Spectrometer (Tasks 2 & 3)

SBS polymer content has a significant influence on the performance of the SBS modified asphalt binder. One of the critical requirements of polymer-modified binders is the homogenous mixture of polymer in asphalt binders. However, during construction, SBS polymer tends to separate from SBS modified asphalt binder under static heated storage conditions. Therefore, quality control in the production and process of SBS modified binder in the field is a challenging task. On the other hand, manufacturers tend to achieve high PG specifications adding other non-elastomeric polymer instead of SBS polymer to

lower the production expense. Thus, it is crucial to determine SBS content during the process and application of SBS modified asphalt binder in the pavement construction for quality assurance purposes.

Many studies were performed during the past few decades to establish a precise polymer content determination technique. Still, there is no accepted rheological, mechanical, or chemical test method that is widely accepted for determining the SBS content in asphalt binder. The FT-IR spectroscopy could be a suitable option for SBS content determination, as it is a rapid, portable, non-destructive technique. Again, it requires minimal sample preparation and minimal training of operators. AASHTO T302-15 proposed a standard test method for polymer content determination in polymer modified emulsified asphalt residue and asphalt binder using FT-IR spectroscopy from laboratory prepared binders. However, its implementation in the field binders was not addressed adequately. Following the AASHTO standard in the field is not feasible because this standard requires a calibration equation for each specific binder and each specific SBS polymer type. Developing a calibration equation is time consuming because it has to be developed with SBS modified binder of different SBS contents.

None of the previous studies, which followed the AASHTO standard, considered the influence of sources of PG binders, the difference in SBS polymer structures, and the presence of the cross-linking agent. Application of the developed SBS content determination method was not verified using the unknown plant modified, or refinery supplied binders. Therefore, this study was initiated to study these variables and develop a universal regression model that can be used to predict SBS content in asphalt binder.

1.3.3 Determination of SBS Polymer Degradation in Asphalt Binder and Asphalt Mixture due to Oxidative Aging (Tasks 4, 5 & 6)

SBS modified asphalt binder reduces pavement distress and increases the service life. Physical and rheological properties of aged SBS modified asphalt binder are different from the unaged binder because of the oxidation of base binder and the degradation of SBS polymer [15]. Due to aging, the temperature susceptibility of SBS modified asphalt binder decreases, resulting in reduced low temperature cracking resistance of asphalt pavement [16].

As aging reduces the long-term performance of SBS modified asphalt binder, several researchers studied the degradation of SBS polymer due to oxidative aging by different mechanical and chemical tests. However, there is no specific rheological, mechanical, or chemical test that can determine SBS polymer degradation due to aging. Also, the influence of modifiers on aging is still unknown. Therefore, there is a need for a direct test method to evaluate the degradation of SBS polymer in asphalt binder.

1.4 Research Hypothesis and Objectives

The main hypothesis of this study is stated below:

The novel DSR-based extensional deformation test method can be used to polymer content determination and quantification of polymer degradation in asphalt binder. Polybutadiene-based and polystyrene-based regression models can be used for the same purpose.

Two main aspects of this dissertation are quantification of SBS polymer and evaluation of SBS polymer degradation. **Figure 1.2** represents the specific objectives and their respective chapters. The detailed objectives of this research are stated below:

- To develop a DSR-based extensional deformation test method for polymer content determination in asphalt binder.
- To investigate the effects on the polybutadiene functional group of the FT-IR spectrum due to the differences in PG binders, differences in SBS polymer structure, and the presence of cross-linking agents.
- To develop a universal regression model for SBS content determination in asphalt binder based on polystyrene functional group.
- To investigate the DSR-based extensional deformation test parameters for the evaluation of SBS polymer degradation in asphalt binder due to oxidative aging.
- To evaluate the degradation of SBS polymer in asphalt aggregate mixture due to laboratory aging using the extensional deformation test parameters.
- To understand the chemical changes of unmodified and modified asphalt binder after oxidative aging.

1.5 Outline of the Dissertation

The findings of this study are presented five individual articles. Three of them have been published in peer-reviewed journals and presented at conferences. Chapters 2 to 5 contain an article, and Chapter 7 is the conclusion and recommendations for future work.

A novel DSR-based extensional deformation test was developed for polymer content determination in Chapter 2. In this test method, the SER was used inside the DSR host system to obtain the rheological properties of polymer modified asphalt binder and polymer modified asphalt emulsion. Different types of modifiers (SBS, SBR latex, crumb rubber, HDPE, and PPA) were used to modify the asphalt binder. From the extensional deformation test parameters, it was found that SBS, SBR latex, and crumb rubber can be

identified easily. Later, calibration equations were developed for latex modified asphalt binder and latex modified asphalt emulsion using the specific test parameter. In contrast, the DSR temperature sweep test parameter and the MSCR test parameters did not show any relation to the polymer content in any asphalt binder or emulsion. This chapter is a published paper in the International Journal of Pavement Research and Technology.

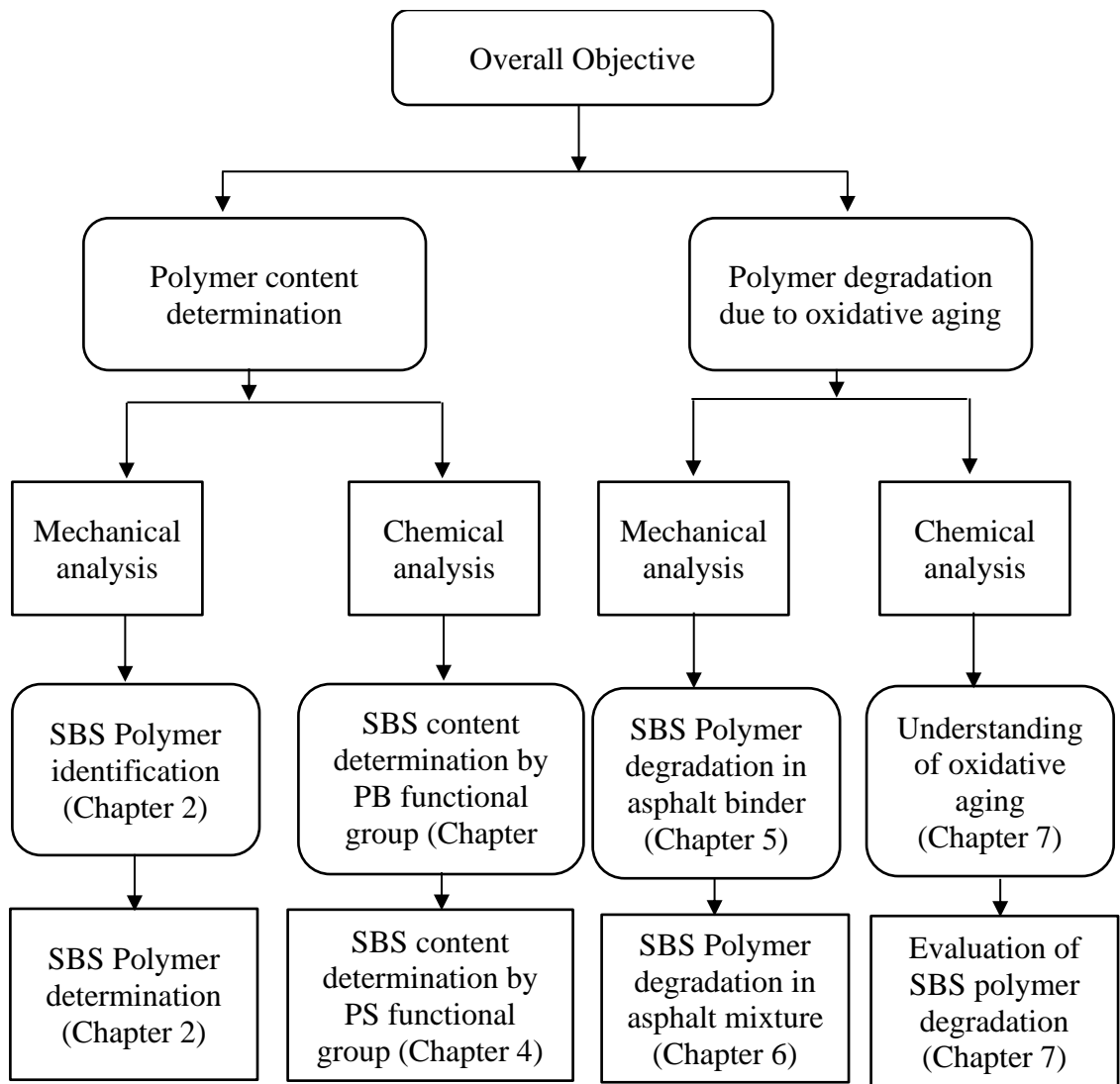


Figure 1-2: Research objectives and outline.

In Chapter 3, effect analysis was performed on the polybutadiene functional group obtained from the FT-IR spectrum due to the differences in binders' performance grades, sources, different types of SBS polymers and their sources, and the presence of a cross-linking agent. A model was developed to predict SBS content in SBS modified asphalt binder considering the polybutadiene (PB) functional group. Using the PB model, the SBS content can be predicted without using any reference of a calibration curve. One plant was visited to implement the model by predicting the SBS content in the plant's modified binders. Furthermore, four refinery supplied binders were used to validate the model as the actual SBS content in the plant's modified binders were known only in a range. This chapter is ready to be submitted in a peer-reviewed journal soon.

In Chapter 4, a universal model was developed considering the polystyrene (PS) functional group. Eleven SBS modified binders were used to predict SBS content supplied from three different refineries. The prediction result was reported to the refineries, and the refinery personnel confirmed that the model predicted the exact content. Variations in PG binders, SBS polymers, and the presence of a cross-linking agent were studied to understand the effect on the PS functional group. Statistical analysis showed that the predicted results from the PS model were within a 95% confidence level. Finally, new laboratory prepared binders were used to predict SBS content with the verified PS model. This chapter will be submitted in a peer-reviewed journal after adding some more work.

In Chapter 5, the degradation of SBS polymer was evaluated by the extensional deformation test parameters. In this study, one SBS modified asphalt binder was collected from a local plant. Different percentages of SBS were mixed in the laboratory. The rolling thin film oven (RTFO) aging and the pressure-aging vessel (PAV) were performed to

simulate the short-term and long-term aging of the SBS modified asphalt binders. UV aging was performed to understand the effect of UV radiation on SBS modified asphalt binder. All these original and aged binders were used to perform the extensional deformation test. It was found that aging degraded the performance of the SBS modified asphalt binder after analyzing the test parameters. The chapter is published in Transportation Research Record: A Journal of Transportation Research Board.

Chapter 6 investigates the SBS polymer degradation in asphalt mixture. SBS modified asphalt binder was prepared in the laboratory. Asphalt aggregate mixture was prepared using the SBS modified asphalt binder. The mixture was kept inside the forced draft oven at 135°C for four hours to simulate the short-term aging. After four hours, some mixture was placed in the forced draft oven for five consecutive days at 85°C. Again, some mixture was placed in the forced draft oven for one day at 135°C. Both types of aging were performed to simulate long-term aging. Later, the asphalt binder was collected from the mixture using the centrifuge extractor and rotavapor. The extracted binder was used to perform the novel extensional deformation test. The aging behavior of the extracted SBS modified binder was evaluated from the elongation force parameters. This chapter is a published conference proceeding in *International Airfield and Highway Pavements 2021*.

Chapter 7 represents the chemical analysis of aged original and SBS modified asphalt binder. One performance graded binder, namely PG 64-22 binder, was used in this study to understand the aging mechanism after RTFO and PAV aging. First, FT-IR spectrometer and DSR test were performed to investigate the correlation between the changes in functional groups and rheological properties of aged asphalt binder. Later, the plant supplied SBS modified asphalt binders were used to evaluate the degradation of SBS

polymer in asphalt binder using the FT-IR spectrometer. The findings of these studies were published as conference proceedings at RILEM International Symposium on Bituminous Materials 2020, and International Conference on Transportation and Development 2020.

Chapter 8 summarizes the conclusions of the chapters and provides recommendations for future works.

CHAPTER 2

A NOVEL EXTENSIONAL DEFORMATION TEST FOR IDENTIFICATION AND DETERMINATION OF ELASTOMERIC POLYMER*

2.1 Introduction

For polymer modified binders and emulsions, the applicability of the Superpave Performance Graded (PG) specifications and test methods was found to be invalid. Thus, the Department of Transportation (DOT) in most states have added supplemental specifications, also known as the PG-Plus test, to identify the presence of polymers and modifiers. Louisiana is among the states that are currently using a PG-Plus specification. Separation of polymer, force ductility (AASHTO T300), and elastic recovery tests are the required tests for the Louisiana Department of Transportation and Development's (LADOTD's) PG-Plus specifications.

Extensional flows are very sensitive to crystallinity and polymer long-chain branching. Those can be far more descriptive regarding polymer characterization than any other type of bulk rheological characterization. Therefore, several states use PG Plus tests

* This chapter or portions thereof has been published in the *International Journal of Pavement Research and Technology*, under the title "A Novel method for polymer content determination in asphalt binder and emulsion", Vol. 12, Issue 6, 2019. The current version has been formatted for this dissertation.

for asphalt binder characterization. Recently introduced Sentmanat extensional rheometer (SER) has been designed for use as a detachable fixture on commercially available rotational rheometer host systems. This fixture can convert a conventional rotational rheometer host system into a universal testing station capable of performing extensional melt rheology experiments, all within the controlled environment of the host system's environmental chamber [17].

A small percent of modifiers such as styrene-butadiene-styrene (SBS), styrene-butadiene-rubber (SBR) latex, ethylene/vinyl acetate (EVA), polyolefin, and polyphosphoric acid (PPA), etc. by weight of asphalt binder has extensively been added in road construction [13], [18], [19]. Due to this wide application, it is crucial to understand the physical and rheological properties of polymer modified asphalt binder (PMAB) and polymer modified asphalt emulsion (PMAE).

SBS is an elastomeric polymer. SBS polymer and maltenes controlled the low temperature properties of SBS modified asphalt [10]. At high temperature, SBS modified asphalt binder showed the highest recovery on strain with non-recoverable creep compliance [11]. PPA is an inorganic polymer of orthophosphoric acid (H_3PO_4). PPA modification increased the performance grade of asphalt binder [20]. In addition, the rutting resistance of asphalt binder increased significantly after PPA modification [21].

PMAE has obtained much attention since its use. PMAE is mostly used for slurry seal and micro-surfacing to address minor distresses, correct ruts, improve surface texture, enhance ride quality, and ultimately extend pavement life [22]. PMAE can be prepared by adding various polymers such as SBR latex, SBS triblock copolymer, and EVA [22], [23]. In general, it is difficult for SBS, or EVA modified asphalt to be emulsified. However, SBR

latex, because of its liquid form, has a significant advantage in an emulsion formulation. Pavement constructed with the SBR latex modified asphalt emulsion has an excellent rut filling capability [24].

Shafii et al. [25] investigated the physical properties of asphalt emulsion modified with natural rubber latex. It was concluded that the softening point, ductility, penetration, plasticity index values were improved after latex modification. Chen et al. [26] performed Composite Specimen Interface Cracking (CSIC) test on PMAE under repeated tensile loading and monitored the rate of damage development. The results indicated that the polymer modification significantly improves reflective cracking resistance. Latex modification decreased the rate of deformation of the asphalt mixture by increasing the dynamic stability [27]. Also, latex modification enhanced the thermal stability and viscosity of the asphalt binder at high temperature [28]. There are several advantages of latex modification in the asphalt binder. Latex is less expensive than other types of polymers. It mixes homogeneously with the asphalt binder at a low temperature, and less time is required for mixing. As a result, latex increases the durability of the road surface. The disadvantages of latex mixing with asphalt binder are foaming, ammonia vapor, and heat loss.

Crumb rubber (CR) is collected from waste automotive and truck tires. CR improved the viscoelastic properties, temperature resistance and reduced the activation energy of the sulfur modified asphalt binder [29]. HDPE is a polyethylene thermoplastic. HDPE increased the elastic properties of the asphalt binder at high temperature where permanent deformation affects the pavement. With the increment of percentage of HDPE, improvement in mechanical behavior increased [30].

To this end, this study has been initiated to identify the elastomeric polymer in modified asphalt binder and determine the polymer content in the PMAE and PMAB. Hossain *et al.* [31] developed a sample preparation method and test procedure for the DSR-based extensional deformation test. By analyzing the extensional deformation parameters, identification and determination of elastomeric polymers are performed.

2.1.1 Objective

The main objectives of this study are to initiate a new extensional deformation test method and correlate the test parameters with the percent of polymer content in the PMAEs and PMABs. The specific objectives are as follows:

1. To improve the sample preparation method for extensional deformation test, recommended by Hossain *et al.* [31].
2. To determine the effectiveness of elastomers using the second peak elongation force, F_2 .
3. To investigate the correlation between the polymer percent and F_2 value.
4. To compare the $G^*/\sin\delta$, and non-recoverable creep compliance, J_{nr} with the proposed new parameter F_2 for quantifying the percent of the polymer.

2.2 **Materials and Experimental Plan**

One neat PG binder, namely, PG 64-22, is selected so that different percentages of modifiers (SBS, PPA, SBR latex, CR, and HDPE) can be added in the laboratory. A mechanical mixer is used for premixing modifiers with the base binder PG 64-22. Mixing of modifiers (SBS, PPA, SBR latex, CR, and HDPE) with an asphalt binder is developed in the laboratory using a high shear mixer (**Figure 2-1**). Sample preparation and test procedure are developed for the novel extensional deformation test. **Table 2-1** represents

the materials and experimental plan in detail. We performed temperature sweep (DSR) tests according to AASHTO T315 and MSCR tests are performed according to AASHTO T350 for PMAB and PMAE.

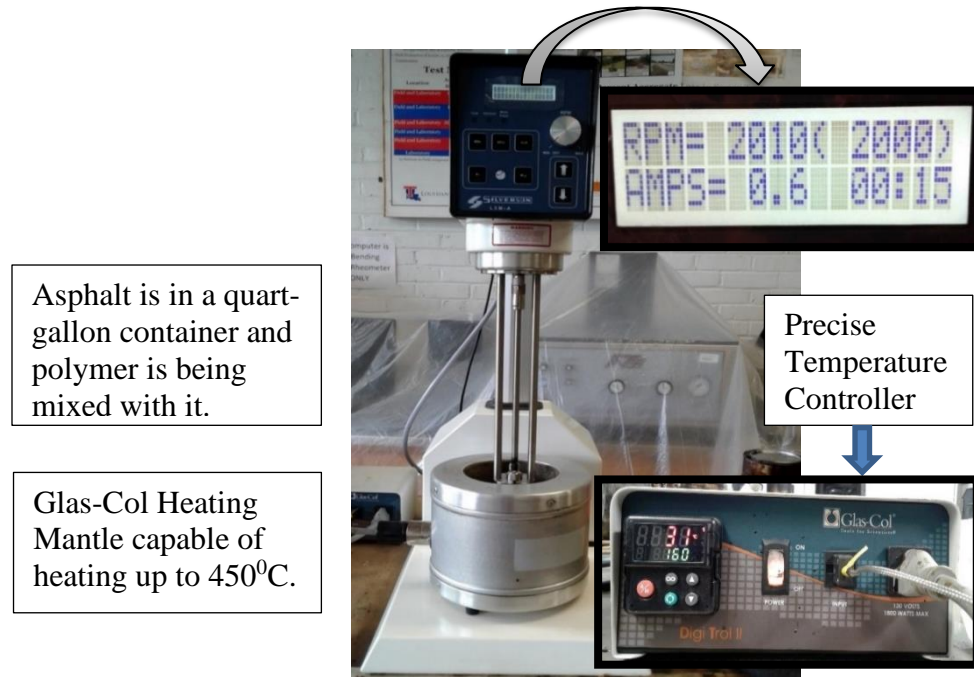


Figure 2-1: Mixing of polymer with asphalt binder by the high shear mixer at a fixed temperature and a fixed speed.

Table 2-1: Materials and experimental plan.

Modifier type	% of modifier	Test	Test Temperature
SBS	2%, 4% & 6%	Extensional deformation	4°C, 12°C and 16°C
PPA	1%, 1.5% & 2%		
CR	5%, 10% & 15%		
HDPE	3.5%, 4%, 6% & 8%		
SBR Latex (PMAE)	0%, 2.5%, 4% & 5.5%	Extensional deformation	4°C
		DSR	58, 64, 70 & 76°C
		MSCR	58, 64, 70 & 76°C
SBR Latex (PMAB)	0%, 2%, 4% & 6%	SER	4°C, 12°C and 16°C
		DSR	58, 64, 70 & 76°C
		MSCR	58, 64, 70 & 76°C

2.2.1 Materials and Preparation of Modified Asphalt Binder.

The mixing techniques of different modifiers with asphalt binder are sated below:

2.2.1.1 SBS Mixing

In this study, 2%, 4%, and 6% SBS by weight of base binder are added with PG 64-22. Mixing of SBS polymer is divided into three stages: (1) Large-sized (passing #4) SBS polymer particles are grinded with a mechanical grinder for 20 minutes into small size (passing #16) particles, (2) The SBS are mixed with the base binder by a mechanical mixer for 15 minutes and sheared for 2 hours with a high shear mixer at 180°C. The speed is set to 4000 rpm, and (3) The second step is repeated.

2.2.1.2 SBR Latex Mixing

Latex is mixed more cautiously as foaming occurs on the surface of the base binder immediately after adding; 2%-6% latex by weight of base binder is mixed with PG 64-22 with 2% interval. Latex mixing is done in two stages: firstly, the latex is added slowly in small quantities. After adding each small quantity, there is a waiting period of 30 seconds, and then a mechanical mixer is used for 5 minutes. Following this procedure, the percentage of latex is added with the base binder. It takes 20 minutes, 30 minutes, and 40 minutes to mix 2%, 4%, and 6% latex with the base binder, respectively. Secondly, the mixed sample is sheared at 160°C for 2 hours with a speed of 2000 rpm.

2.2.1.3 PPA Mixing

PPA is a viscous liquid, so the speed of the high shear mixer is set to 2000 rpm. Three different percentages (1%, 1.5%, and 2%) of PPA are added by weight of PG 64-22 binder. The mixing of PPA is done in two stages: firstly, the PPA is mixed with a

mechanical mixer for 15 minutes. Secondly, the mixed sample is sheared at 180°C for 30 minutes using the high shear mixer.

2.2.1.4 CR Mixing

In this study, three different percentages (5%, 10%, and 15%) of CR is mixed with PG 64-22 binder. The particle size of CR is #16 passing and #40 retained. A high shear mixer at 4000 rpm shears CR for 1 hour. Before sheared, CR is mixed with PG 64-22 binder by a mechanical mixer for 15 minutes. All the mixing technique is done at 180°C.

2.2.1.5 HDPE Mixing

As the melting point of HDPE is 190°C, mixing of the HDPE with PG 64-22 binder is done at 190°C; 3.5%, 4%, 6%, and 8% HDPE are mixed by a mechanical mixer for 15 minutes and then sheared at 4000 rpm for 1 hour.

2.2.2 Principle of DSR-based Extensional Deformation Test

As described in detail by Sentmanat [17], the SER consists of a paired master and slave wind-up drums mounted on the bearing housed within a chassis and mechanically coupled via interlocking gears. The rotational motion of the rheometer spindle energizes the rotation of the drive shaft, which results in the rotation of the master drum, and an equal opposite rotation of the slave drum. Consequently, the two ends of the sample are stretched over the unsupported length, which causes the sample to coil up onto the drums. Both ends of the sample remain secured by the clamps onto the drums.

According to Sentmanat [17], the Henky strain rate ($\dot{\epsilon}_H$) applied on the sample can be expressed as

$$\dot{\epsilon}_H = \frac{2\Omega R}{L_0} \quad \text{Eq. 4-1}$$

where Ω is the angular rotation rate, R is the radius of the equally dimensioned drums and L_0 is the unsupported length. The resistance of the stretch applied (Torque, T) on both the drums can be expressed as

$$T(t) = 2RF(t) \quad \text{Eq. 4-2}$$

where F(t) is the tangential force. The instantaneous cross-sectional area (A) can be expressed as

$$A(t) = A_0 \exp[-\varepsilon_H t] \quad \text{Eq. 4-3}$$

Again, the tensile stress function, (η_E^+) can be written as

$$\eta_E^+(t) = \frac{F(t)}{\varepsilon_H A(t)} \quad \text{Eq. 4-4}$$

2.2.3 Sample Preparation

In this study, the sample preparation method of Hossain *et al.* [31] is followed after some modifications. PMAE and PMAB (latex modified and unmodified PG 64-22 binder) samples are prepared using the following steps:

2.2.3.1 Preparing the Binder

- a. The binder in the main can (5 gal) is heated in the oven at 163°C for 45 minutes.
- b. Around 100 g of the binder is placed in a small metal can (8 oz.) to reduce the aging that occurs due to the repeated heating process (**Figure 2-2a**).
- c. The binder in the small can is heated in the oven at 163°C for 20-30 minutes until it liquefies.

2.2.3.2 Controlling the Sample Thickness

- a. The binder is poured in a 1 in. diameter silicon mold to control the amount of binder needed (**Figure 2-2b**). Silicon is selected to be the molding material because asphalt does not adhere to the silicon. The mold's size is selected to be 1-in. in diameter to

simplify the thickness control process by reducing the amount of binder under the loads.

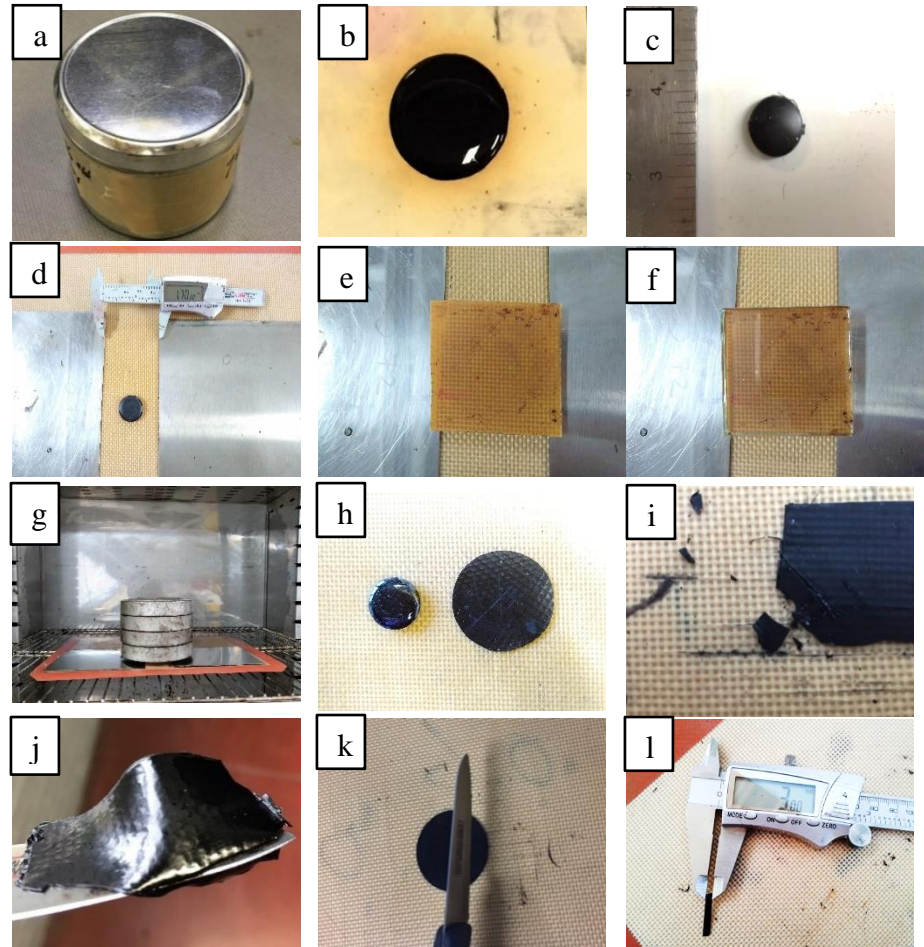


Figure 2-2: (a) Binder placed in a small can, (b) Binder poured in the silicon mold, (c) Binder's shape after being removed from the silicone mold, (d) Binder placed between two stainless steel plates, (e) Silicone mat placed above the binder, (f) A thick glass placed over the silicon mat, (g) The loads placed over the thick glass, (h) Binder's shape after removing the loads, (i) Cracked during the cutting process due to a long cooling period, (j) Sticking to the metal edge due to a short cooling period, (k) Cutting the sample to the desired length, (l) Specimen with desired dimensions.

- b. The liquid binder poured in the silicon mold is at room temperature for 15 to 20 minutes until it cools down. Then it is removed from the silicon mold, as shown in

Figure 2-2(c).

- c. The sample is placed onto a silicon mat between two stainless steel plates with the exact desired thickness, (**Figure 2-2d**), to control the sample's thickness. After a few trials, 1.7 in is found to be the suitable spacing dimension between the two stainless-steel plates to allow the binder to spread in a uniform thickness.
- d. A minimum of 2 in x 2 in silicon mat is placed over the sample overlapping with the stainless-steel plate, as shown in **Figure 2-2(e)**, to block the adhesion between the asphalt sample and the glass plate from the next step. The overlapping ensures that the silicon mat will not slip from the stainless-steel plates and affect the sample's thickness control process. The dimension of the silicon mat is to ensure that the sample is covered after spreading.
- e. A 2 in x 2 in thick glass plate is placed over the silicon mat, overlapping with the stainless-steel plates, as shown in **Figure 2-2(f)**, to ensure a uniform distribution of the loads over the sample.
- f. 20 lb. of loads are placed over the thick glass plate. The loads are kept over the sample for 3 hours (**Figure 2-2g**). Several trials of 2, 4, and 5 hours were made, but the sample's thickness increased by around 1 mm after removing the loads due to delayed elastic recovery if the loading period is less than 3 hours [32].
- g. The whole system of preparing the sample is kept in an oven at 58°C, as shown in **Figure 2-2(g)**. The oven temperature is selected at 58°C after several trials of temperatures (50°C, 55°C, and 65°C) at which the sample's thickness remains the same after unloading.
- h. The loads are removed along with the glass plate and the silicon mat, as shown in **Figure 2-2(h)**.

2.2.3.3 Cutting the Sample to the Desired Dimensions

- a. The sample is placed in a refrigerator at 5°C for 1 to 2 minutes and is removed carefully from the big silicon mat to a smaller 4 in x 4 in silicon mat.
- b. Then the sample is placed in a refrigerator at 5°C for 2 to 3 minutes. If the sample is left at 5°C longer than 2 to 3 minutes, the sample will crack during the cutting process, as shown in **Figure 2-2(i)**. If the sample is left at 5°C for less than 2 to 3 minutes, the sample will stick to the metal edge during the cutting process, as shown in **Figure 2-2(j)**.
- c. Immediately after removing the sample from the refrigerator, the sample is cut with a sharp metal edge to the desired dimensions (2-2 k). The sample is measured by a slide caliper to ensure the desired dimensions (**Figure 2-2l**).

2.2.4 Test Procedure

Measurements are performed on a Universal Testing Platform model SER3-G, manufactured by Xpansion Instruments LLC, connected to DSR model AR2000 Ex with a controlled environmental chamber.

- a. After starting the DSR, the smart swap is inserted. Then, the SER bracket is fixed in the DSR as shown in **Figure 2-3(a)**.
- b. The sample is loaded and secured at each end by clamps as shown in **Figure 2-3(b)**, and then the chamber is closed. The clear distance between the two drums is always kept at 12.7 mm.
- c. In the beginning, the samples slipped several times during the tests because of the high stresses resulting from the solid tensile testing as shown in **Figure 2-3(c)**.



Figure 2-3: (a) The SER fixture before loading the specimen, (b) SER fixture after loading the specimen, (c) Clamps kicked out due to the high stresses, (d) Double-sided adhesion tape fixed to the drums, (e) Loading the sample post to the double-side adhesion tape, (f) Software screenshot shows the test Parameter, (g) Software screenshot shows the DSR control panel, (h) Sample during the extensional deformation test, (i) Sample after the end of the test.

- d. Therefore, an ultra-thin double-sided adhesion tape with a thickness of 0.1 mm is placed onto the drums prior to the sample loading to prevent the sample from

slipping as shown in **Figure 2-3(d)**. The sample is loaded in the SER by placing on the double-sided adhesion tape as shown in **Figure 2-3(e)**.

- e. As for the test parameters, the environmental control is set to 4°C, the soak time is 600 s, and the wait for temperature option is activated to ensure temperature equilibrium. The solid density is set to 1.0 g/cm³, and the melt density is set to 0.95 g/cm³ (**Figure 2-3f**). The final strain is 3.7 rad, with a strain rate of 0.1 s⁻¹. For more accurate measurements, the fast-sampling option is activated (**Figure 2-3g**).
- f. **Figure 2-3(h)** shows the sample during the extensional deformation. **Figure 2-3(i)** shows the sample at the end of the test. Upon completion of the test, the sample is removed immediately, and the drums are carefully cleaned with a soft wipe, and paint thinner is used as needed.

2.3 Results and Discussions

2.3.1 Elongation Force

Polymer modified binder is a non-homogeneous material. In the elongation force vs. step time graph, the first peak indicates the original asphalt property, and the second peak indicates the polymer's effect on the asphalt binder. The first peak reflects the asphalt yielding due to the tensile force, and the second peak depends on the type and level of the polymer modification [7].

2.3.2 Elongation Force vs. Step Time Curve Characterization

Figure 2-4 shows the elongation force vs step time curves for PMAE and PMAB with different percent of polymer. The figures show the differences in the curve characterizations between the four-different polymer percent. **Figure 2-4 (a)** shows 0 N second peak elongation force; F_2 for 0% PMAE that is due to the non-polymer content in

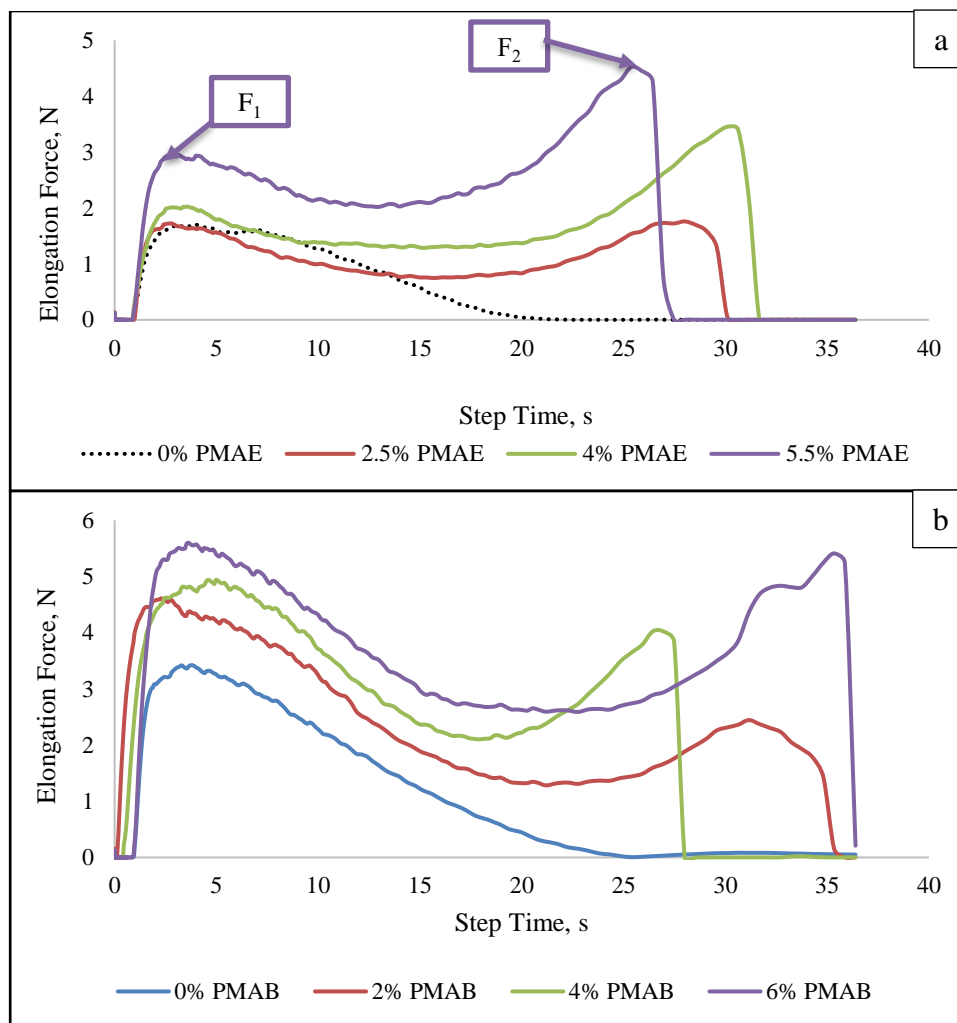


Figure 2-4: Elongation Force vs Step Time at 4°C (a) for PMAE and (b) for PMAB.

the emulsion. For 2.5%, 4% and 5.5% PMAE, it can be observed that, as the percent of the polymer in the PMAE increases, the inflection point is decreasing. This is due to the improvement in the emulsion's extensional property. It is also observed that as the increment of polymer percentage F_2 increases, then the maximum F_2 is found from the maximum percent of PMAE. F_2 is increased by about 96% when 4% latex added compared to 2% PMAE, and F_2 is increased by about 31% when 6% latex added compared to 4% PMAE. It is shown from the figure that 2% and 4% latex could not change the F_1 value

significantly, but 6% latex modification increases the value of F_1 by 72% as well as the value of F_2 compared to 0% PMAE.

In the case of **Figure 2-4 (b)**, PMAB shows almost the same trend as **Figure 2-4 (a)**. No F_2 is found from 0% PMAB. It is observed that with the increment of polymer percentage, F_2 increases then the maximum F_2 is found from the maximum percent of PMAB. F_2 is increased by about 64% when 4% latex is added compared to 2% PMAB, and F_2 is increased by about 39% when 6% latex is added compared to 4% PMAB. It is shown from the figure that when compared to 0% PMAB, 2%, 4%, and 6% latex modification increase the F_1 value about 35%, 44%, and 72%, respectively.

2.3.3 Stiffness of Different Types of Modified Asphalt Binders.

Figure 2-5 (a), (b), and (c) show the F_1 and F_2 values of the different types of the modified binder at 4°C, 12°C, and 16°C, respectively. It is obvious from the figures that the highest stiffness can be found from 8% HDPE. PPA modified binders also show a higher F_1 value than other types of modified binders. SBS, latex, and CR modified binder have almost similar types of stiffness. As HDPE is a plastomer and PPA is a chemical modifier, both do not show any F_2 value at the three tested temperatures. These modifiers only modify the binder itself and increase the binder's stiffness. HDPE and PPA modified binder fail after reaching the F_1 value.

On the other hand, SBS, latex, and CR modified asphalt binder increase the binders' stiffness in a small amount and show elastomeric rubber property by F_2 value. SBS, latex, and CR modified asphalt binder do not fail after immediately reaching F_1 value; rather, these binders elongated more to achieve F_2 value before failure. Among the elastomeric rubber modifier, SBS modified binder show a higher second peak, which indicates that the

SBS modified binder can take more load than the latex and CR modified asphalt binder. It can be concluded that the SBS modified binder is more effective than the other two modified asphalt binders are.

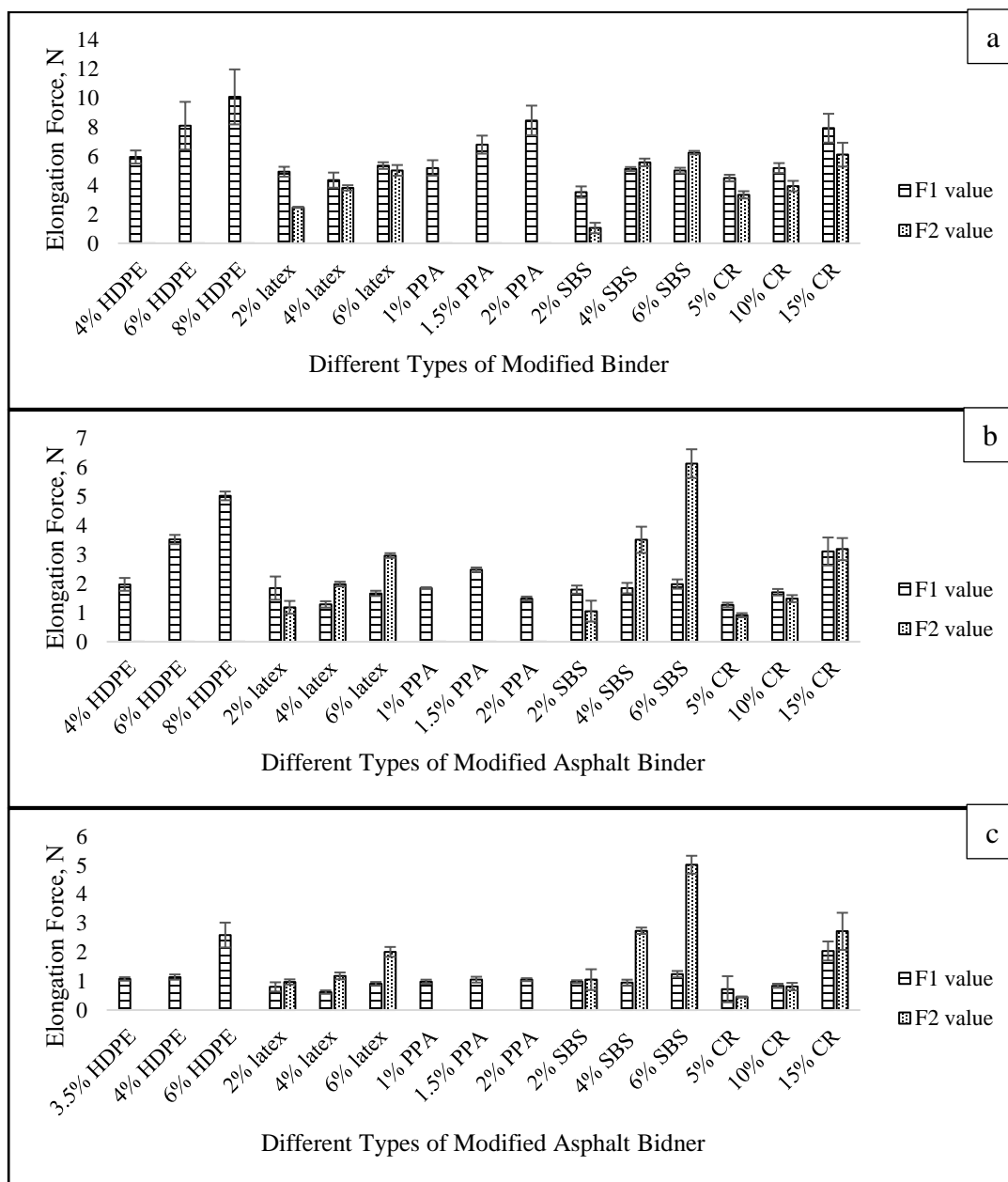


Figure 2-5: Elongation force (F_1 and F_2) of different types of binders at (a) 4°C, (b) 12°C, and (c) 16°C.

2.3.4 Second Peak Elongation Force, F_2 , at Similar Stiffness

Figure 2-6 (a), (b), and (c) show the F_2 value of the different types of the samples with similar stiffness at 4°C, 12°C, and 16°C, respectively. The stiffness of the original PG 64-22 binder increases after modification for all five modifiers. It is observed that in the case of 1% PPA, 10% CR, 4% SBS, 2% latex, and 3.5%/4% HDPE, similar stiffness (F_1 value) can be found as shown in **Table 2-3**. As mentioned earlier, 1% PPA, 3.5%, and /4% HDPE do not have any F_2 value as shown in **Figure 2-6 (a), (b), and (c)**. On the other hand, at 4°C, with a similar F_1 value, 10% CR, 4% SBS, and 2% latex have an F_2 value equal to 3.93, 5.56, and 2.47 along with standard deviation of 0.36, 0.26, and 0.04, respectively (**Figure 2-6 a**).

Table 2-2: Similar Stiffness (F_1) Value of Different Types of Modified Binders.

Modified binder name	F_1 value at 4°C	F_1 value at 12°C	F_1 value at 16°C
1% PPA	5.18	1.84	0.98
10% CR	5.17	1.7	0.84
4% SBS	5.1	1.84	0.95
2% latex	4.92	1.84	0.80
3.5%/ 4% HDPE	4.93	1.97	1.08

At 12°C, the F_2 value is equal to 1.48, 3.50, and 1.18, along with a standard deviation of 0.12, 0.45, and 0.22, respectively, as shown in **Figure 2-6(b)**. Similarly, at 16°C, the F_2 value is equal to 0.81, 2.74, and 0.97, along with a standard deviation of 0.13, 0.11, and 0.09, respectively, as shown in **Figure 2-6(c)**. It is clear from the figures that for the same PG graded binder, 4% SBS has the highest F_2 value. It indicates that SBS modified asphalt binder performs better than the latex and CR modified binder.

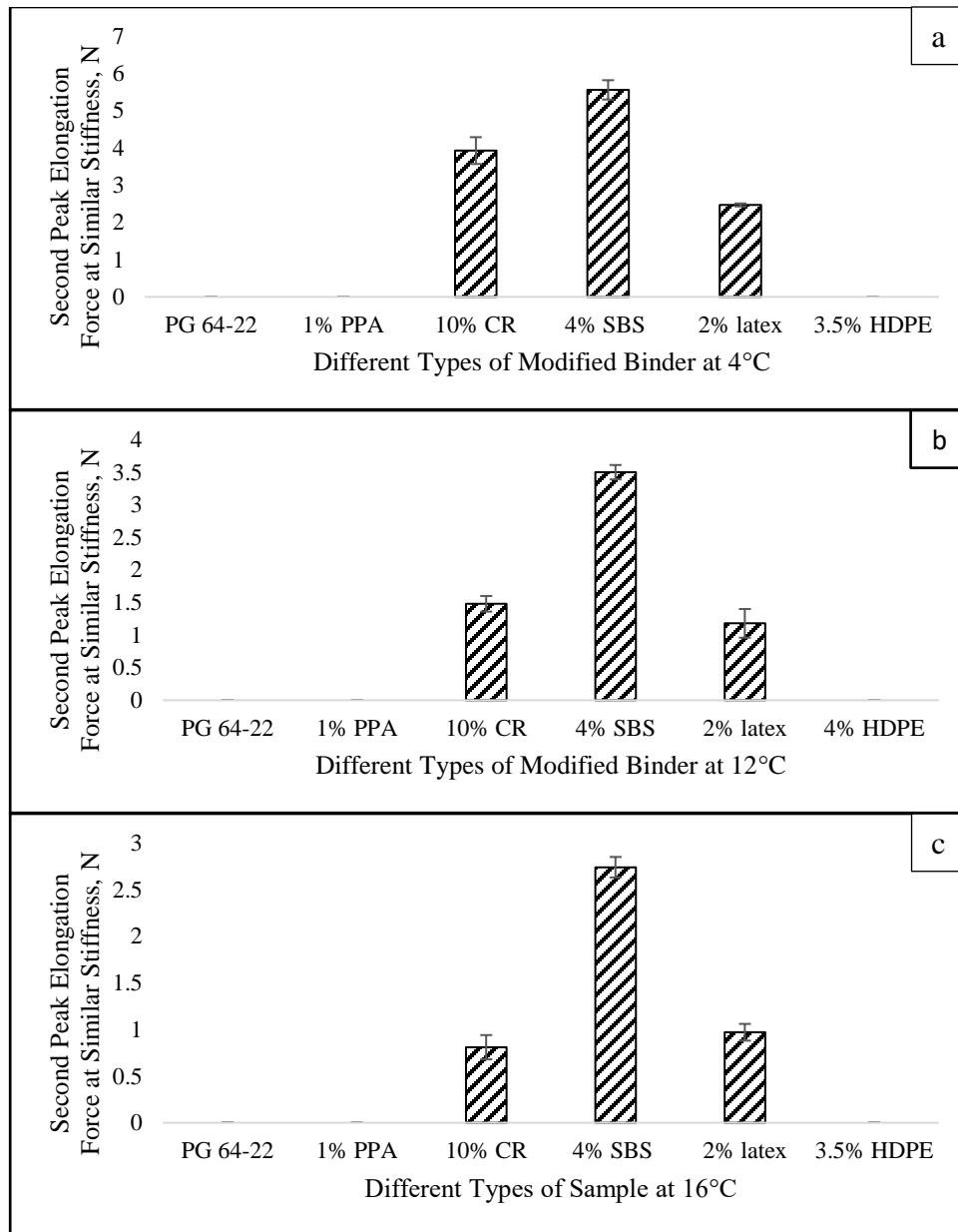


Figure 2-6: F_2 at similar stiffness for different types of modified binder at (a) 4°C, (b) 12°C, and (c) 16°C.

2.3.5 Polymer Content Determination

Shirodkar *et al.* [33] studied the correlation between polymer modification and mechanical properties of the binder. It was concluded that the percent recovery from

MSCR along with non-recoverable creep compliance may specify PMAB. The relationship between polymer content and the parameters of this new test method is presented below.

2.3.5.1 Polymer (latex) Modified Asphalt Emulsion (PMAE)

Zhang *et al.* [34] performed the penetration test, the softening point test, and ductility tests on SBR latex PME with a different percent of the polymer. Tests were performed for every 1% between 1% to 8%. The results did not show a linear correlation with the increment of percentage of polymer for all the performed tests. PMAEs with four different percentages of latex are tested to establish a correlation between the polymer percentage in the PMAE and the investigated parameter. The investigated parameters are F_1 and F_2 . The four different percentages of latex are 0%, 2.5%, 4%, and 5.5%.

Figure 2-7 indicates the F_1 and F_2 vs percent of latex for PMAE at 4°C. From Figure 2-7 (a), it is found that there is no correlation between F_1 value and the percent of latex. For 0%, 2.5%, 4% and 5.5%, F_1 value is equal to 1.81, 1.66, 2.24 and 2.88 with standard deviation of 0.10, 0.06, 0.29 and 0.32, respectively. From **Figure 2-7 (b)**, it can be observed that with the increment of the latex percentage, F_2 increases, and this is due to the improvement in the PMAE because of the latex additives. For 0%, F_2 is equal to 0 N, for 2.5% F_2 is equal to 2.43 N, for 4% F_2 is equal to 3.25 N, and for 5.5% F_2 is equal to 5.17 N with standard deviations of 0, 0.01, 0.24 and 0.08, respectively. Therefore, it is linearly increasing with R^2 value of 0.9934. From the figure, the equation of the straight line is equal to $0.8007x$ where slope is equal to 0.8007. This indicates that F_2 increases by 0.8007 N per percent increase in latex.

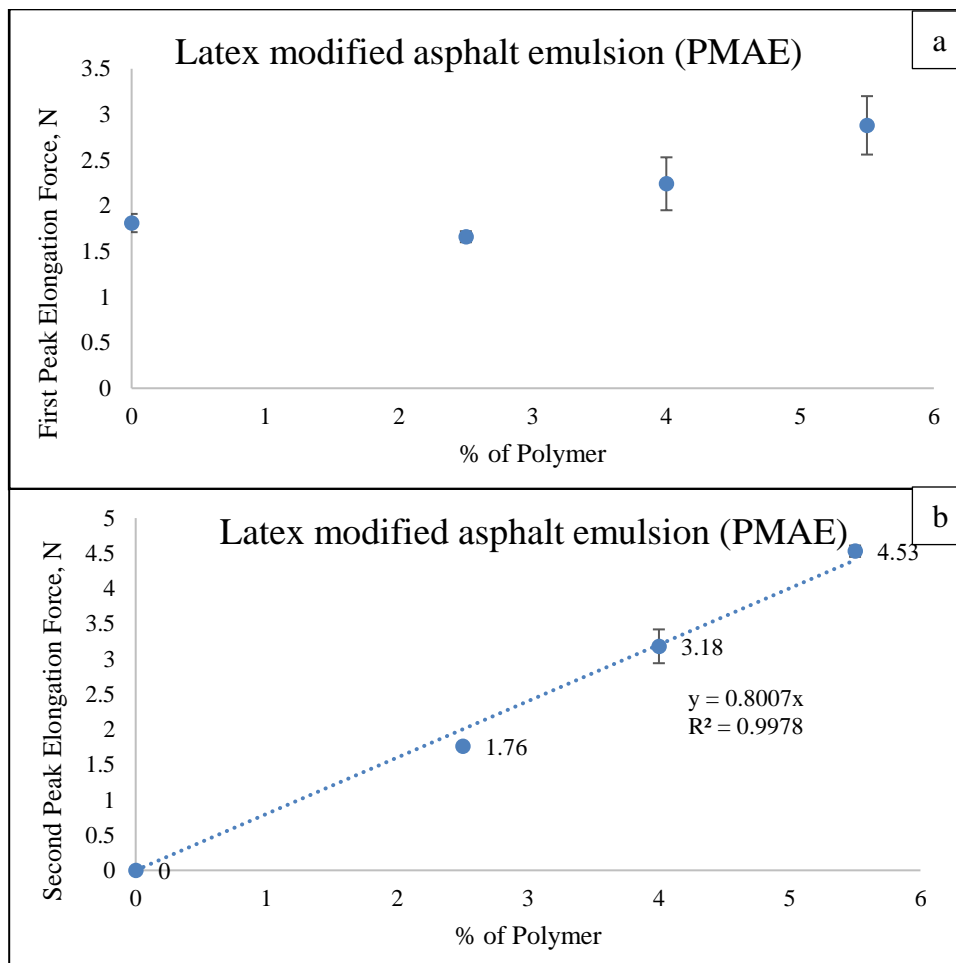


Figure 2-7: (a) First peak elongation force vs. the percent of polymer for PMAE at 4°C, and (b) Second peak elongation force vs. the percent of polymer for PMAE at 4°C.

2.3.5.2 Latex Modified Asphalt Binder (PMAB)

F_1 has no correlation with the percent of polymer as shown in **Figure 2-8(a)**. For 0%, 2%, 4%, and 6% PMAB, the F_1 value is equal to 3.58, 4.92, 4.34, and 5.34 with the standard deviations of 0.17, 0.34, 0.52, and 0.23, respectively, which indicate that no linear correlation exists. There is a linear correlation between F_2 vs. the percent of polymer for PMAB at 4°C as shown in **Figure 2-8(b)**. No F_2 is found from the 0% PMAB (i.e. unmodified PG 64-22). When 2% latex is added, F_2 is found to be 2.47N.

F_2 increases to 3.81 N when 4% latex is added. F_2 further increases to 5.01 N when 6% latex is added. The standard deviations are 0, 0.03, 0.18 and 0.37, respectively. The coefficient of determination (R^2) value is found to be 0.9535. The slope of the straight line is equal to 0.8971. This indicates that F_2 increases at 0.8971 N per percent increase in the latex. This rate is higher than that of 0.8007 N per percent of latex for latex modified asphalt emulsion.

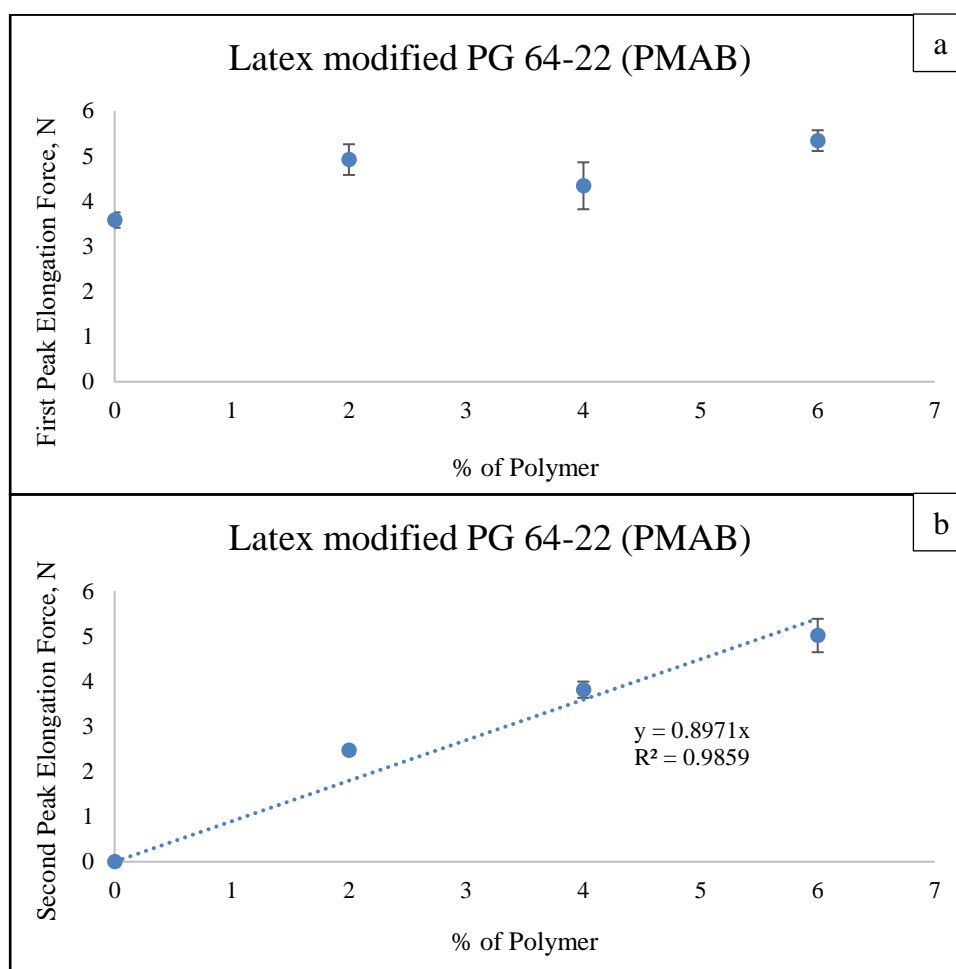


Figure 2-8: (a) First peak elongation force vs. percent of polymer at 4°C, and (b) Second peak elongation force vs. percent of polymer at 4°C.

From 4-8, it can be concluded that F_2 reflects the level and the type of the polymer. From the figure, it is clear that F_2 has a strong correlation with the percent of the polymer.

It is observed from the figures that the linear curve of PMAB is steeper than PMAE, which indicates latex improves asphalt binder property more than asphalt emulsion.

2.3.6 Temperature Sweep (DSR) Test Results

Figure 2-9 presents the results of the temperature sweep tests performed at temperatures 58°C, 64°C, 70°C, and 76°C for latex modified asphalt emulsions and binders, respectively. It can be observed that at each temperature tested, rutting factor $G^*/\sin\delta$ increases with an increase in the percent of latex in PMAE.

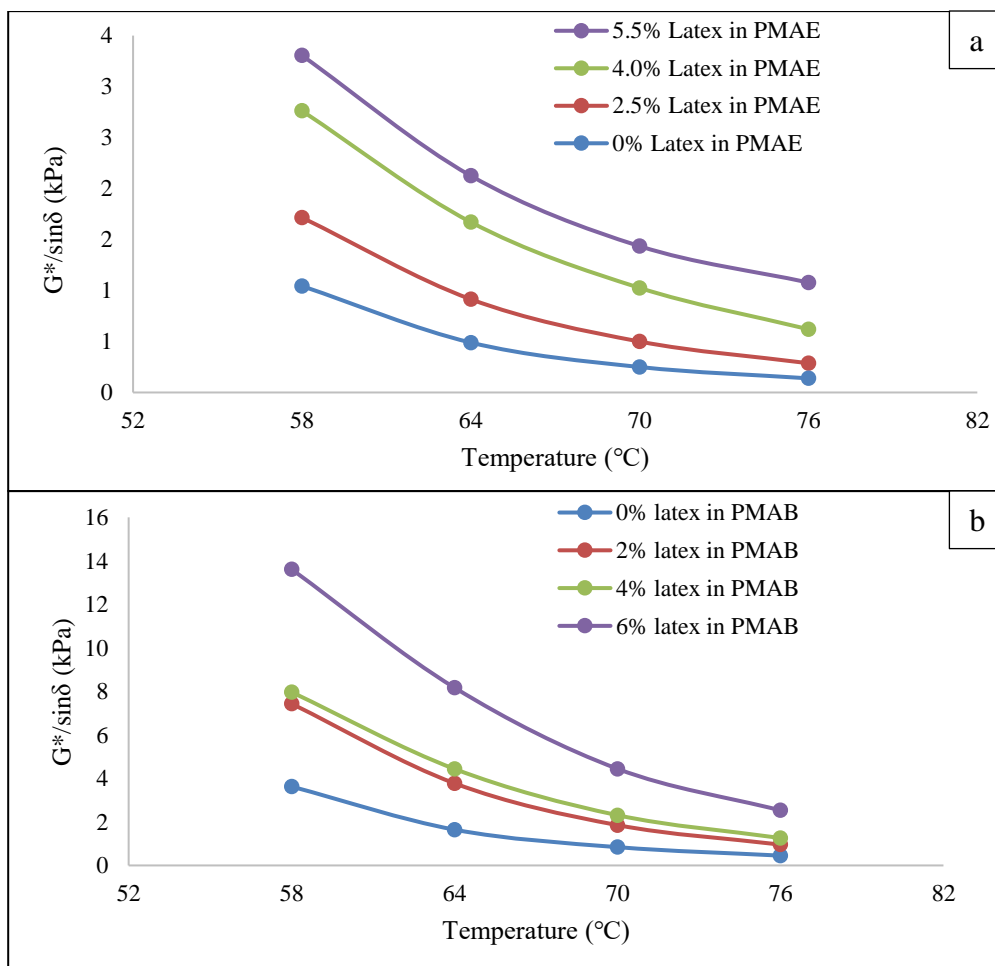


Figure 2-9: $G^*/\sin\delta$ at different temperatures of (a) PMAE and (b) PMAB.

However, the higher stiffness (higher $G^*/\sin\delta$) is not a polymer indicator and should not be considered as a measure for polymer content determination in polymer modified asphalt binder and emulsion. For example, 0% latex modified emulsion and binder have $G^*/\sin\delta$ value, but 0% latex modified emulsion and binder do not have any F_2 value.

2.3.7 Multiple Stress Creep Recovery (MSCR) Test Results

Figures 2-10 and **2-11** show the results of the multiple stress creep recovery tests of PMAE and PMAB at 58°C, 64°C, 70°C, and 76°C. **Figure 2-10** shows recovery values at 3.2 kPa for PMAE and PMAB, respectively. **Figure 2-11** shows the non-recoverable creep compliance values at 3.2 kPa for PMAE and PMAB, respectively. **Figure 2-10** indicates that at 58°C, 64°C, 70°C, and 76°C, percent recovery increases with an increase in the percent of latex polymer in both the PMAE and PMAB.

Figure 2-11 indicates that non-recoverable creep compliance (better rutting susceptibility) reduces with an increase in the percent of latex polymer in the case of PMAE and PMAB. However, it is also clear that non-recoverable creep compliance (J_{nr}) value reduces with the decrease in temperature as the binder becomes stiffer. Stiffness is not an indicator of presence of polymer and so, non-recoverable creep compliance cannot be used as a parameter for the polymer percent determination in PMAE or PMAB. In the proposed new method in this study, 0% latex modified emulsion does not have any F_2 value, whereas any binder has a J_{nr} value. Therefore, the proposed method is better in identifying the polymer and quantifying the percent of polymer.

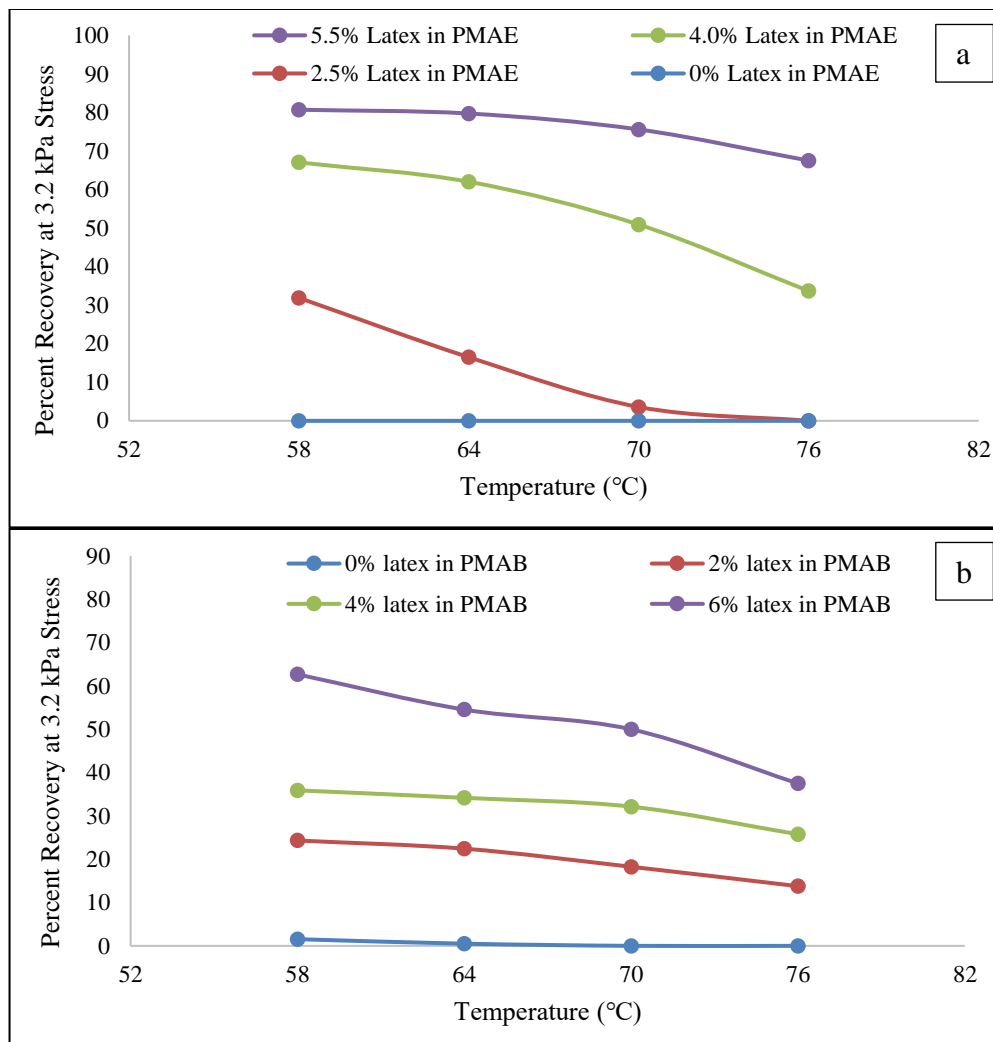


Figure 2-10: Multiple stress creep recovery at 3.2 kPa stress of (a) PMAE and (b) PMAB.

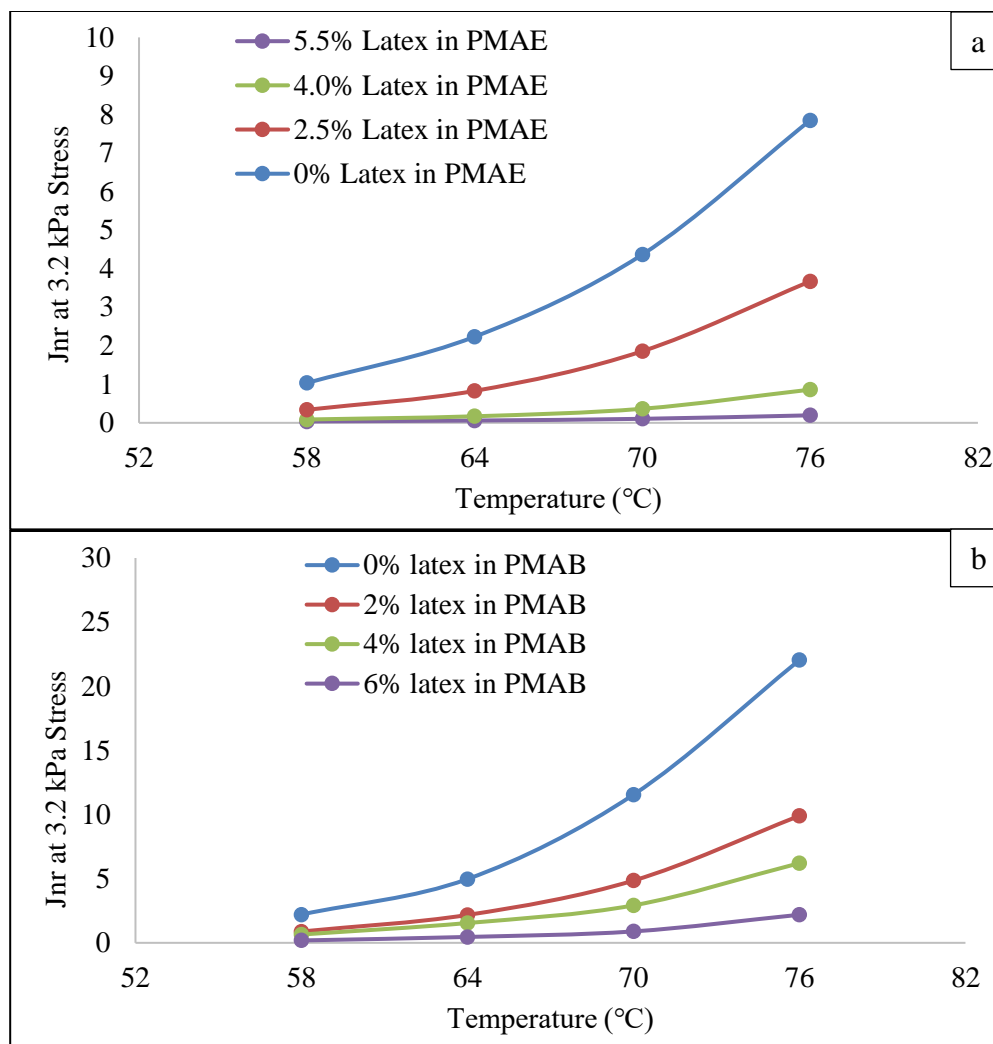


Figure 2-11: Non-recoverable creep compliance (Jnr) at 3.2 kPa stress of (a) PMAE and (b) PMAB.

2.4 Conclusion

This study identifies the different types of modifiers (SBS, PPA, latex, CR and HDPE) and their effectiveness. In addition, determination of the SBR latex in modified asphalt emulsion (PMAE) and binder (PMAB) is performed. Different percentages of modifiers are added with the base binder PG 64-22 in the laboratory. The novel DSR-based extensional deformation test method is followed to find out the modifier's effectiveness

and determine the SBE latex content. The following conclusions can be drawn from this study:

- First peak elongation force, F_1 , is the binder's stiffness and the second peak elongation force, F_2 , is the modifier's stiffness. From the five modifiers, SBS, SBR latex, and CR modified binder show the F_2 value, and PPA and HDPE do not show any F_2 value.
- Stiffness values of PPA and HDPE modified asphalt binder are more than the stiffness values of SBS, SBR latex, and CR modified binder. Among SBS, SBR latex, and CR modified binder, SBS modified binder shows a higher F_2 value, which indicates it can take on more of a load than the other two types of modified binders. Based on the F_2 value, it can be concluded that SBS modified binder is more of an effective binder than SBR latex and CR modified binder.
- For the first peak elongation force, F_1 has no linear correlation with the percent of polymer in case of both PMAE and PMAB.
- For the second peak elongation force, F_2 is investigated to correlate it with the percent of the polymer in the PMAE and PMAB. F_2 has a linear correlation with the percent of the polymer in the PMAE and PMAB with R^2 values equal to 0.9934 and 0.9535, respectively.
- Temperature sweep tests and multiple stress creep recovery tests indicate that the F_2 value proposed in this new test method is a better indicator of polymer content compared to rutting parameter, $G^*/\sin\delta$ and non-recoverable creep compliance, J_{nr} .

CHAPTER 3

SBS CONTENT DETERMINATION BY EVALUATING POLYBUTADIENE FUNCTIONAL GROUP

3.1 Introduction

The modification of the asphalt binder becomes a common practice as the traffic loads and the volume has increased enormously over the last few decades. Therefore, the use of modifiers, such as SBS, styrene-butadiene rubber (SBR), polyphosphoric acid (PPA), ethylene vinyl acetate (EVA), etc., has enhanced tremendously to improve the pavement performance [35]. Among these modifiers, SBS is the most used polymer. SBS modified asphalt binder reduces rutting and increases the fatigue and thermal cracking resistance of the pavement [36]. But the quality control of SBS modified asphalt binder is a challenging task in the field for several reasons. Firstly, SBS polymer tends to separate from the SBS modified asphalt binder under static heated storage conditions, including segregation and thermal decomposition [37], [38]. Secondly, the supplier may use lower SBS content and other additives in the asphalt binder to achieve a higher PG binder for making more profit [39]. Hence, a quantification standard is necessary for quality control in the field as the SBS modified binder's performance depends on the SBS content [40].

Studies on the quantification of SBS content were performed by different methods such as elastic recovery [41], extensional deformation [40], phase separation [42], gel

permeation chromatography [42]–[45], nuclear magnetic resonance [46], and IR [41], [46]–[49], etc. Lu *et al.* [50] reviewed different mechanical and non-mechanical tests, including the FT-IR spectrometer, to select the appropriate SBS quantification method. The handheld FT-IR spectrometer was found to be the best suitable method for quantifying SBS content. From FT-IR spectra analysis, several calibration curves were proposed for SBS quantification in different types of SBS modified PG binders.

Similarly, Sun *et al.* [51] established a calibration curve to quantify SBS in SBS modified asphalt binder considering the peak absorbance ratio using FT-IR spectrometer. Another researcher, Hu *et al.* [52], considered all the variabilities in SBS mixing with asphalt binder for SBS quantification in laboratory measurement. **Table 3-1** represents some of the previous studies that used FT-IR spectroscopy to characterize and quantify the polymers in the modified asphalt binder.

In summary, these previous studies only considered laboratory binders and developed a calibration curve for each specific asphalt binder. These studies did not investigate the effect of a variety of PG binders from several sources, the impact of different SBS polymer types from different sources and cross-linking agent on the peak absorbance height or area of the PB functional group.

In 2005, AASTHO standardized a test method for polymer content determination of laboratory prepared polymer modified emulsified asphalt residue and asphalt binder using FT-IR spectroscopy (AASTHO T 302-15). Still, its implementation in field binders was not adequately addressed. Following the AASHTO standard in the field is not feasible because it requires a calibration curve in each binder's specific case. Developing a

calibration curve in the field is not always possible for each specific binder due to proprietary reasons.

Table 3-1: Polymer content determination by FT-IR spectrometer in previous studies.

Authors	Index Used	Polymer Type	Comment	Verification (field binder)
AASHTO T302 (2015)	Peak ratio 965/1375 Peak area at 965 cm ⁻¹	SBS, SBR, and SB	Calibration curve	No
Wang <i>et al.</i> , [53]	Peak area at 966 and 699 cm ⁻¹	SBS	Calibration curve using partial least square regression	No
Ye <i>et al.</i> , [21]	Peak ratio 966/1375 and 700/1375	SBS	Peak height curve, R ² = 0.98 and peak area curve, R ² = 0.99	No
Diefenderfer <i>et al.</i> [41]	Peak ratio 965/1375	SBS and SB	Calibration curves, R ² = 0.99	No
Fernandez, <i>et al.</i> [54]	Peak at 815, 960 and 700 cm ⁻¹	Natural rubber and SBR	Calibration curves, R ² = 0.99	No
Luo <i>et al.</i> , [39]	Peak area at 966 and 813 cm ⁻¹	SBS	Calibration curve using linear regression analysis, R ² = 0.98	No
Curtis <i>et al.</i> , [47]	Peak ratio 965/1375 (latex), 1242/1375, 1736/1375 (EVA), and 966/1375 (SBS)	SBR latexes, EVA and SBS	Calibration curves, R ² = 0.92 to 0.99	No
Nasrazadani, <i>et al.</i> [55]	AASHTO T302 was followed	SBS, SBR and SB	Calibration curve, R ² = 0.99 Calibration curve, R ² = 0.99	No

Note: SBR- Styrene butadiene rubber, SB- Styrene-butadiene, EVA- ethylene vinyl acetate

In this study, the FT-IR spectrum's absorbance intensity for each specific characteristic functional group was quantified by both height and area method. The effects of the differences in PG binders and sources, SBS polymer sources and structures, and cross-linking agents on peak absorbance height of the PB functional group were studied. After that, a model was developed to predict SBS content in SBS modified binder using a handheld FT-IR spectrometer with a diamond attenuated total reflectance (ATR) sensor. We visited an asphalt plant to measure the required time to determine SBS content in *in-situ* condition with the newly developed model. Finally, for validation, four modified

binders with unknown SBS content were obtained from two refineries. The SBS contents were determined using the developed model without any calibration curve, and the results were sent to the refineries for verification with the actual SBS content. The model predicted all the refinery supplied binders with a minimal error.

3.1.1 Objective

The following points summarize the objectives of this study:

- Investigating the effects of the different PG binders and sources of the binders, the different SBS polymer types and sources, and the cross-linking agent on the PB functional group of the FT-IR spectra.
- Developing a model that can successfully predict the SBS content in any unknown binder without a calibration curve with a handheld FT-IR spectrometer.

3.2 Materials and Experimental Plan

3.2.1 Materials

In this study, three different base binders, namely PG 52-34, PG 58-28, and PG 64-22, were used. PG 58-28 was collected from Louisiana (source A) and Texas (source B). PG 64-22 was obtained from two different sources: one from Louisiana (source A) and the other from North Carolina (source C). For the polymer modified binder preparation, two types of SBS polymer structure, triblock and di-block, were considered. For triblock SBS copolymers, both linear and radial molecular configurations were examined [56]. As a result, three types of SBS copolymers named linear, radial, and di-block were used to prepare the polymer-modified asphalt binder. SBS polymer was collected from two different sources in powder and pellet form. A reagent grade 100-mesh particle size sulfur

was used as a cross-linking agent for avoiding the phase separation of SBS modified asphalt binder [57].

3.2.2 Preparation of SBS Modified Binders in Laboratory

SBS modified asphalt binders were prepared in the laboratory using a high shear mixer. SBS polymer was added to the asphalt binder based on the total weight of the binder. SBS polymer (1%, 2%, 3%, and 4% by weight of base binder) was added to the base binders employing the following method:

- Around 600 gm of asphalt binder was collected in a quart can from the supplier's bucket.
- Then the quart can was placed in the melting pot, as shown in **Figure 3-1(a)**. The temperature of the melting pot was set at 170°C. When the binder achieved its workability, the rotation speed of the high shear mixer was set at 5000 rpm. At this time, the addition of SBS polymer began little by little and continued for the next 30 minutes (**Figure 3-1b**).
- The mixing procedure continued for 30 minutes at 5000 rpm and then for another 2 minutes at 8000 rpm. This mixing process was continued for 2.5 hours by changing the speed after every 30 minutes. **Figure 3-1(c)** represents the high shear mixer that was used in this study.
- The increment in temperature of the melting pot was monitored by adjusting the speed of the high shear mixer so that it could not exceed the temperature of 185°C.
- On the other hand, for the addition of the cross-linking agent (0.5% sulfur) in the SBS modified binder, the mixing process, as mentioned earlier, was followed for 1.5 hours. Then sulfur was mixed in the SBS modified binder all at a time and

continued the mixing technique for one more hour as the mixing process mentioned earlier.

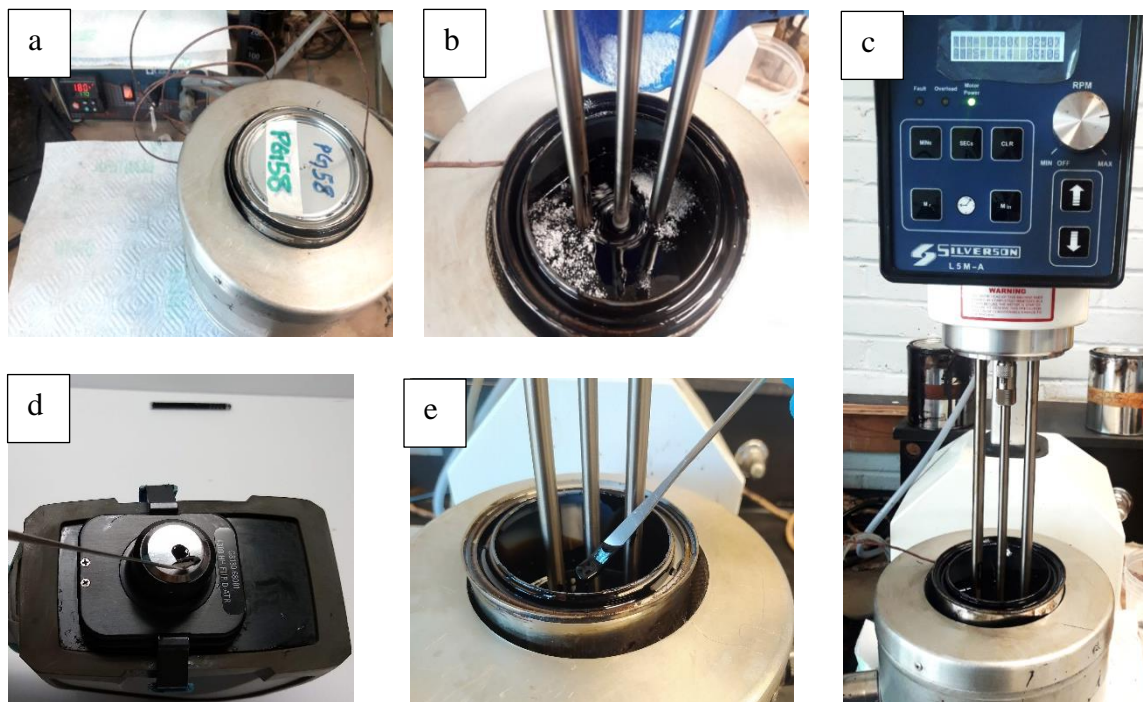


Figure 3-1: (a) Heating samples in a quart can in the melting pot, (b) Adding powder SBS in the liquid asphalt binder, (c) Mixing in the high shear mixer for 2.5 hours, (d) Sample collection using a spatula, (e) Placing sample on diamond ATR sensor of FT-IR spectrometer.

- In this process, a total of twenty-six binders was prepared for different percentages of SBS.
- For repeatability data collection on different days, remixing was conducted in high shear mixer at 170°C for 30 minutes at 5000 rpm. After 15 minutes, speed was increased to 8000 rpm, and mixing was continued for 2 minutes. After that, the speed was reduced to 5000 rpm to complete the 30-minute cycle of remixing.

Table 3-2 shows the number of cases (26), and the number of samples ($26 \times 50 = 1,300$) tested in this study. Here, “Batch” indicates the SBS modified binders prepared by the

same procedure for the second time. “Days” indicates the repeatability in data collection for different days from the same batch.

Table 3-2: Materials and test matrix.

Binder	Type of polymer	Source of polymer	%SBS	Batch	Day	No. of samples	No. of cases	
PG52-34 (Source C)	Radial	Source 1	0, 1, 2, 3, 4	1	1	50	1	
					2	50	2	
				2	3	50	3	
					1	50	4	
PG58-28 (Source A)	Radial	Source 1	0, 1, 2, 3, 4	1	1	50	5	
					2	50	6	
					3	50	7	
				2	4	50	8	
					1	50	9	
					2	50	10	
PG58-28 (Source B)	Radial	Source 2	0, 1, 2, 3, 4	1	1	50	12	
					1	1	50	13
						2	50	14
PG64-22 (Source A)	Radial	Source 1	0, 1, 2, 3, 4	1	3	50	15	
					1	50	16	
				2	2	50	17	
					1	50	18	
PG64-22 (Source C)	Radial	Source 1	0, 1, 2, 3, 4	1	1	50	19	
					2	50	20	
	Linear	Source 1	0, 1, 2, 3, 4	1	1	50	21	
					2	50	22	
	Diblock	Source 1	0, 1, 2, 3, 4	1	1	50	23	
					2	50	24	
Radial+ 0.5% S	Source 1	0, 1, 2, 3, 4	1	1	50	25		
				2	50	26		

3.2.3 FT-IR Spectroscopy

The handheld FT-IR spectroscopy is considered more robust to implement in the field for quick identification and quantification of chemical compounds [58]. The principle of FT-IR spectroscopy involves passing an infrared beam through the material and

identifying their molecular structure based on their rotational and vibrational frequency [59]. The chemical bonds in a material absorb the infrared beam in a specific wavenumber and are displayed as an absorbance spectrum in FT-IR spectroscopy.

In most cases, FT-IR spectrometer reported a spectrum in 400 cm^{-1} - 4000 cm^{-1} region where 600 cm^{-1} - 1500 cm^{-1} is known as the fingerprint region due to complex functional groups that differ from sample to sample [60]. After analyzing this absorbance spectrum, chemical functional groups of a material can be identified and quantified. In this study, a 4300 handheld FT-IR spectrometer was used to obtain the spectra considering its flexibility, robustness, carrying capability for field data collection, and easy sampling procedure. The diamond ATR sensor was used since the collected spectra remained unaffected by the sample amount placed on the sensor (AASTHO T302 2015). Again, the sensor has corrosion and scratching resistivity, which makes it suitable for field measurement.

3.2.4 Data Collection from Laboratory Prepared SBS Modified Binders

Ten samples were taken from each laboratory prepared SBS modified binders using a spatula for data collection (**Figure 3-1d**). Before each scan, background spectra were collected to check if the sensor was adequately clean. Then the sample was placed on the sensor area after collecting using a spatula. The connection between the sample and the sensor of the instrument was ensured. Each spectrum collected by the FT-IR spectrometer was converted to the absorbance spectra by the default Microlab PC software provided with the instrument. Twenty-four scans for each sample were conducted in $650\text{-}4000\text{ cm}^{-1}$ region and reported in 4 cm^{-1} resolutions. **Figure 3-1(e)** shows the data collection technique with the 4300 handheld FT-IR spectrometer.

3.2.5 In-Situ Data Collection from Plant Modified Binders

We visited one plant to estimate the required time for predicting the SBS content in SBS modified asphalt binders in the in-situ condition. The following steps summarize the FT-IR spectrometer data collection in the plant:

- At first, the plant modified asphalt binders was collected in a 1-gallon can from the asphalt plant's designated tank (**Figure 3-2a** and **3-2b**).
- After that, the background spectrum was checked, and the asphalt binder was placed on the ATR sensor using a spatula, as shown in **Figure 3-2(c)** and **3-2(d)**.
- Then the FT-IR spectrum was collected by Microlab mobile software.
- In this process, ten samples were collected from each binder (**Figure 3-2e** and **3-2f**).
- After collecting each sample, we used a solvent to clean the sensor.
- The required time was 20 minutes for data collection from each binder including cleaning and background checking.
- It took 10 minutes for data processing, data analysis, and predicting the SBS content.

In summary, a total of 30 minutes was required to predict SBS content in the in-situ condition from SBS modified asphalt binder.

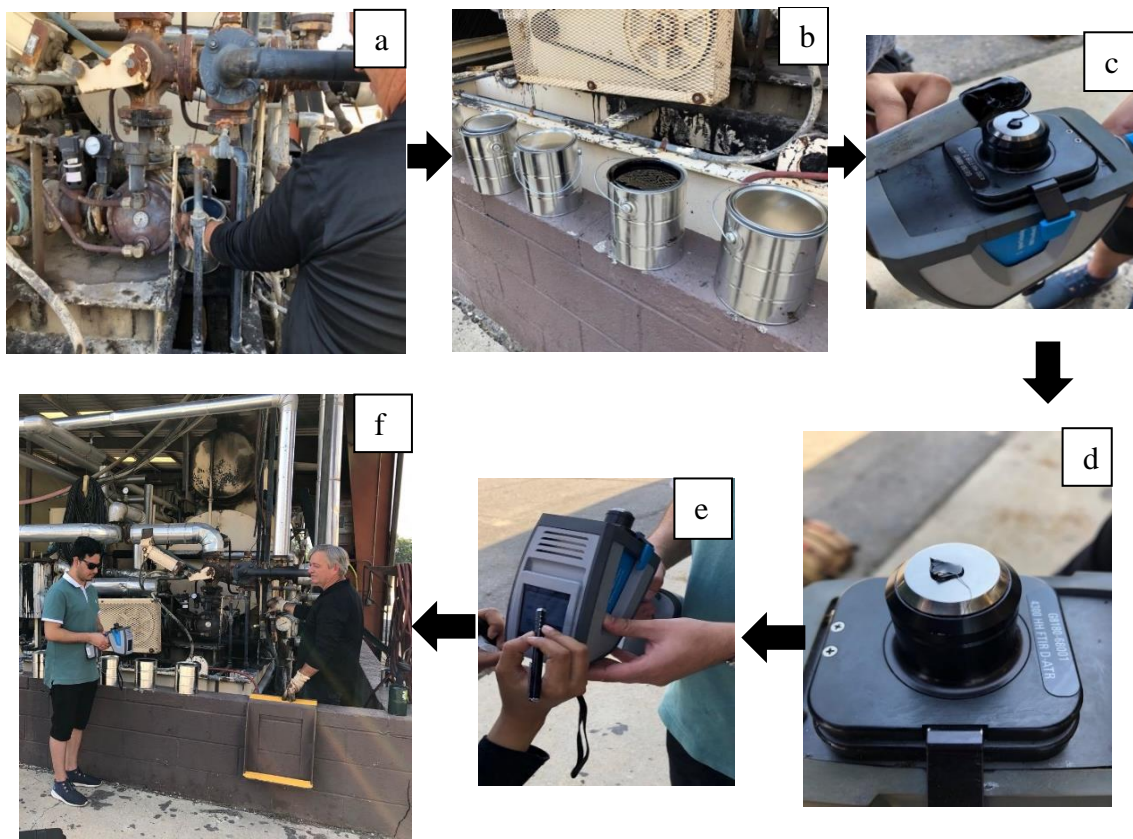


Figure 3-2: (a) Collecting the hot sample from the asphalt tank, (b) Storing samples in gallon cans in the plant, (c) Placing the sample on the ATR sensor by a spatula, (d) Ensuring a good connection between sensor and sample, (e) Collecting FT-IR spectra and (f) Repeating the same procedure for other samples.

3.2.6 Data Collection from Refinery Supplied SBS Modified Binders

Four SBS modified binders were supplied from two refineries with unknown SBS content. The binders were heated in the forced draft oven at 170°C for 2.5 hours. The binder was then placed over the hot plate, and the temperature of the hot plate was 170°C. The hot plate temperature was maintained at 170°C throughout the data collection period by continually checking with a digital thermometer. A small amount of binder was collected from the quart can using a spatula and directly placed over the diamond ATR

sensor (**Figure 3-1e**). Then the FT-IR spectrum was collected by following the procedure mentioned earlier.

3.3 Results and Discussion

3.3.1 Qualitative Analysis of FT-IR Spectrum

The effect of SBS modification in the asphalt binder was analyzed qualitatively by studying FT-IR spectra of unmodified and modified asphalt binders, respectively. This analysis occurred by overlapping both spectra and categorizing the inclusion of any unknown functional group in the fingerprint region of $650\text{-}1800\text{ cm}^{-1}$. **Figure 3-3** shows the characteristic functional groups present in an unmodified and SBS modified asphalt binder in the fingerprint region.

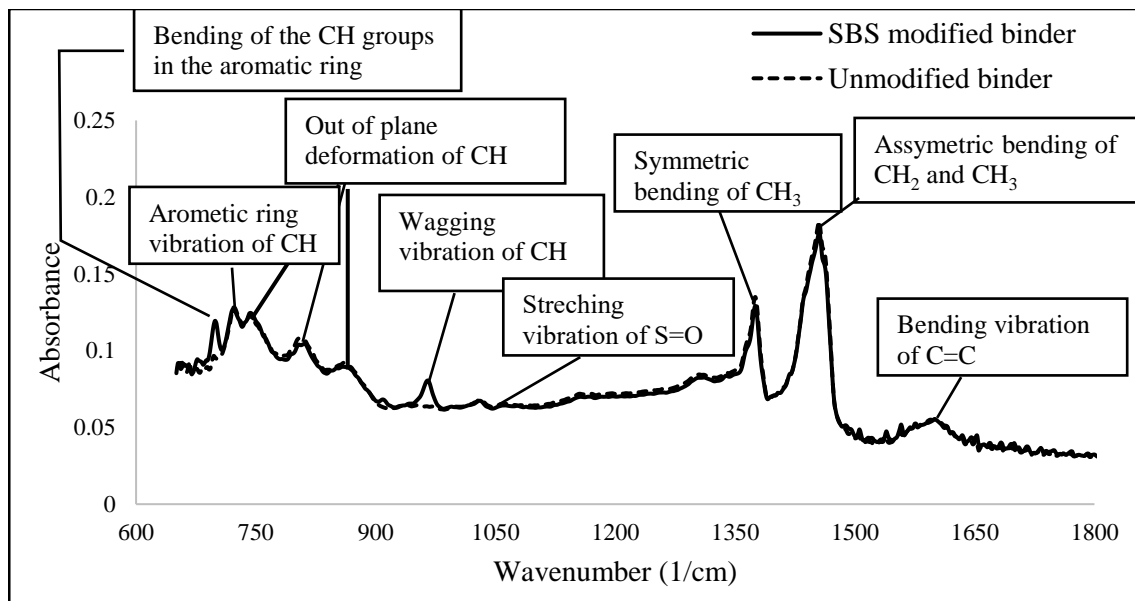


Figure 3-3: Typical FT-IR spectrum of unmodified and SBS modified asphalt binder.

It was observed that the key functional groups in the unmodified asphalt binder were bending vibration of $C = C$ at 1600 cm^{-1} , asymmetric bending of CH_2 and CH_3 at 1455 cm^{-1} , symmetric bending of CH_3 at 1375 cm^{-1} , stretching vibration of $S = O$ at 1034

cm^{-1} , out-of-plane deformation of CH at 870 cm^{-1} , 817 cm^{-1} , and 745 cm^{-1} , and aromatic ring vibration of CH at 721 cm^{-1} . These functional groups were persistent in all the unmodified base binders used in this study. From this, it can be inferred that functional groups in FT-IR spectra of all unmodified base binders remained identical even though their performance grade (PG) were different.

However, when base binders were modified with SBS polymers, two other functional groups were added (a) out-of-plane (wagging) vibrations of the CH groups at 965 cm^{-1} , which was accountable for PB block, and (b) out-of-plane bending of the CH groups in the aromatic ring at 699 cm^{-1} for polystyrene block [61]. No other functional groups were added due to the difference in SBS polymer structure and sulfur as a cross-linking agent. Besides, peak positions and peak shapes of these functional groups were also unaffected by these changes in the material. In this study, only the PB functional group was considered to develop the first-order linear curves from laboratory prepared binders.

3.3.2 Quantitative Analysis of FT-IR Spectrum

According to Beer's law, the absorbance intensity in terms of peak height or peak area is directly proportional to the content [60]. **Figure 3-4** shows the increasing pattern in absorbance intensity of the FT-IR spectra at wavenumber 965 cm^{-1} due to different contents of SBS in the asphalt binder. In this study, the absorbance intensity of the characteristic functional group was quantified by both height and area method to find the appropriate method that would provide repeatable measurements. These two methods were selected, considering their ability to eliminate noise and baseline shift effects [60].

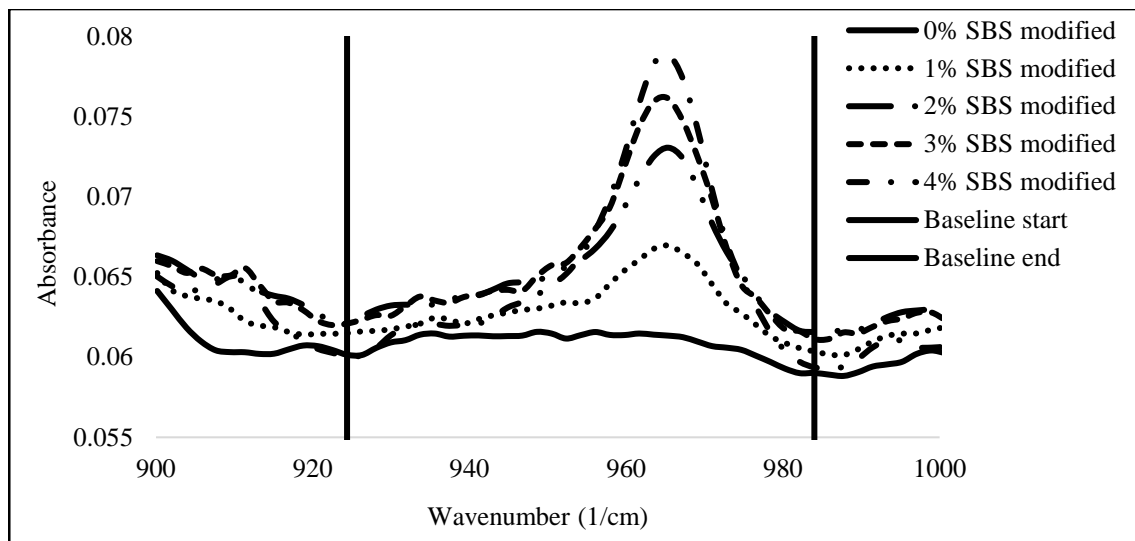


Figure 3-4: Effect of different percentages of SBS content in asphalt binder on the absorbance intensity at wavenumber 965 cm^{-1} .

For the peak height method, the height of the functional group was determined by drawing a baseline considering the two lowest points on either side of the characteristic functional group. After that, the top point of the peak and the baseline were added to determine the peak's height (**Figure 3-5**). For the peak area method, the absorbance area was calculated by the trapezoidal rule method. The baseline was drawn following a similar process as the peak height method.

We subtracted the area under the baseline from the total area under the peak, which provided the desired area. Following these procedures, the peak absorbance heights, and areas at wavenumber 965 cm^{-1} for different percentages of SBS were measured using the MATLAB programming tool. However, for unmodified samples (0% SBS), negligible peak height, and the area were encountered due to the IR beam's scattering effect [62]. Also, no pretreatment of the raw spectra was conducted since the proposed method was intended to apply for *in-situ* data measurement.

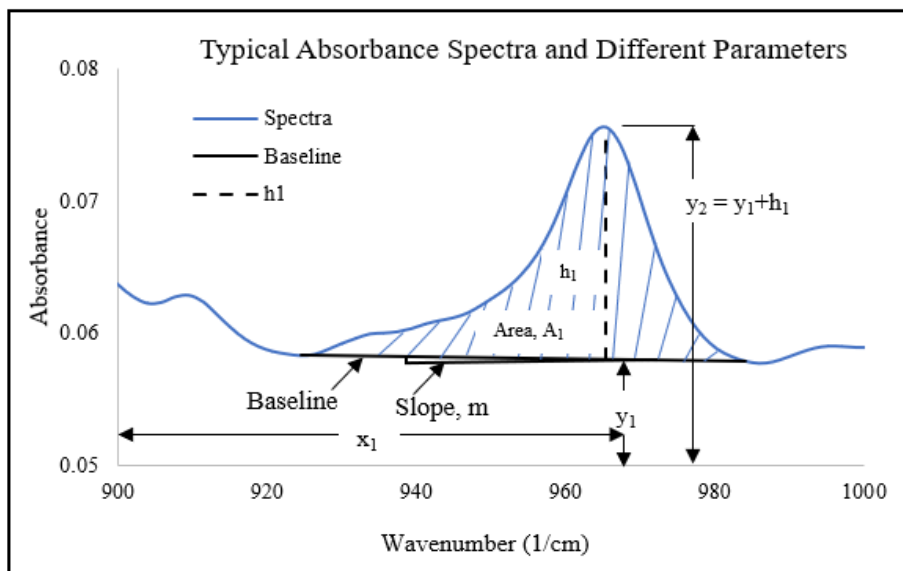


Figure 3-5: SBS quantification in peak height and peak area method.

3.3.3 Effect of Binder's Performance Grades and Sources on Peak Absorbance

Height

In the Superpave system, the binder's performance grade significantly impacts the physical and rheological properties such as stiffness, penetration, viscosity, etc., of asphalt binder. Similarly, the absorbance intensity of the FT-IR spectrum can be influenced by different PG binders and their sources. On the other hand, the plotting of calibration curves for different types of asphalt binder grades with respect to the SBS content can lead to a potential error for the dependency on specific samples [41].

Therefore, in this study, the effect of the different PG binders and their sources on the peak absorbance height of the PB functional group was investigated. The average heights of the peak absorbance were plotted against SBS contents to analyze the correlation better. As shown in **Figure 3-6(a)**, in different PG binders, the average peak heights differed by 3-8% for different SBS content except for 0% SBS modified binder. The

average peak height variation was about 31% between 0% SBS PG 52-34 and 0% SBS modified PG 58-28 binder. This difference arose for two reasons: no preprocessing of raw data and absolute height calculation from two of the lowermost points of the valley. The spectrum of unmodified (0% SBS) asphalt binder did not have any fixed valley under the peak 965 cm^{-1} .

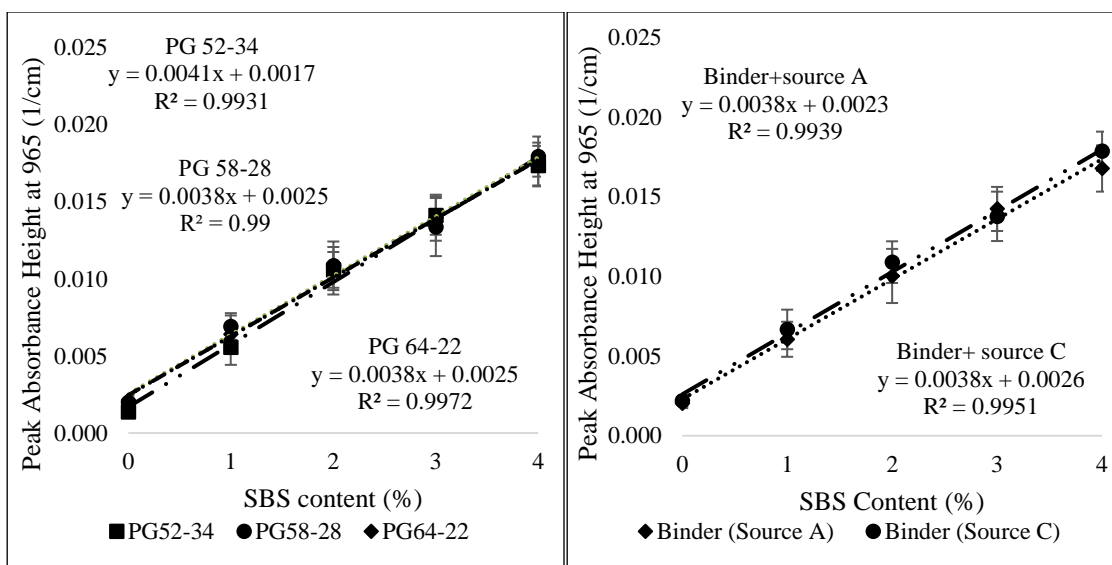


Figure 3-6: Relation between peak absorbance height and SBS content considering (a) different PG binders and (b) different sources of same PG binder.

Likewise, the difference among the average peak heights was 3 to 9% in the case of the same PG binders from different sources, as shown in **Figure 3-6(b)**. It can be inferred that different PG binders did not affect the peak absorbance height at 965 cm^{-1} . Also, the same PG binders from different sources did not influence the peak absorbance's height at 965 cm^{-1} . Moreover, the peak absorbance height of different PG binders and the same PG binders from different sources with SBS modification showed a high correlation with the SBS content. These figures depicted a significant finding, which confirms that the binders of different grades and binders from different sources would not need different calibration

curves. The peak absorbance height of different PG binders and binders from different sources can be used collectively to develop the linear regression model.

3.3.4 Effect of Cross-linking Agent on Peak Absorbance Height

Sulfur is often added to the SBS modified asphalt binder to increase storage stability [63]. Sulfur added polymer modified binder showed better compatibility [51], improvement in high temperature properties [64], the highest recovery in multiple stress creep recovery (MSCR) test and increment in viscosity [65]. Therefore, in this study, sulfur was added to the SBS modified asphalt binder to observe the peak height difference at 965cm^{-1} due to sulfur addition.

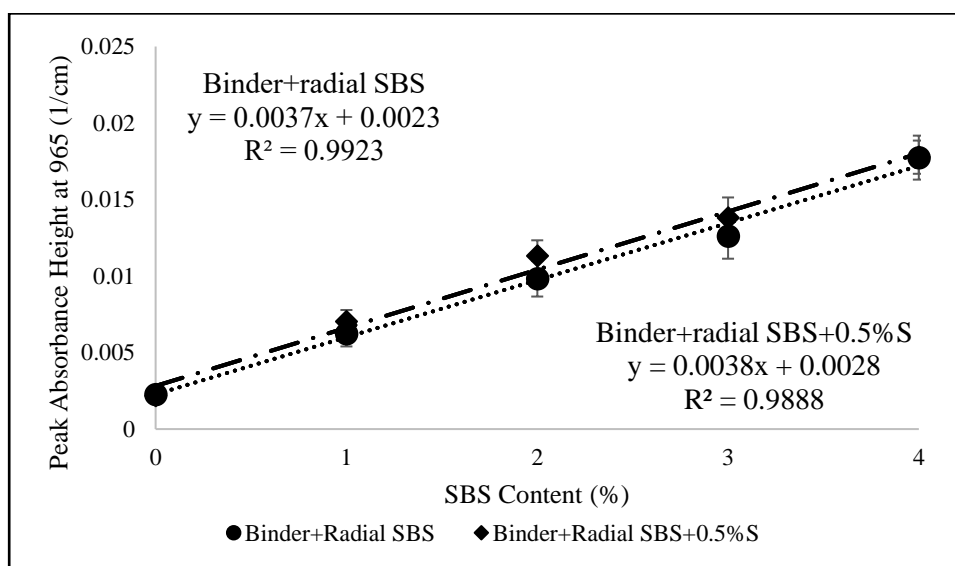


Figure 3-7: Relation between peak absorbance height and SBS content considering the effect of cross-linking agent.

Figure 3-7 represents the peak absorbance height at 965 cm^{-1} with different SBS content. It was observed that the difference in average peak absorbance height between the binders varied from 0.1% to 9.5%. Besides, peak height increased linearly with the increment in SBS content in both binders. This correlation indicated the addition of sulfur

as a cross-linking agent in radial SBS modified asphalt binder did not affect the peak absorbance height. It can be concluded that no additional calibration curve was needed if any binder was sulfur modified.

3.3.5 Effect of SBS Polymer Sources and Structures on Peak Absorbance Height

Triblock (linear and radial) and diblock SBS polymers are widely used to modify the asphalt binder. There is a significant difference in the physical and rheological behavior of triblock and diblock SBS modified asphalt binder. The rheological properties (elasticity, stiffness, and viscosity) of the radial SBS modified binder are better than the linear SBS modified binder [21], [66].

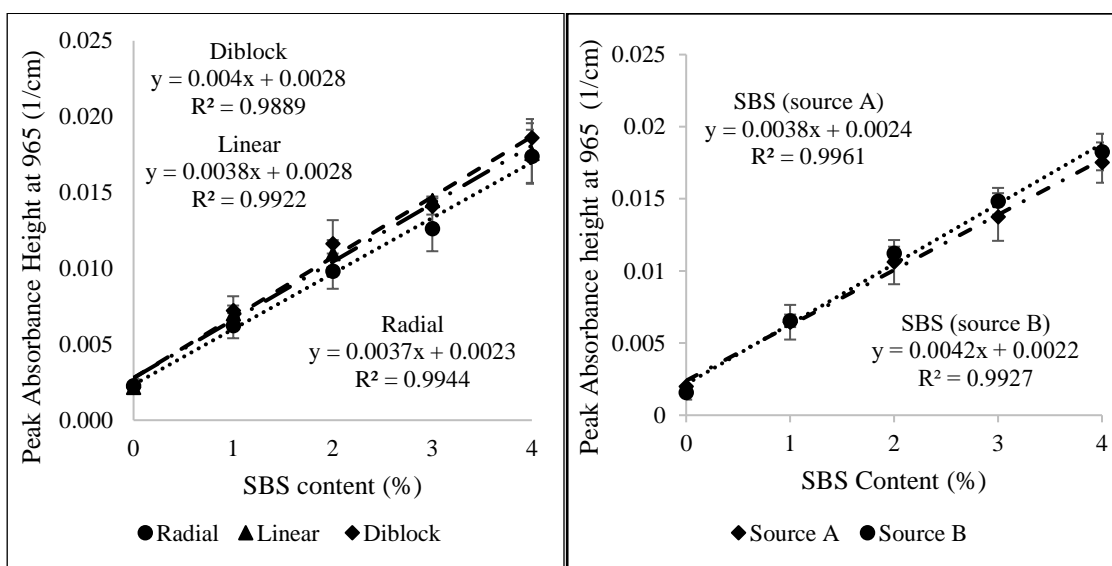


Figure 3-8: Relation between absorbance height and SBS content considering (a) three different SBS polymer structure, (b) two different SBS polymer sources.

However, the Florence micrograph showed poor polymer distribution in the radial SBS modified binder [67]. On the other hand, the stability and macro network formation of the triblock SBS modified binder are better than the stability and macro network formation of the diblock SBS modified binder [12]. But influences in absorbance intensity

of FT-IR spectrum due to the difference in SBS polymer structure and sources were not studied before.

Therefore, three different types of SBS polymer from two different sources were used in this study to investigate the effect of types and sources of SBS polymer on the peak absorbance height. **Figure 2-8** represents the absorbance height vs. SBS content at 965 cm^{-1} for three different types of SBS polymer (radial, linear, and diblock) from two different sources (Source A and B). It was observed that the difference in average peak absorbance height was varied from 0% to 14.7% for different SBS polymer structures.

Similarly, in different polymer sources, the variation was 1.5% to 7.9% on average for peak absorbance height. Additionally, peak height increased linearly with the increment of SBS content in all the cases of different SBS polymer sources and structures. In conclusion, different SBS types or SBS from different sources did not affect the peak absorbance height at 965 cm^{-1} in a statistically significant manner.

3.3.6 Evaluation of Variability

Repeatability indicates the repetition of data collection in the identical condition of the same sample. Reproducibility implies the variation in the same sample measurements in different conditions (different operators, instruments, etc.). In this study, the same binder was used for FT-IR spectrometer data collection on different days to evaluate the FT-IR spectrum variability. Also, different operators collected the data in different batches when all other conditions were identical. Statistical hypothesis analysis (Student's t-test) was performed on the peak absorbance height at 965 cm^{-1} of the SBS modified asphalt binder on different days and in different batches. **Table 3-3** represents the statistical hypothesis analysis result of different SBS modified asphalt binder's peak absorbance height.

The null hypothesis was that the mean value of the two different binders' peak absorbance height would be equal. The alternative hypothesis was that the mean of the peak absorbance height of a binder would be higher or less than the mean of the other binder's peak absorbance height. From the table, it can be observed that the null hypothesis cannot be rejected, which indicated the mean values of the peak absorbance height of the binders are the same in all the different cases. It can be concluded that the prediction of SBS content using peak absorbance height at 965 cm^{-1} could be repeatable and reproducible.

Table 3-3: Statistical hypothesis analysis result.

Binder ID	T_0	DF, ϑ	$t_{\frac{\sigma}{2},\vartheta}$ (From standard T- table)	p- value	Rejection criteria: $ t_0 > t_{\frac{\sigma}{2},\vartheta}$, $p < 0.05$	Comments
Binder + 3% SBS (Day 1 & 2)	-1.513	18	2.101	0.148	$1.513 < 2.101$ $0.148 > 0.05$	Null hypothesis cannot be rejected
Binder + 4% SBS (Day 1 & 2)	-1.333	18	2.101	0.199	$1.333 < 2.101$ $0.199 > 0.05$	Null hypothesis cannot be rejected
Binder + 1% SBS (Batch 1 & 2)	-1.757	58	2.002	0.083	$1.757 < 2.002$ $0.083 > 0.05$	Null hypothesis cannot be rejected
Binder + 4% SBS (Batch 1 & 2)	-0.847	58	2.002	0.400	$0.847 < 2.002$ $0.400 > 0.05$	Null hypothesis cannot be rejected

3.3.7 Linear Regression Analysis Considering Peak Height and Peak Area

The peak absorbance height at 965 cm^{-1} did not vary with different binder grades and sources, SBS polymer sources and structures, and the cross-linking agent. So, the FT-IR spectrum peak at 965 cm^{-1} could be used to develop a model both in peak height and peak area method. **Figure 2-9** represents the correlations among peak height, peak area, and SBS content considering all 1300 data points obtained from 26 cases. From **Figure 3-9(a)** and **Figure 3-9(b)**, it can be observed that peak height showed a slightly higher correlation with SBS content compared to the peak area measurements (**Figure 2-9c** and

Figure 3-9(d). It was also observed that 2% and 4% SBS content included some outlier values in both analysis methods.

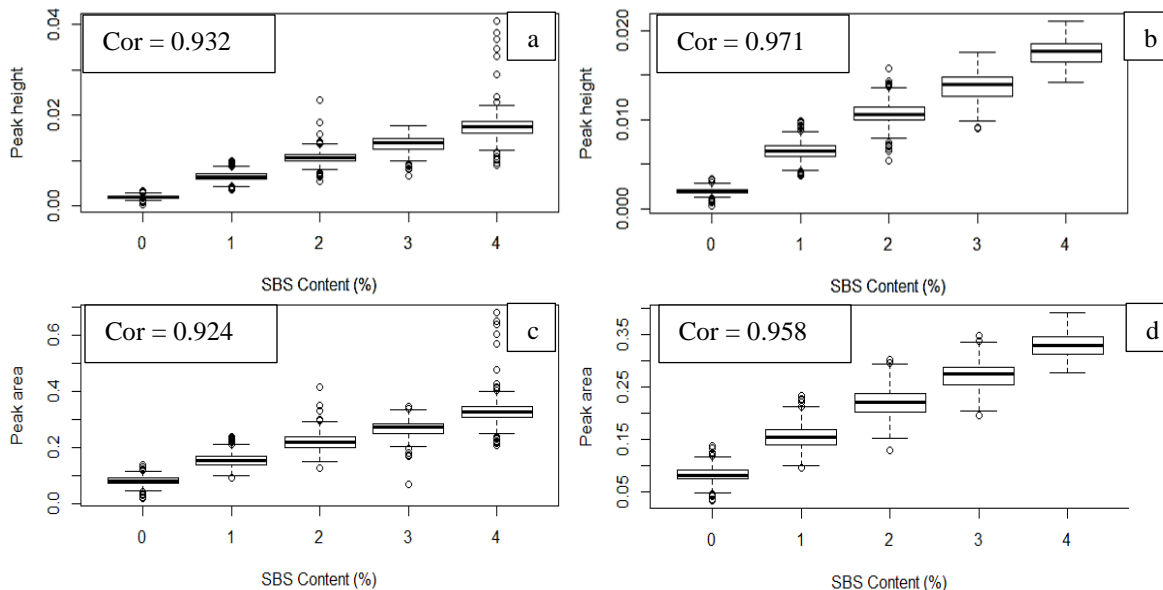


Figure 3-9: Correlation between SBS content and (a) peak height at 965 cm^{-1} with outlier data points, (b) peak height at 965 cm^{-1} without outlier data points, (c) peak area at 965 cm^{-1} with outlier data points, and (d) peak area at 965 cm^{-1} without outlier data points.

Note: W/O = without

In this study, Cook's distance [68] algorithm was applied to remove the outliers. The influential points that negatively affected the regression model [69], [70] were selected when the Cook's distance of an observed value was greater than four times the average Cook's distance. Among 1300 data points, 50 (for peak height), and 44 (for peak area), data points were identified as outliers. After deleting these points, the regression model was built again, and their correlation was observed. It was found that the correlation coefficient increased to 0.971 in the case of peak height measurement. Similarly, in peak area measurement, the correlation coefficient increased to 0.958, as illustrated in **Figure 3-9(b)** and **Figure 3-9(d)**.

The linear regression model found in all the cases are stated below:

With outlier: Peak height at $965\text{ cm}^{-1} = 0.00383*\text{SBS content}+0.002403$ **Eq. 2-1**

Without outlier: Peak height at $965\text{ cm}^{-1} = 0.00386*\text{SBS content}+0.002373$ **Eq. 2-2**

With outlier: Peak area at $965\text{ cm}^{-1} = 0.06084*\text{SBS content}+0.090338$ **Eq. 2-3**

Without outlier: Peak area at $965\text{ cm}^{-1} = 0.06061*\text{SBS content}+0.089474$ **Eq. 2-4**

From the models, the coefficients of the regression models did not change significantly after removing the outlier data points. However, the correlation coefficient improved significantly. **Table 3-4** represents the statistical analysis of all the models. Higher F-statics and lower p-value (< 0.05) were found from the statistical analysis of the regression models.

Table 3-4: Statistical analysis of peak height or peak area vs. SBS content at 965 cm^{-1} .

Statistical parameters	Peak height	Peak height (W/O Outlier)	Peak area	Peak area (W/O Outlier)
t-value	91.83	140.88	86.24	116.55
F-statics	8433	19850	7437	13580
p-value	$< 2.2\text{e-}16$	$< 2.2\text{e-}16$	$< 2.2\text{e-}16$	$< 2.2\text{e-}16$
Upper 95% CI	0.939	0.974	0.916	0.953
Lower 95% CI	0.925	0.967	0.932	0.962
Correlation	0.932	0.971	0.924	0.958
Multiple R-squared	0.869	0.942	0.854	0.917
Adjusted R-squared	0.869	0.942	0.854	0.917
Residual standard error	0.0021	0.0013	0.0356	0.0255

These values also indicate that the prediction from these models will not be interpreted as coincidental events. Since the correlation coefficient between peak height and SBS content was higher, the final linear regression model was selected based on the peak height measurement without outlier data points.

3.3.8 Prediction of SBS Content in Laboratory Prepared Binders

A total of eight laboratory prepared SBS modified asphalt binders were used to predict the SBS content by four different operators using the regression model 2 (**Eq. 2-2**)

developed in the preceding section. The operators were not informed about the actual content of SBS before predicting the result. **Table 3-5** shows the prediction result of the laboratory prepared binders. Among these eight binders, binders 1 and 2 were used to develop the regression model, whereas the remaining ones were not used in the regression analysis. Four different operators carried out the measurements to ensure repeatability and reproducibility in predicting SBS content. Here, the predicted SBS percentages were reported to the nearest 0.1%. Besides, standard deviation (SD), coefficient of variation (CV), and 95% CI (confidence interval) were calculated. The differences between observed and predicted values in all eight measurements were found in the range of 0%-6%, which indicated the model's high accuracy in predicting SBS content.

Table 3-5: SBS content prediction of the laboratory-prepared binders.

Sample ID	Sample used in regression analysis	Operator	Avg. height	Predicted SBS (%)	SD	CV	CI	Actual SBS (%)	% error
1	Yes	A	0.018	4.1	0.002	4.745	0.0014	4.0	2.50
2	Yes	B	0.014	3.0	0.001	3.856	0.0008	3.0	0.00
3	No	A	0.017	3.8	0.003	7.814	0.0022	4.0	5.00
4	No	A	0.017	3.9	0.001	1.940	0.0006	4.0	2.50
5	No	B	0.015	3.3	0.003	8.802	0.0021	3.5	5.71
6	No	C	0.010	2.0	0.001	9.278	0.0010	2.0	0.00
7	No	D	0.018	4.0	0.001	5.454	0.0010	4.0	0.00
8	No	C	0.010	2.0	0.001	5.481	0.0004	2.0	0.00

3.3.9 Model Implementation on Plant Modified Binders

We visited one plant to understand the feasibility of the prediction model in the practical field. Four different SBS modified asphalt binders were collected from the plant and tested using the handheld FT-IR spectrometer. In each case of the binders, ten samples were collected. The average peak height was measured after collecting the spectrum. The maximum allowable CV was 10% to avoid the variation in measurement caused by non-

homogeneous polymer phase distribution in the asphalt binder [46]. Then the binders' SBS content was predicted using model 2 (**Eq. 2-2**), without any calibration curve.

Table 3-6 represents the prediction results of the SBS modified asphalt binders. For case 1, the binder was SBS modified PG 76-22. Since the actual percentage of SBS was unknown in this case due to supplier trade guidelines, a range for predicted SBS content was reported. On the other hand, for cases 2, 3, and 4, the manufacturer specified the SBS content range. Results showed that predicted SBS content falls within the specified range mentioned by the manufacturer.

Table 3-6: Field trial results of SBS quantification model.

Plant binder	Avg. peak height	SD	CV (%)	CI	95%CI Upper	95%CI Lower	Predicted SBS (%)	Actual SBS (%)
1	0.007	0.001	5.10	0.0420	1.1	1.1	1.1	unknown
2	0.015	0.0015	9.95	0.0010	3.2	3.2	3.2	> 3
3	0.011	0.002	9.00	0.0014	2.2	2.2	2.2	1-3
4	0.010	0.001	7.10	0.0011	2.1	2.1	2.1	1.5-3

3.3.10 Model Validation from Refinery Supplied SBS Modified Binders

In field trials, the actual amount of SBS contents were provided in a range rather than a specific percentage value (**Table 3-7**). Therefore, further validation of the model was performed using the refinery supplied SBS modified binders. SBS content was predicted from four different refinery binders with unknown SBS content. The SBS content of the binders was predicted using model 2 (**Eq. 2-2**) without any calibration curve.

All four binders were supplied from the refinery, and data collection was performed in the laboratory. For all four binders, ten samples were collected in each case. **Table 3-7** shows the results obtained from the refinery binders. For refinery binders 1, 2, 3, and 4

predicted SBS content was 2.1%, 2.1%, 4.8%, and 1.8%. The predicted results were reported to the refinery and verified with the actual content where the actual SBS content was 2%, 2%, 5%, and 2%, respectively. The percentage error in prediction was 4-10% with respect to the actual value. All predicted results of the refinery binders were reported to the nearest 0.1%. The CI of all the measurements did not vary that much, which indicated the measurement's prediction accuracy.

Table 3-7: Validation of the prediction model with refinery supplied binders.

Refinery	Binder	Avg. peak height	SD	CV	CI	Predicted SBS (%)	Actual SBS (%)	% Error
1	1	0.011	0.0003	2.60	0.0002	2.1	2%	5%
	2	0.011	0.0006	2.80	0.0004	2.1	2%	5%
2	1	0.021	0.0008	3.89	0.0006	4.8	5%	4%
	2	0.009	0.0003	3.01	0.0002	1.8	2%	10%

3.4 Conclusion

This study's principal goal was to understand the effect of variation in PG binders, SBS polymers, and the addition of cross-linking agent on the peak absorbance height at 965 cm^{-1} . A prediction model was developed by the linear regression analysis after observing the negligible effect of the factors mentioned earlier. The model can be used to predict the SBS content in SBS modified asphalt binder with unknown SBS content. The main findings from this study are stated below:

- The qualitative analysis showed that SBS addition in the asphalt binder incorporated two additional functional groups at 965 cm^{-1} accountable for polybutadiene (PB) block and at 699 cm^{-1} named as the polystyrene block.

However, the difference in SBS polymer structure (linear, radial, and diblock) and the cross-linking agent (sulfur) did not add any new functional group to the asphalt binder.

- The peak shape and position at 965 cm^{-1} were unaffected by the variation in PG binders and binder sources, SBS polymer sources and structures, and the cross-linking agent's presence.
- The regression model developed in this study was based on the relation between peak height measurement and SBS content with $R^2 = 0.942$. The peak height was highly correlated to the SBS content with a correlation value of 0.971.
- The whole process for SBS content prediction required 30 minutes in the *in-situ* condition using the handheld FT-IR spectrometer.
- The percentage error was ranged from 0-6% for predicting SBS content in the case of laboratory prepared binders.
- The prediction results of the refinery-supplied binders were justified by the supplier. The percentage error of the predicted SBS content ranged from 4-10%.

CHAPTER 4

SBS CONTENT DETERMINATION BY EVALUATING POLYSTYRENE FUNCTIONAL GROUP

4.1 Introduction

SBS polymer is the most widely used polymer in asphalt binder modification. It is a thermoplastic block copolymer, which is composed of polystyrene (PS) outer blocks and a polybutadiene (PB) inner block. PS is a glassy material that acts as a cross-linker for the elastomeric network and imparts strength. On the other hand, PB is a rubbery material that provides an elastic property. The addition of SBS in the asphalt binder significantly changes the binder's properties. SBS modified asphalt binder reduces rutting and increases the cracking resistance of the asphalt pavement [71].

However, phase separation and thermal decomposition can lead to poor rutting performance at high temperature and poor cracking resistance at low temperature [72]. The phase separation occurs during the transportation or storage of the SBS modified asphalt binder. In addition, thermal degradation can take place due to the long-term high temperature during storage, construction, and pavement usage [73]. Therefore, it is required to quantify SBS polymer in the SBS modified asphalt binder before and during the construction for quality assurance purposes.

SBS modified asphalt binder is mainly obtained from factory manufacturing [74]. However, the manufacturer does not mention the SBS content due to propriety issues. On the other hand, binders' performance grade (PG) can be obtained using other polymers or additives along with SBS polymer, which helps the manufacturer to profit more [39]. For these reasons, it is crucial to determine the SBS content for quality control in the field by a quick, simple, accurate, precise, and universal method.

Several researchers [40], [41], [44], [75], [76] studied the quantification technique of SBS polymer in modified asphalt binder using different methods for the last few decades. Among these techniques, the FT-IR spectrometer method showed the highest accuracy in predicting SBS content in the laboratory prepared SBS modified binders [47]–[49], [77]–[79]. AASHTO published a standard in 2005 to quantify SBS polymer in the SBS modified asphalt binder (AASHTO T302-15).

Later, Diefenderfer [41] followed the AASHTO standard to quantify SBS polymer using different SBS modified high PG binders. No correlation was found between the binder grading and the polymer content in that study. It was found that the same PG binder can have different polymer content because the final PG binder is dependent on the base PG binder. Also, the same base binder collected from the different suppliers can give a different result, which was not studied. In the report of the Strategic Highway Research Program (SHRP) [76], we followed the AASHTO standard for the identification and quantification of SBS polymer in SBS modified different types of PG binders. Calibration curves were plotted for different types of SBS polymers and binders, considering the PB and PS functional groups.

A detailed and comprehensive study was performed by Lu and Guo [50] using partial least square (PLS), principal component regression (PCR), stepwise multiple linear regression (SMLR) analysis. No significant advantages were obtained from these complicated regression analyses compared to the simple linear regression analysis. Also, the prediction error of the SBS content of a modified binder that contains more than 5% SBS might be unacceptable if calibration curves are used. Again, increased test replicates can reduce this error.

Table 4-1 represents the previous studies on SBS quantification in SBS modified asphalt binder. All these studies have one thing in common and that is the determination of SBS polymer requires calibration curves for all individual SBS polymer, PG binder, additives, and cross-linking agents. However, developing a calibration curve in the field is not feasible because the manufacturer does not always provide the same SBS polymer, which was used for the modification. Even if they do, it is a time-consuming process to build a calibration curve.

To this end, this study was initiated to address the issue related to quality control by developing a universal model for determining the SBS content in any SBS modified asphalt binder. Another model was developed following the AASHTO T302 standard to compare with the newly developed universal model. These models were developed considering all the variabilities such as different PG binders from different sources, different types of SBS polymer from different sources, and a cross-linking agent (sulfur). Therefore, no calibration curves were required to quantify the SBS content of the refinery or plant modified asphalt binders.

4.1.1 Objectives

The main objective of this study was to develop a universal model that can be used to quantify SBS content in the SBS modified asphalt binder without any calibration, standard, or reference curve. The specific objectives were to

- Develop PS and PB model from the linear regression analysis considering different PG binders from different sources, different SBS polymers from different sources, and the presence of a cross-linking agent (sulfur).
- Compare the models based on the predicted, and actual SBS content of the refinery supplied binders,
- Validate the models from the refinery supplied binders, and
- Verify the predicted results from the statistical analysis.

4.2 **Materials and Methods**

4.2.1 Materials

Three PG binders (PG 52-34, PG 58-28, and PG 64-22) were used in this study. These binders were supplied from three different sources (Sources 1, 2 & 3). Two types (triblock and diblock) of SBS polymers were used to modify the PG binders. Both linear and radial triblock molecular configurations were utilized to understand their morphological difference [56]. These SBS polymers were collected from two different sources (Source A and Source B). A reagent grade 100 mesh particle size sulfur was used as a cross-linking agent to modify the PG binders.

Table 4-1: Previous studies on the quantification of SBS in Asphalt Binder.

Authors	Wavenumber (cm ⁻¹)	Type of Analysis	Type of SBS/Binder	Observation	Study on Refinery/Plant Binder
Masson et al., [48]	699, 966	-	Linear, branched, star	Calibration curves at 699 and 966	No
Ye et al. [67]	700, 966	Absorbance peak and area	Linear, branched	Calibration curve at 966/1375	No
Wang et al., [80]	965, 1375	Ratios of Absorbance peak and area	PG 76-22 binder	Calibration curve at 965/1375	No
Wang et al., [81]	910, 966	Spectral band	-	Calibration curve	No
Hu et al., [52]	966	Peak area ratio	Linear, branched	Calibration curve at 966	No
Sun et al., [51]	700, 966	Absorbance ratio	-	Calibration curve at 966/810	No
Luo et al., [39]	966	Peak area ratio	Linear	Calibration curve at 966/813	No

4.2.2 Experimental Plan

Figure 4-1 represents the experimental plan, which was used in this study. Data collection was performed for different Batches and different Days for twenty-five cases total. Batch indicates the SBS modified binders, which were prepared following the same procedure for the second time. Days indicates the repeatability in data collection for different days from the same Batch of binders. In each case, a total of fifty FT-IR spectrometer data were collected. In this way, data was collected for a total of 1250 times to develop the universal model.

4.2.3 Principle of FT-IR Spectroscopy

The principle of FT-IR spectroscopy involves passing an infrared beam through the material and identifying their molecular structure based on their rotational and vibrational frequency [59]. The chemical bonds in a material absorb the infrared beam in a specific wavenumber and are displayed as an absorbance spectrum in FT-IR spectroscopy. In most cases, the FT-IR spectrometer reported a spectrum in 400 cm⁻¹-4000 cm⁻¹ region where 600

cm^{-1} - 1500 cm^{-1} is known as the fingerprint region due to the presence of complex functional groups which differs from sample to sample [60]. After analyzing the absorbance spectrum, chemical functional groups of a material can be identified and quantified. In this study, a 4300 handheld FT-IR spectrometer with a diamond attenuated total reflectance (ATR) sensor was used for the spectra collection.

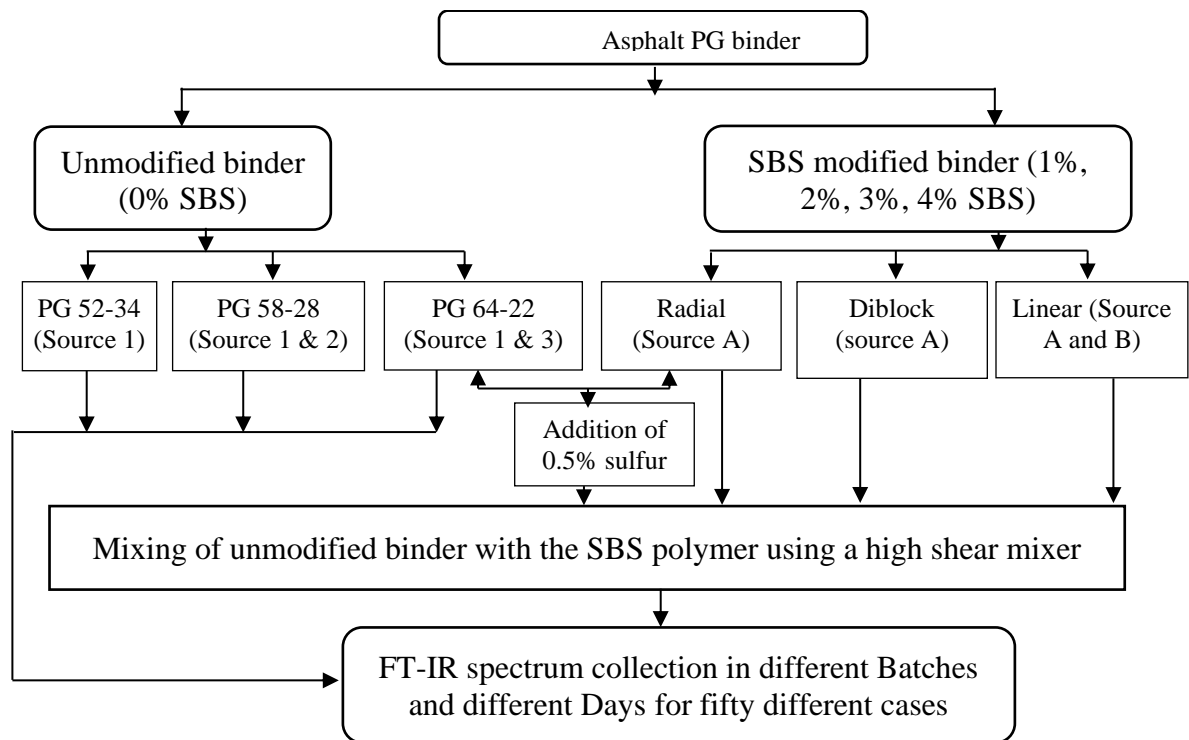


Figure 4-1: Materials and experimental plan.

4.2.4 Preparation of SBS Modified Asphalt Binder in the Laboratory

SBS polymer was mixed with asphalt binder in the laboratory by the following steps:

- At first, around 600 gm of asphalt binder was taken in a quart can from the supplier's bucket. We heated the quart can at 170°C to melt the asphalt properly. In

the meantime, the high shear mixer and melting pot were being prepared for mixing SBS with the binder.

- After 1.5 hours of heating, the quart can was moved into the melting pot to adjust the heating of the melting pot (**Figure 4-2a**). The melting pot with the quart can was heated for another 30 minutes before starting the high shear mixer.
- The speed of the high shear mixer was fixed at 5000 rpm at the beginning and SBS was mixed little by little within the first 30 minutes (**Figure 4-2b**).
- After every 30 minutes, the speed was increased to 8000 rpm for 2 minutes to mix SBS polymer uniformly with the binder. Otherwise, a little bit of SBS polymer remained floating on the surface of the binder. The total time of mixing was 2.5 hours including the speed increment (**Figure 4-2c**).
- When speed was increased to 8000 rpm, temperature also increased [1]. The increment in speed was monitored carefully so that the temperature cannot be more than 180°C.
- In the case of a cross-linking agent, (sulfur) addition in the SBS modified asphalt binder, all the sulfur was added after 1.5 hours of mixing.

All other steps were followed as before.

4.2.5 Data Collection from Laboratory Prepared Binders

Immediately after 2.5 hours of mixing, the binder was collected using a spatula for FT-IR spectrometer data collection (**Figure 4-2d**). After collecting, the binder was directly placed over the diamond ATR sensor before it cooled down (**Figure 4-2e**). The connection between the sample and the sensor was ensured. If the binder cooled down before being

placed over the sensor, the crystal might not be covered perfectly, and the spectrum of the sample could be incorrect.

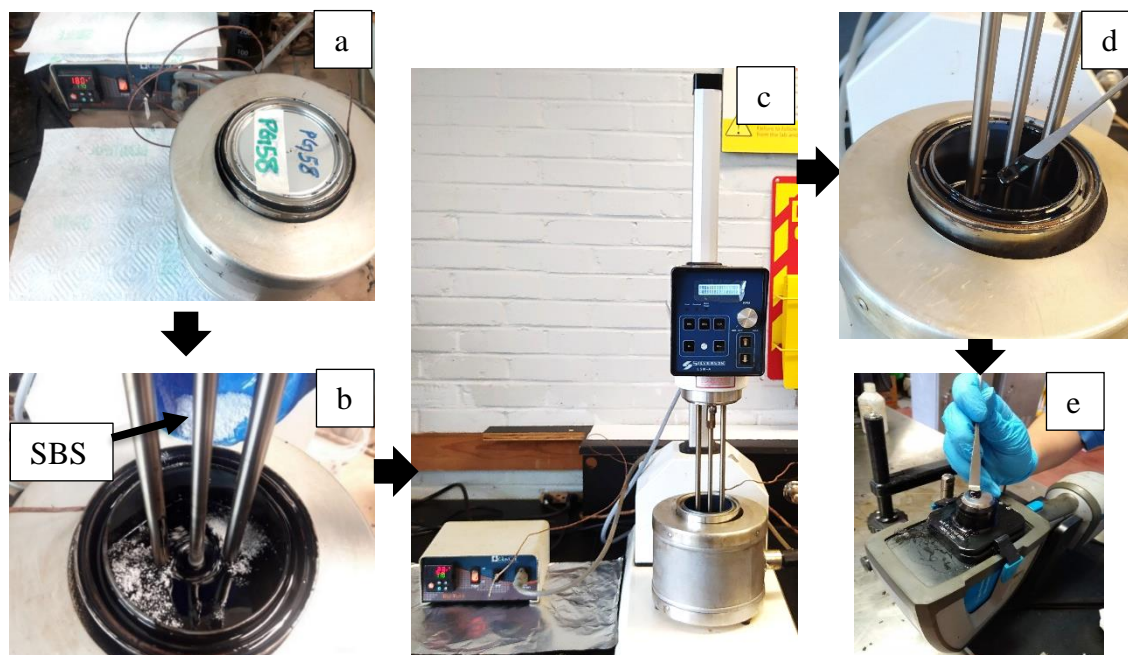


Figure 4-2: (a) Heating binder can inside a melting pot, (b) Adding powdered SBS in the liquid asphalt binder, (c) Mixing of SBS using high shear mixer for 2.5 hours, (d) Collecting sample with a spatula for FT-IR spectroscopy, and (e) Placing sample on the diamond ATR sensor of the handheld FT-IR spectrometer.

Mixing continued with the high shear mixer until the binder collections for 10 times were finished. Each spectrum collected by the FT-IR spectrometer was converted to absorbance spectra by the default Microlab PC software provided with the instrument. A total of 24 scans for each sample was conducted in $650\text{-}4000\text{ cm}^{-1}$ region and reported in the form of 4 cm^{-1} resolution. Before each scan, the background spectra were collected to check if the sensor was properly clean. In the case of repeatability, the high shear mixer was used for mixing the modified binder again for 30 minutes at the speed of 5000 rpm. After 15 minutes, speed was increased to 8000 rpm for two minutes. When 30 minutes of remixing was done, sample was collected using the spatula. The high shear mixer was used

for remixing continually until all the data collection was performed. The temperature was kept at 170°C throughout the data collection.

4.2.6 FT-IR Spectrometer Data collection form Refinery Supplied Binders

In this study, eleven SBS modified asphalt binders total were supplied from three different refineries with unknown SBS content. At first, the binders were kept in the forced draft oven at 170°C for 2.5 hours. Then the binder was placed over the hot plate at a temperature of 170°C. The temperature of the hot plate maintained at 170°C throughout the data collection period by constantly checking with a digital thermometer. A small amount of the binder was collected from the binder can using a spatula and directly placed over the diamond ATR sensor (**Figure 4-2e**). Then the FT-IR spectrum was collected by following the above-mentioned procedure.

4.2.7 Spectral Analysis

According to Beer's law, the absorbance intensity in terms of peak height or peak area is directly proportional to the content [60]. In this study, the absorbance intensity of the characteristic functional group of PB and PS was quantified by the peak absorbance area and height method, respectively, to find the appropriate one which would provide repeatable measurements. These methods were selected considering their ability to eliminate noise and baseline shift effects [82]. The peak absorbance area was calculated by the trapezoidal rule method within the selected baseline. For the peak height measurement, at first, the height of the functional group was determined by drawing a baseline considering the two lowest points on either side of the characteristic functional group. After that, the baseline and top point of the peak was added to determine the peak height as shown in **Figure 4-3**.

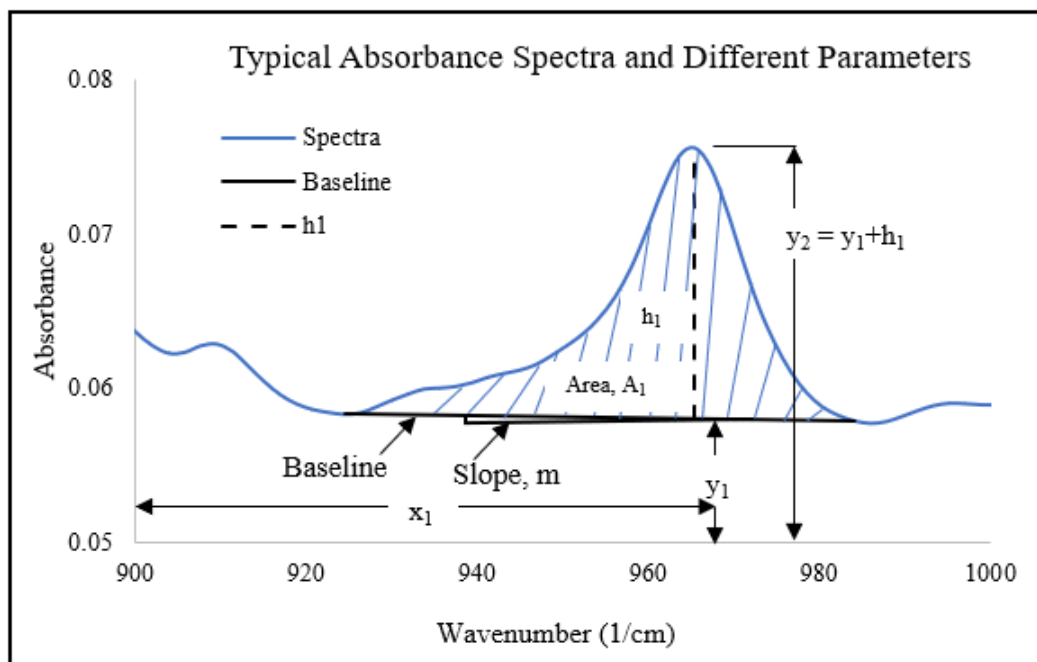


Figure 4-3: Measurement of peak absorbance area and peak absorbance height.

The procedure for the peak area and peak height measurement was automated using a computational code in the MATLAB environment. Peak area and peak height values were analyzed in terms of standard deviation (SD) and coefficient of variation (CV) to visualize the effect of SBS polymer structures and sources, different PG binder and binder sources, and presence of the cross-linking agent. Regression analysis for peak area and peak height was performed to visualize the relationship between the absorbance intensity and the content of the modifier. Outlier analysis was performed using the cook's distance [68]. After eliminating the outlier values, a regression analysis was performed again in both cases. The PB and PS models with all the values and without outlier values were used to predict the SBS content of the refinery supplied binders. The final model was selected based on the best correlation between the actual and predicted SBS content. All statistical analysis was performed in RStudio programming language.

4.3 Results and Discussion

4.3.1 Qualitative Analysis of FT-IR Spectrum

This analysis was done by overlapping both spectra and categorizing the inclusion of any unknown functional group in the fingerprint region of $650\text{-}1800\text{ cm}^{-1}$. The key functional groups in the unmodified asphalt binder are bending vibration of C=C at 1600 cm^{-1} , asymmetric bending of CH₂ and CH₃ at 1455 cm^{-1} , symmetric bending of CH₃ at 1375 cm^{-1} , stretching vibration of S=O at 1034 cm^{-1} , out-of-plane deformation of CH at 870 cm^{-1} , 817 cm^{-1} , 745 cm^{-1} , and aromatic ring vibration of CH at 721 cm^{-1} . These functional groups were persistent in all the unmodified base binders used in this study. From this observation, it can be inferred that the functional groups in the FT-IR spectra of all the unmodified base binders remained identical even though their performance grade (PG) was different.

However, when the base binders were modified with SBS copolymers, two additional functional groups were added (a) out-of-plane (wagging) vibrations of the CH groups at 965 cm^{-1} , which was accountable for PB block, and (b) out-of-plane bending of the CH groups in the aromatic ring at 699 cm^{-1} for PS block as shown in **Figure 4-4** [61]. No additional functional groups were added due to the difference in SBS polymer structure and the presence of sulfur as a cross-linking agent. Besides, peak positions and peak shapes of these functional groups were also unaffected by these above-mentioned changes in the material. In this study, PB and PS functional groups were considered for developing the first-order linear curves from the laboratory prepared binders and quantifying the SBS content in the refinery-supplied binders.

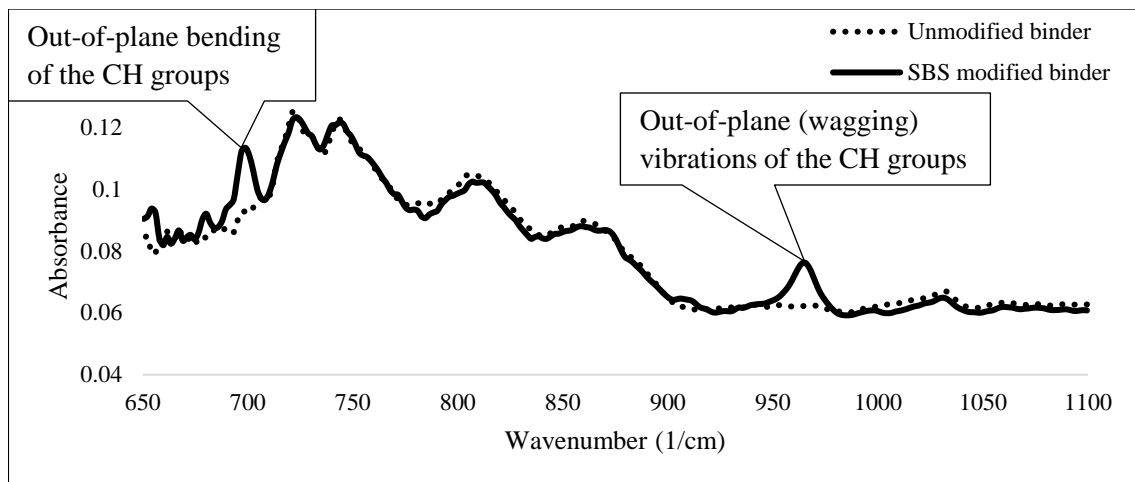


Figure 4-4: Typical FT-IR spectrum of unmodified and SBS modified binder.

4.3.2 Quantitative Analysis for Linear Regression

In this study, fifty curves were developed in consideration of two-analysis methods, PB peak area and PS peak height, considering all contributing factors such as the difference in SBS polymer structure and sources, presence of sulfur as a cross-linking agent, and different PG binders from different sources. **Figures 4-5(a)** and **4-5(b)** showed the increasing pattern in absorbance intensity of the FT-IR spectra at wavenumber 965 cm^{-1} and 699 cm^{-1} due to the addition of a different percentage of SBS in asphalt binder.

For the PB model, peak area measurement was performed for linear regression analysis according to the AASHTO standard. The area of the valley was measured under the peak at the wavenumber 965 cm^{-1} and between the baselines. The baseline was drawn at the two lowermost points of the valley under the peak at wavenumber 965 cm^{-1} .

For the PS model, peak height measurement was performed for linear regression analysis. The height of the PS block was measured between the baseline and the peak at wavenumber 699 cm^{-1} . The baseline was drawn at the two lowermost points of the valley under the peak at wavenumber 699 cm^{-1} . Using these two analysis methods, absorbance

peak areas and peak heights of the PB and PS functional groups was measured at wavenumber 965 cm^{-1} and 699 cm^{-1} , respectively, for different percentage of SBS (0%, 1%, 2%, 3%, and 4%).

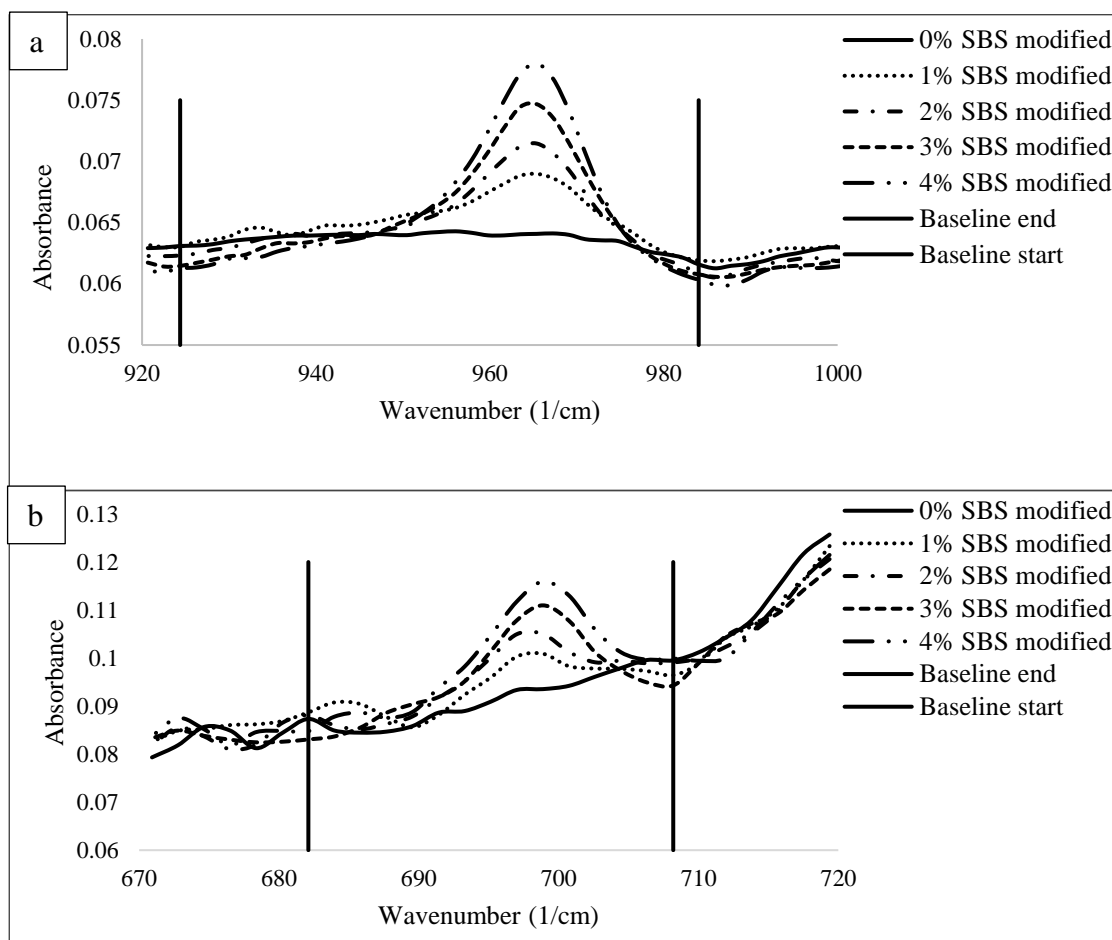


Figure 4-5: Effect of SBS content (%) on (a) wavenumber 965 cm^{-1} and (b) wavenumber 699 cm^{-1} .

4.3.3 Peak Absorbance Area and Height Analysis

The peak absorbance height and area were obtained from the built-in function of the MATLAB numerical computing environment for both PB and PS functional groups at 965 cm^{-1} and 699 cm^{-1} respectively. **Figure 3-6** represents the relation between SBS content, peak absorbance height, and peak absorbance area considering the different

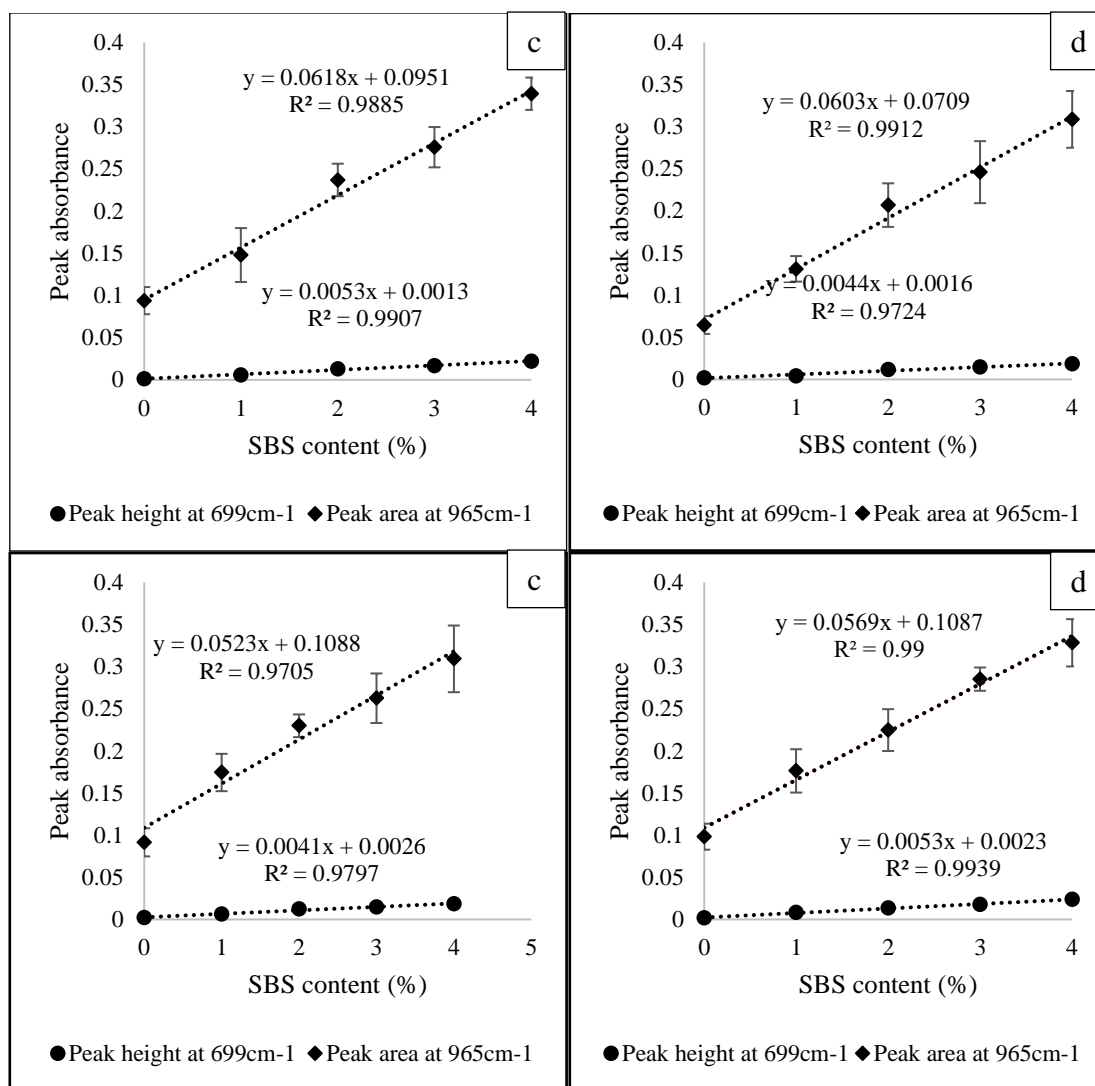


Figure 4-6: Relationship between peak absorbance height and area at the wavenumber 699 cm^{-1} and 965 cm^{-1} , and SBS content (%) considering (a) SBS modified PG 64-22, (b) SBS modified PG 52-34, (c) SBS modified PG 58-28, and (d) addition of sulfur in SBS modified PG 64-22 binder.

binders (linear SBS modified binder), and the addition of crosslinking agent (sulfur). It can be observed that in all the cases, both the peak absorbance area and peak absorbance height of the PB and PS functional groups, respectively, have a good relationship with the SBS content. All the R^2 value was more than 0.97. Therefore, the peak absorbance area and peak absorbance height of the PB and PS functional groups, respectively, can be used to develop the regression models for predicting SBS content.

4.3.4 Developments of the Model

Since the quantitative measurement of PB and PS peak absorbance areas and peak absorbance heights were not affected by the mentioned factors and were only governed by the SBS content, correlation (Corr.) among these three variables was determined. Figure 4-7 shows the correlation among these three variables considering 1250 data points obtained from twenty-five cases for peak area and peak height measurement individually. From Figures 4-7(a) and 4-7(c), it can be observed that peak area data points of the PB model showed a slightly greater correlation (0.918) with SBS content compared to the peak height data points of the PS model (0.892). It was also observed that 2% and 4% SBS data points contained some outlier values in both analysis methods.

To remove the outliers, Cook's distance [68] algorithm was applied. In this study, influential points which negatively affected the regression model [69], [70] were selected when the Cook's distance of an observed value was greater than four times of the average Cook's distance. Among 1250 data points, 50 and 56 data points were identified as influential points for the PB and PS regression model, respectively. After deleting these points, the regression model was built again, and their correlation was observed. It was found that correlation among the variables increased significantly, which is illustrated in **Figures 4-7(b) and 4-7(d)**. For the PB model, the peak height data point's correlation increased to 0.954, where for the PS model and peak height measurement correlation increased to 0.965.

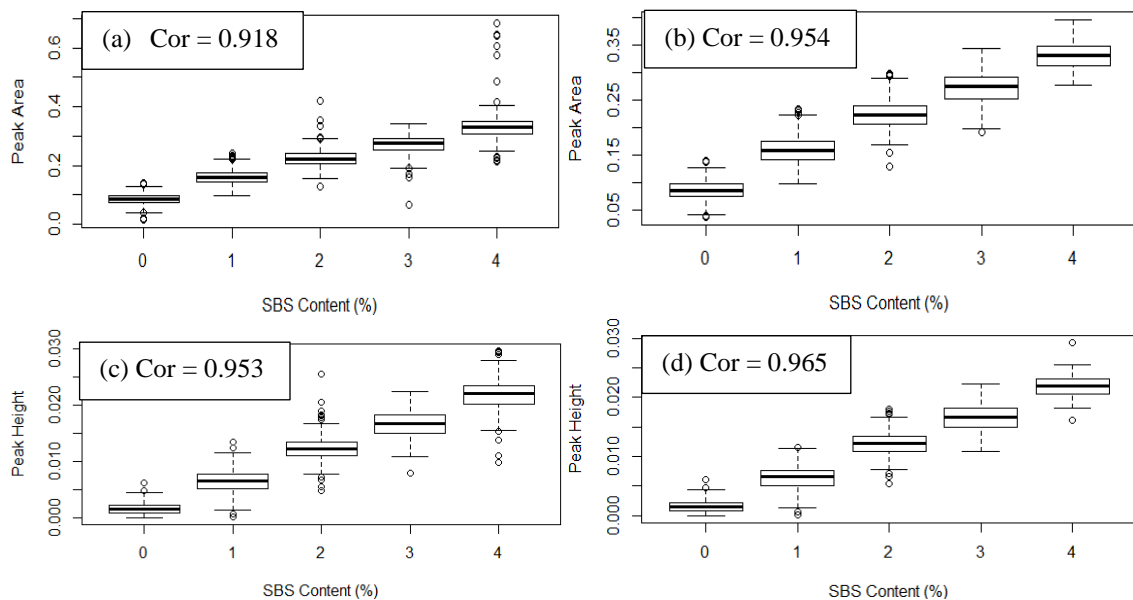


Figure 4-7: Correlation among SBS content (%) and (a) peak area at 965 cm^{-1} with all the data points, (b) peak area at 965 cm^{-1} without outlier data points, (c) peak height at 699 cm^{-1} with all the data points, and (d) peak height at 699 cm^{-1} without outlier data points.

The regression equation found in all the cases stated below:

- PB model-1: $\text{SBS content (\%)} = 16.6197 \cdot \text{peak area} - 1.57969$
- PB model-2: $\text{SBS content (\%)} = 16.7160 \cdot \text{peak area} - 1.59455$
- PS model-1: $\text{SBS content (\%)} = 198.3733 \cdot \text{peak height} - 0.32216$
- PS model-2: $\text{SBS content (\%)} = 196.8117 \cdot \text{peak height} - 0.30526$

4.3.5 Accuracy of the Models

Table 4-2 shows the parameters of the regression models considering all data and without outlier data points. By comparing other parameters obtained from the developed regression models, it can be observed that the t-value increased when the outlier data points were deleted, thus directing to the improvement of the regression model. P-value was the same in all the cases, lower than 2×10^{-16} , which indicated that the estimations of the

coefficients were significant. After that, the accuracy of both models was compared based on RSE (residual standard error), multiple R^2 , adjusted R^2 , and F-statistics.

Here, the RSE value reduced in both models, which indicated that the regression model developed without an outlier was more fitted, and thus provided less of a prediction error compared to the model developed with the outlier data points. Both multiple R^2 and adjusted R^2 increased, directing to the fact that the regression model developed without the outlier can explain more variations in the outcome. Besides, higher F-statics and lower p-value (< 0.05) were also observed in the regression model developed without outlier represented that the developed model is a highly significant prediction model, and the prediction from this model will not be interpreted as a coincidental event. Here, 0.05 represented the significance level for a 95% confidence interval (CI).

Table 4-2: Statistical analysis of SBS content and peak height at 965 cm^{-1} and 699 cm^{-1} .

Statistical parameters	PB model-1	PB model-2	PS model-1	PS model-2
t-value	81.15	109.45	110.38	127.26
p-value	$< 2.2\text{e-}16$	$< 2.2\text{e-}16$	$< 2.2\text{e-}16$	$< 2.2\text{e-}16$
95% lower CI	0.909	0.947	0.947	0.961
95% upper CI	0.927	0.959	0.958	0.969
RSE	0.0367	0.02629	0.002274	0.00191
Multiple R^2	0.8434	0.9102	0.908	0.932
Adjusted R^2	0.8432	0.9101	0.908	0.932
F-statistics	6585	11980	12180	16190

4.3.6 Application in Refinery Supplied Binders

The developed PB and PS models from the linear regression analysis with all the data points and without the outlier points were used to predict the SBS content in the refinery supplied binders. The validity of a predictive model depends on the relationship between the actual and the predicted value. In this study, refinery supplied binders were

used to select the final model, which would validate the model as universal. **Table 4-3** represents the actual and the predicted values of the eleven refinery supplied binders. It was observed that the PS models predicted the SBS content better than the PB models.

Table 4-3: Actual and predicted SBS content (%) of the refinery supplied binders.

Refinery	Sample ID	Actual (%)	PB model-1	% Avg. dev.	PB model-2	% Avg. dev.	PS model-1	% Avg. dev.	PS model-2	% Avg. dev.
Refinery 1	A	1	0.1	50.8	0.1	50.3	0.8	4.8	0.8	5.8
	B	2	1.3		1.3		1.9		2.0	
	C	5	4.1		4.1		4.9		5.1	
	D	2.3	0.0		0.0		2.3		2.3	
	E	1.8	0.0		0.0		1.8		1.8	
	F	5.75	0.3		0.3		6.1		6.3	
Refinery 2	G	2	1.7	1.7	2.0	2.0				
	H	2	1.2	1.2	1.9	1.9				
Refinery 3	I	2.1	1.5	1.5	2.1	2.2				
	J	2.86	2.7	2.7	3.3	3.4				
	K	3.1	2.1	2.3	3.1	3.2				

Note: % Avg. dev. = percent average deviation

4.3.7 Selection of the Final Model

For selecting the final model, the predicted SBS content from all the models were plotted against the actual SBS content, as shown in **Figure 4-8**. The R^2 value was found 0.1642, 0.1665, 0.9876, and 0.9873 from the predicted SBS content using the PB model-1, PB model-2, PS model-1, and PS model-2, respectively. A higher R^2 value indicates the better fit of the model. From the R^2 value, it can be concluded that PS model-1 was better than the other three models for predicting the SBS content in the refinery supplied binders. Based on the R^2 value, PS model-1 was selected as the final model in this study.

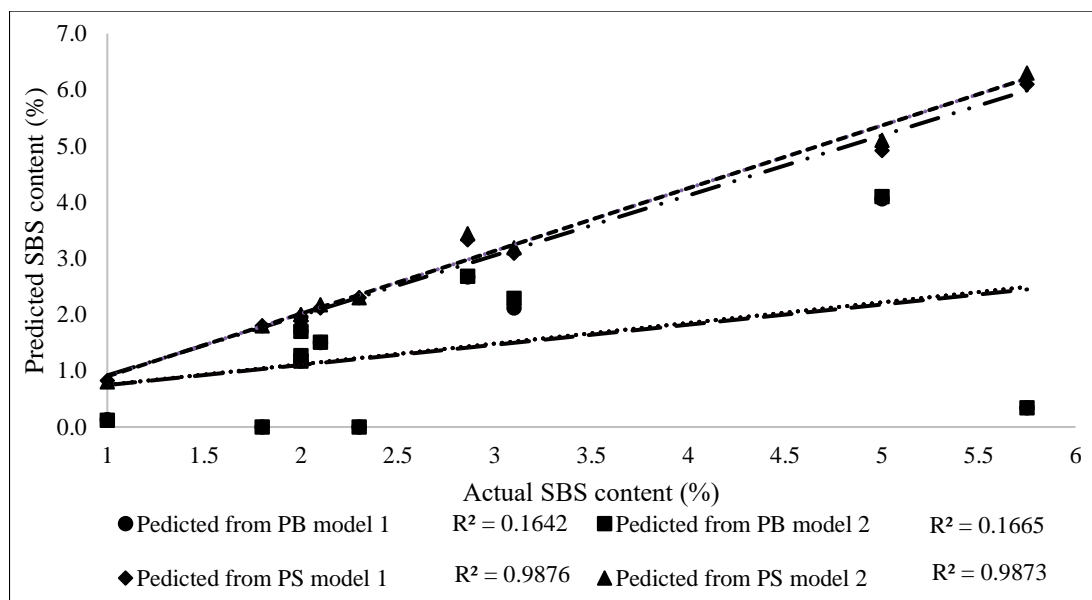


Figure 4-8: Relation between the actual and predicted SBS content considering all the models.

4.3.8 KS-test

The two-sample Kolmogorov-Smirnov (KS) test [83] was performed in this study to compare the distributions of the actual and predicted SBS content. This test measures the maximum difference between the observed and actual cumulative distribution [84]. The null hypothesis (H_0) is that the actual and the predicted values are from the same continuous distribution. The alternative hypothesis (H_a) is that the actual and the predicted values are not from the same continuous distribution.

The hypothesis test was carried out on a 5% significance level. **Table 4-4** represents the KS-test result for all the models. If the D-statistic is small or the p-value is high, then the hypothesis cannot be rejected if the distributions of the two samples are the same. The chance of similarity in distribution between the actual value and the predicted value can be estimated from the p-value. It can be observed from **Table 4-4** that there is a 99.99% chance

of similarity in distribution between the predicted values from the PS model-1 and the actual values.

Table 4-4: KS-test result of all the prediction models.

KS test parameter	Predicted from PB model 1	Predicted from PB model 2	Predicted from PS model 1	Predicted from PS model 2
D-statistic	0.63636	0.63636	0.09091	0.18182
P value	0.02074	0.02074	0.99999	0.99709

4.3.9 Effects of SBS Polymer Sources, Binder Grades and Sources, and Cross-linking Agents

For establishing the universal model, effects due to the differences in SBS polymer sources, binder grades, binder sources and addition of sulfur on the peak absorbance height were studied. **Figure 4-9** represents the effect analysis on peak absorbance height. The differences in peak absorbance height of radial SBS modified asphalt binder without and with sulfur were 3%, 2%, 4%, and 0.6% in the case of 1%, 2% 3%, and 4% SBS modified binders, respectively (**Figure 4-9a**). In the case of 1%, 2%, 3%, and 4% SBS modified PG 52-34 and PG 64-22, differences in peak absorbance height were observed as 5%, 4%, 2%, and 7%, respectively (**Figure 4-9b**). These differences are very low and can be ignored.

Similarly, SBS polymers from two different sources did not affect the peak absorbance height at 965 cm^{-1} as shown in **Figure 4-9(c)**. The same PG binders were collected from two different sources. However, no significant difference was observed in the peak absorbance height (**Figure 4-9d**).

4.3.10 Model Validation with New Laboratory Modified Binders

Laboratory prepared five SBS modified asphalt binders were used to validate the PS model. One operator, X, prepared the binder, and another operator, Y, collected the FT-

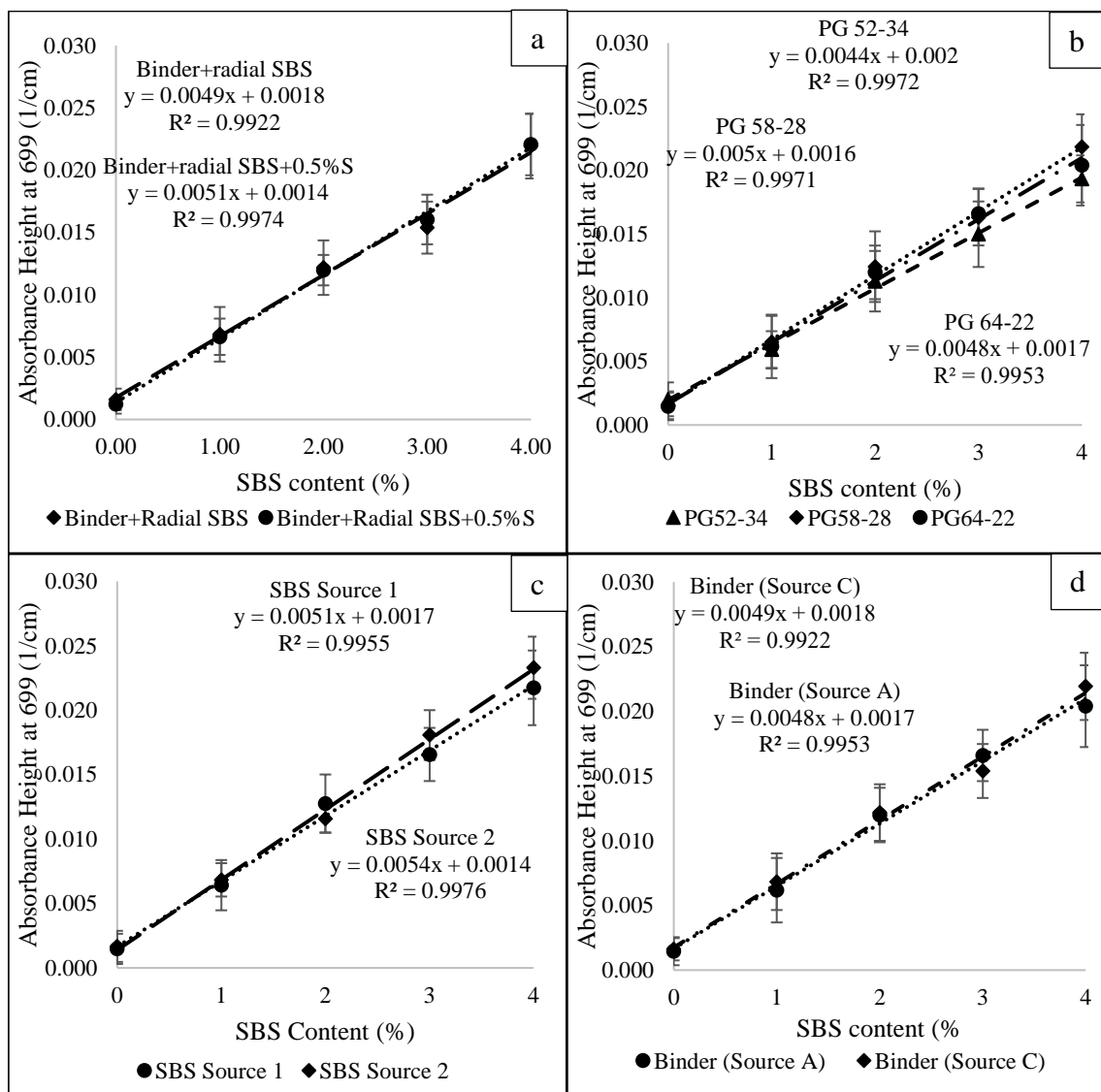


Figure 4-9: Effect on peak absorbance height due to (a) addition of sulfur as a cross-linking agent, (b) difference in base binder, (c) difference in SBS polymer sources, and (d) difference in base binder sources.

FTIR spectra were analyzed and SBS content was predicted. Operator Y remained blind to the actual SBS content until the prediction. **Table 4-5** represents the actual and predicted SBS content of the laboratory prepared SBS modified asphalt binder. The percent average deviation is only 10%, which indicates the PS model can predict the SBS content in the refinery supplied binders as well as in the laboratory prepared binders.

Table 4-5: Actual and predicted SBS content of the laboratory prepared SBS modified binders.

Laboratory prepared sample	Source of SBS	Actual SBS content (%)	PS Model-1	% avg. dev.
Linear SBS modified PG 52-34 binder	A	4	4.0	
Linear SBS modified PG 58-28 binder	B	2	2.2	
Linear SBS modified PG 58-28 binder	A	3	3.3	10
Radial SBS modified PG 64-22 binder	A	2	1.7	
Diblock SBS modified PG 64-22 binder	A	4	3.8	

4.4 Conclusion

This study was performed to develop a universal model for the quantification of SBS polymer in the SBS modified asphalt binder. Using the universal model, unknown SBS content can be determined of any SBS modified asphalt binder from a refinery or plant. Another model was developed following the AASHTO T302 standard. The following conclusions can be drawn from this study:

- From the qualitative analysis, we found that PB and PS were the characteristic functional groups of the SBS polymer. From the quantitative analysis, it was observed that the absorbance peak area at 965cm^{-1} and absorbance peak height at 699 cm^{-1} can be analyzed to find a correlation with the SBS content.
- Three different types of SBS polymer from two different sources were mixed with three different PG binders collected from three different sources. Sulfur was added in the SBS modified asphalt binder as a crosslinking agent. No changes were observed in the characteristic functional groups, or in the linear correlation between the peak absorbance and the SBS content due to these variations.

- PB model was developed following the AASHTO T302 standard, and the PS model was developed from the peak absorbance height measurement. Both models were obtained from the linear regression analysis. Using Cook's algorithm, the outliers were deleted to improve the models statistically.
- Eleven SBS modified asphalt binders were supplied from three different refineries with unknown SBS content. Using the developed models, SBS content in those binders was predicted, and the results were sent to the refinery to verify the actual SBS content. PS model obtained from all the data points showed the best correlation between the actual and predicted SBS content. In addition, the % average deviation was the lowest when the PS model was used.
- KS test was performed on the results obtained from the PB and PS models. The highest p-value and lowest d-statistics were found from the PS model-1. All these analyses indicated that the PS model-1 can predict the SBS content in any SBS modified asphalt binder without any calibration equation. Prediction of SBS content from the laboratory prepared unknown SBS modified binders also proved the same.
- Finally, the handheld FT-IR spectrometer can be implemented as a quality control tool in the field for the quantification of the SBS polymer in the SBS modified asphalt binder.

CHAPTER 5

A NOVEL EXTENSIONAL DEFORMATION TEST FOR EVALUATING SBS DEGRADATION DUE TO AGING OF ASPHALT BINDER*

5.1 Introduction

Due to heavy loads and increased traffic volume, modification of the asphalt binder with different modifiers has become very common to enhance the asphalt's pavement service life. These modifiers include polymers (such as elastomers and plastomers), fillers (such as fly ash and Portland cement), extenders (such as sulfur and lignin), antistrips (such as lime and organo-metallics), antioxidants (such as carbon black and amines), stiffening agents such as (PPA and gilsonite), etc. [85], [86]. Among these modifiers, SBS and PPA are frequently used.

SBS is an elastomeric block copolymer. It has three chains: polystyrene, polybutadiene, and polystyrene. Polystyrene is a hard plastic that gives durability and stiffness, and polybutadiene gives rubbery properties. Polymer and maltenes control the low temperature properties of the SBS modified asphalt binder [10]. At high temperature,

* This chapter or portions thereof has been published previously in the *Transportation Research Record: Journal of Transportation Research Board* under the title "Evaluation of Degradation of SBS Modified Asphalt Binder Because of RTFO, PAV, and UV Aging using a Novel Extensional Deformation Test", Vol. 2673, Issue 6, 2019. The current version has been formatted for this dissertation.

SBS modified asphalt binder shows the highest recovery on the strain with non-recoverable creep compliance [11].

PPA is an inorganic polymer of orthophosphoric acid (H_3PO_4). PPA raises both the saturates and asphaltenes at the expense of the cyclic and resins. As saturates convert into asphaltenes, asphaltenes increase, and the molecular weight (M_w) decreases. PPA affects the dispersed phase and the matrix of the asphalt, and as a result, the two main phases in the asphalt stiffens. As a result, the rutting resistance of the asphalt pavement and the performance grade of the PPA modified asphalt binder increases significantly after PPA modification [20].

PPA is more effective when SBS modified binder is used for PPA modification. Several researchers investigated PPA and SBS modified asphalt binders separately and combined. The results indicated that PPA modification provides better results when it is added with SBS modified asphalt binder. As indicated earlier, PPA increases the creep recovery and the non-recoverable creep compliance. However, the effects of PPA are not significant at low temperatures, and SBS modification helps in this regard [21], [87].

Although SBS polymer improves the asphalt binder quality, SBS degrades due to oxidative aging. Hao *et al.* [16] studied aged SBS modified binders with Gel Permeation Chromatography (GPC) and indicated that the effect of the polymer is reduced due to aging. The peaks of the Gel Permeation Chromatography (GPC) curves increase in height and width, which indicates that M_w decreases, and the number of molecules increases after aging which also indicates the polymer's effect is reduced after aging. The fluorescence micrograph showed almost no SBS copolymer after UV aging, which indicates that the influence of UV aging is obvious on the degradation of SBS polymer [88]. Cortizo *et al.*

[8] performed size exclusion chromatography to investigate the SBS degradation in the modified asphalt binder. Chromatographic profiles of SBS modified asphalt binder have shown that the second average molecular weight of fraction (F_2) decreases, and the elution volume remains stable after aging. The first average molecular weight of fraction (F_1) slightly increases, and the elution volume slightly decreases after aging. The researchers concluded that it is the clear consequence of degradation of the polymer due to oxidation.

Dehouche *et al.* [89] investigated the aging characteristics of SBS modified asphalt binder and observed that aging causes both oxidation and SBS degradation. After aging, the colloidal instability index values increase for both the base binder and the SBS. Aging lowers the aromatics' content and simultaneously increases the resins and asphaltenes' contents, with an insignificant change in the saturate contents. These changes have occurred due to the oxidation of the asphalt binder and chemical reaction between the binder and SBS.

The current Superpave Performance Grade (PG) tests are primarily developed for unmodified binders. Recently introduced ASTM D 7405 Multiple Stress Creep Recovery (MSCR) tests are performed only at high temperatures for high temperature performance grading. Some states follow PG Plus tests to identify and quantify the polymer at intermediate and low temperatures. Hossain *et al.* [31] introduced a DSR-based extensional deformation test using an SER inside a DSR. The SER fixture can be used inside a host system like DSR, detachable, and can provide the extensional rheological characteristics in a controlled environment. In a broad sense, the polymer can be characterized by an extensional flow rheometer [17]. To this end, this study has been initiated to investigate the degradation of SBS polymer using the newly introduced extensional deformation test.

5.1.1 Objectives

The main objective of this study is to investigate the degradation of SBS polymer due to RTFO, PAV, and UV aging at different temperatures. The specific objectives are to:

- (a) Establish a suitable polymer mixing procedure to be used in this study,
- (b) Compare the effectiveness of different polymer modifications: SBS, PPA, and SBS-PPA,
- (c) Understand the second peak extensional elongation force, F_2 value of stiffer binder due to aging (by increasing the testing temperature until stiffness (F_1) of aged binder becomes the same as the unaged state),
- (d) Evaluate how different percentages of SBS affect degradation, and
- (e) Investigate the effect of UV aging on the degradation of SBS compared to oven aging.

5.2 Methodology

5.2.1 Extensional Rheology Tests in DSR Platform Using SER Fixture

SER – the extensional rheometer can be used inside a rotational rheometer as an optional fixture. It consists of one master and one slave drum, and both the drums are dimensionally equal. The drums are joined together with intermeshing gears. The slave drum rotates in the equal and opposite direction of the master drum, which results in stretching of the sample over the unsupported length [17].

If Ω is the rate of angular rotation, R is the radius of the drums and L_0 is the fixed unsupported length, then the applied Hencky strain rate to the sample can be written as [17]:

$$\varepsilon_H = \frac{2\Omega R}{L_0} \quad \text{Eq. 5-5-1}$$

Torque, T , is the resistance of the sample to stretch in both drums and it can be measured by the torque transducer attached to the fixture, which can be written as [17]:

$$T(t) = 2RF(t) \quad \text{Eq. 5-2}$$

where $F(t)$ is the tangential force.

The instantaneous cross-sectional area $A(t)$ can be written as [17]:

$$A(t) = A_0 \exp[-\varepsilon_H t] \quad \text{Eq. 5-3}$$

The tensile stress function, $\eta_E^+(t)$, can be written as [5.15]

$$\eta_E^+(t) = \frac{F(t)}{\varepsilon_H A(t)} \quad \text{Eq. 5-4}$$

5.2.2 Materials and Preparation of PMAB

A PG 64-22 and an SBS-modified PG 76-22 are used in this study. SBS polymer and viscous liquid polymer, PPA, are used for modification.

5.2.2.1 SBS Mixing

Different researchers followed different methods for mixing SBS and PPA, as shown in **Table 5-1**. In this study, 2%, 4%, and 6% SBS by weight of the base binder are added with PG 64-22. The mixing of SBS polymer is divided into three stages.

1. Large-sized (passing #4) SBS polymer particles are grinded with a mechanical grinder for 20 minutes into small size (passing #16) particles.
2. We mixed the SBS with the base binder by a mechanical mixer for 15 minutes and then sheared for 2 hours with a high shear mixer at 180°C. The speed is set to 4000 rpm.

3. Repeat the second step.

5.2.2.2 PPA Mixing

As PPA is a viscous liquid, the speed of the high shear mixer is set to 2000 rpm; 0.5%, 2%, and 3.5% PPA by weight of PG 64-22 binder are added. Mixing of the PPA is done in two stages: firstly, the PPA is mixed with a mechanical mixer for 15 minutes. Secondly, the mixed sample is sheared at 180°C for 30 minutes.

5.2.2.3 SBS and PPA Mixing

A separate process is followed to mix both PPA and SBS with the base binder. At first, PPA is mixed, and then SBS is mixed with PG 64-22 binder; 2% PPA by weight of PG 64-22 mixing is mixed by following the same procedure mentioned in the “PPA mixing” section; 0.5%, 2%, and 3.5% SBS by weight of PG 64-22 are mixed with 2% PPA modified PG 64-22 by exactly following the same procedure as mentioned in the “SBS mixing” section.

5.2.2.4 UV Aging

Several researchers have performed UV aging of asphalt binder by following different methods, as shown in **Table 1**. In this study, 2 g of the binder contained in a small can is mixed with dichloromethane (DCM) to make the binder liquid spread on a 14.1 cm circular PAV plate uniformly. A SunRay: high-power UV flood curing system manufactured by Uvitron International is used for UV aging. The UV chamber reaches a constant temperature of 70°C after about two hours. The PAV plate with asphalt binder and DCM solvent is kept under the hood for drying. The dry PAV plate is placed inside the UV chamber when the UV chamber reaches 70°C, as shown in **Figure 5-1(a)**. The

thickness of the asphalt binder film is calculated to be 32 microns, and the intensity of the UV aging chamber is 100 mW/m².

Table 5-1: Literature review on mixing technique of PPA and SBS with base binder and on UV aging procedure.

	Authors	Type of mixer	Speed, rpm	Time	Temp.	Additional polymer	% of Polymer
SBS	Wang <i>et al.</i> [53]	High shear mixer	4000	30 min	175°C	-	4% SBS
	Zhang <i>et al.</i> [88]	Shear mixer	4000 & 2000	40 & 120 min	180°C	-	4% SBS
	Behnood and Olek [36]	High Shear mixer and stirring	4000	30 min	175°C	-	2%, 3% and 4% SBS
	Yan <i>et al.</i> [90]	High Shear mixer and stirrer	4000	30 & 60 min	180°C	0.15% sulfur	4.5%, 6% and 7.5%
PPA	Ge <i>et al.</i> [91]	Shear mixer	1500	30 min	160°C	3% Sasobit	0.5%, 1%, 1.5% and 2% PPA
	Liu <i>et al.</i> [92]	Shear mixer	4000	30 min	160°C	3% and 2.5% SBS	1% and 0.75% PPA
	Liang <i>et al.</i> [93]	High Shear mixer	4000	40 min	160°C	3% SBR	0.5%, 1%, 1.5% and 2% PPA
	Authors	Concentration	Sample weight	Thickness	Temp.	Intensity	UV aging duration
UV aging	Zhang <i>et al.</i> [94]	5% by weight (CS ₂)	50g	1 mm	50°C	20w/m ²	1, 7, 14, 21, 28 and 60 days
	Zeng <i>et al.</i> [95]	5%, 10% 15% and 20% (CS ₂)	-	2.5-15.3μm	50°C	15w/m ²	5h, 10h, 5d and 10d
	Zeng <i>et al.</i> [96]	-	50 g	0.0028 mm	60°C	500 μW/cm ²	-

5.2.3 Experimental Plan

In this study, one hundred and fifty-six extensional deformation tests are performed by DSR-based SER fixture. **Table 5-2** represents the binders, modifier types and their contents, and the total number of extensional deformation tests performed in this study.

Table 5-2: Summary of materials and experimental plan.

Asphalt Binder	Type of Polymer	% of Polymer	Type of Sample	Temperature, °C	No. of Sample	Sample Dimension			
PG 76-22	SBS	----	Original	12 & 16	3*3*2				
			RTFO						
			PAV						
			0%				Original	4, 12 & 16	3*3=9
			2%				Original	4, 12 & 16	3*3=9
							RTFO	12 & 16	3*2=6
							PAV	12 & 16	3*2=6
							Original	4, 12 & 16	3*3=9
			4%				RTFO	12 & 16	3*2=6
							PAV	12, 16, 19, 22, 25 & 28	3*6=18
UV	16 (48 and 60 hours)	3*2=6							
Normal oven	16 (48 and 60 hours)	3*2=6							
PG 64-22	SBS		Original	4, 12 & 16	3*3=9	3 mm* 0.72 mm			
			RTFO	12 & 16	3*2=6				
			PAV	12, 16, 19, 22, 25 & 28	3*6=18				
			UV	16 (48 and 60 hours)	3*2=6				
			Normal oven	16 (48 and 60 hours)	3*2=6				
			PPA	0.5%	Original		4	3*6	
				2%					
				3.5%					
			PPA-SBS	2%-0.5%	Original		4	3*6	
				2%-2%					
2%-									
3.5%									

5.2.3.1 Sample Preparation

In this study, the sample preparation method of Hossain *et al.* [31] is followed with some modifications. After pouring the binder in a 1-inch diameter silicon mold, as shown in **Figure 5-1(b)**, the mold is left at room temperature until it cools down. The sample is placed on a silicon mat between two stainless steel plates with the exact desired thickness to control the sample's thickness. A 50 mm x 50 mm (2 in x 2 in) silicon mat and a similar thick glass plate are placed over the silicon mat, overlapping with the stainless-steel plates.

Then, 20 lb. of loads are placed over the thick glass plate. The loads are kept over the sample for 3 hours. The whole system of preparing the sample is done inside an oven at 58°C, as shown in **Figure 5-1(c)**.

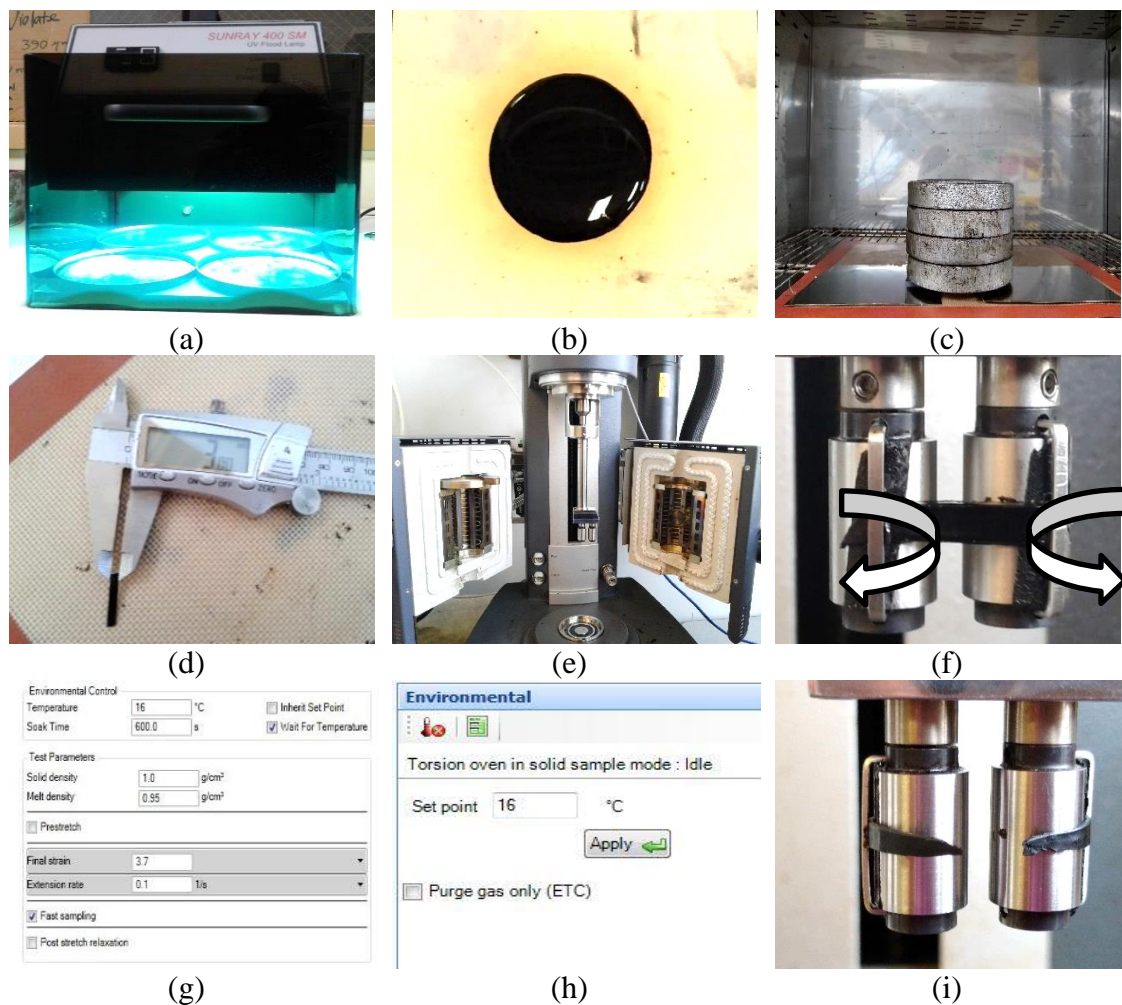


Figure 5-1: (a) Sample over the circular PAV plate inside the UV aging chamber, (b) Sample in the silicon mold, (c) Sample preparation inside the oven, (d) Specimen with desired dimensions, (e) SER fixture before loading the sample, (f) SER fixture after loading the sample, (g) Software screenshot shows test parameters, (h) Software screenshot shows the DSR control panel, and (i) Sample after the end of the test.

After removing the loads, the sample is placed in a refrigerator at 5°C for 1 to 2 minutes. If the sample is left at 5°C for longer than 2 to 3 minutes, the sample will possibly crack during the cutting process. If the sample is left at 5°C for less than 2 to 3 minutes,

the sample will possibly stick to the metal edge during the cutting process. Within 2 to 3 minutes after removing the sample from the refrigerator, the sample is cut with a sharp metal edge to the desired dimensions measured by a slide caliper, as shown in **Figure 5-1(d)**.

5.2.3.2 Test Procedure

Measurements are performed on a Universal Testing Platform model SER3-G, manufactured by Xpansion Instruments LLC. SER is connected to DSR model AR2000 Ex with an environmental chamber. After starting the DSR, the smart swap is inserted, and the SER bracket is fixed, as shown in **Figure 5-1(e)**. The sample is loaded and secured at each end by clamps. An ultra-thin, double-sided adhesion tape with a thickness of 0.1 mm is placed into the drum prior to the sample loading to prevent the sample from slipping, as shown in **Figure 5-1(f)**. As shown in **Figure 5-1(g)** and **5-1(h)**, the environmental control is set to 4°C, the soak time is 600 s, and the wait for temperature option is activated to ensure temperature equilibrium. The solid density is set to 1.0 g/cm³, and the melt density is set to 0.95 g/cm³. The final strain is 3.7 rad, with a strain rate of 0.1 s⁻¹. For accurate measurements, the fast-sampling option is activated. **Figure 5-1(i)** shows the sample at the end of the test.

5.3 Result and Discussion

5.3.1 Effect of Temperature and Speed on Mixing

The shear mixing speed and time affect the size of the agglomerates, which have an impact on the mechanical properties of the composite [97]. It must be noted that an increase in the shear speed of the high shear mixer increases the temperature even if the temperature is set to a certain temperature. This occurs because of the heat generated by

the high shear mixer. This is in **Figure 5-2**. The temperature reading is taken at every 15-minute interval, and the speed is increased after every 30-minute interval from 3000 rpm to 8000 rpm. When the set temperature is 160°C, 180°C, and 200°C, the temperature remains constant up to 4000, 5000, and 5000 rpm, respectively. After that, with the increment of mixing speed, the temperature increases. From the maximum temperature, 260°C is found from the maximum set temperature of 200°C. It can be concluded that for polymer mixing, high shear mixer speed cannot be more than 4000 rpm; otherwise, the temperature cannot be controlled (does not remain stable).

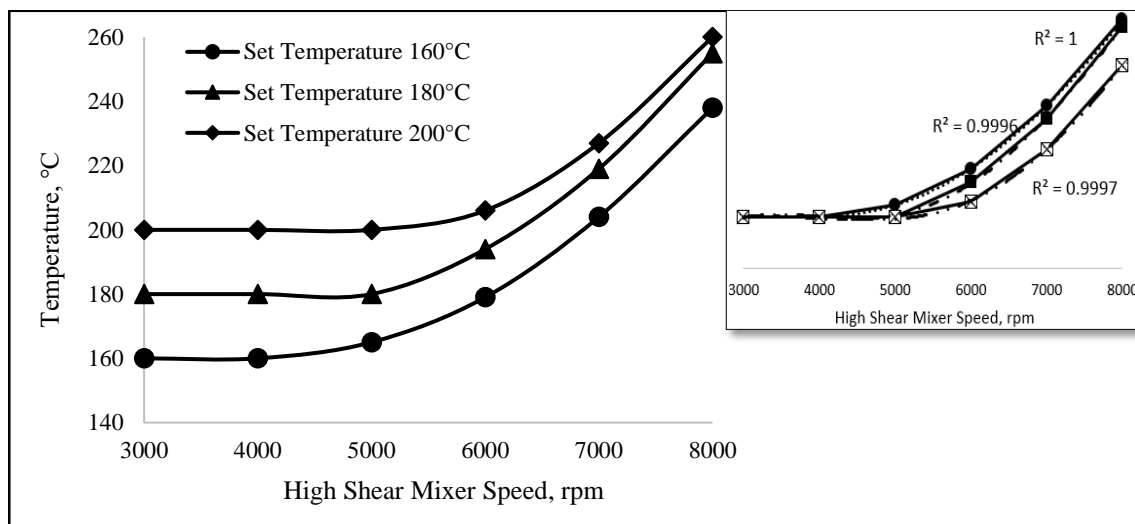


Figure 5-2: High shear mixer speed-temperature curve for original PG 67-22 binder (a) original curve, and (b) Y-axis being dimensionless.

5.3.2 DSR-based Extensional Test Parameter

As mentioned by Hossain *et al.* [31], F_1 is the stiffness of the binder, and F_2 reflects the polymer's characteristics. The value of F_2 increases with the addition of elastomeric polymer content. F_2 is influenced by the increase of F_1 due to aging, so F_2/F_1 value is used to analyze the degradation of the polymer due to aging. In this way, the effect of F_1 on F_2 will be normalized.

5.3.3 Effectiveness of Different Types of Modifiers (SBS, PPA-SBS and PPA)

Four-different percentages of SBS modified PG 64-22 (0%, 2%, 4%, and 6%), four-different percentages of 2% PPA-SBS modified PG 64-22 (0%, 0.5%, 2%, and 3.5%), and four-different percentages of PPA modified PG 64-22 (0%, 0.5%, 2%, and 3.5%) are tested to establish a correlation between the polymer percent and the F_2 . **Figure 5-3** indicates the relationship between F_2 of different types of modifiers (SBS, PPA-SBS, and PPA) and different percentages of the polymer at 4°C. It can be observed that in the case of 2% PPA-SBS and SBS modified PG 64-22, F_2 increases with the increment of the polymer percentages, whereas the addition of only PPA does not show any F_2 .

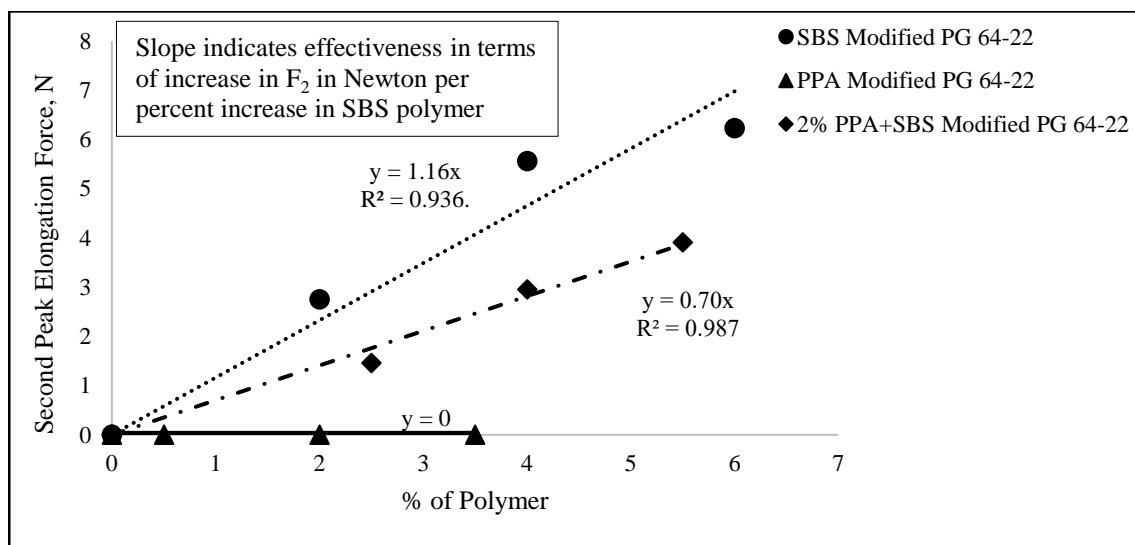


Figure 5-3: Second peak elongation force vs. percent of polymer at 4°C for different types of polymers.

For unmodified PG 64-22 (0% SBS), no F_2 is found. For 2%, 4%, and 6% SBS modified PG 64-22, F_2 is equal to 2.75 N, 5.56 N and 6.23 N, respectively. When 0.5%, 2%, and 3.5% SBS are added with 2% PPA modified PG 64-22, then F_2 is equal to 1.46 N, 2.95 N and 3.91 N, respectively. The slope value is equal to 1.16, 0.70, and 0 for SBS

modified PG 64-22, 2% PPA-SBS modified PG 64-22, and PPA modified PG 64-22, respectively. It is observed from the figure that F_2 increases at the rate of 1.16 N and 0.70 N with the percent of polymer for SBS and PPA-SBS modified PG64-22, respectively. It can be concluded that SBS polymer is the most effective in increasing F_2 . The correlation coefficient of SBS modified PG 64-22, and 2% PPA-SBS modified PG 64-22 is equal to 0.936 and 0.987, indicating that F_2 has a strong correlation with the percent of the polymer.

5.3.4 Polymer Degradation Due to Aging

Polymer degradation is measured by two parameters in this study: reduction in F_2 value and reduction in F_2/F_1 value.

5.3.4.1 Reduction of F_2 Value after RTFO and PAV Aging

F_2 is an indication of the polymer property, so the decrease in F_2 indicates the degradation of the polymer. **Figure 5-4** indicates F_2 of unaged and aged (RTFO and PAV) 2%, 4%, and 6% SBS modified PG 64-22 binder at 12°C and 16°C, respectively. The F_2 values of the original 2% SBS modified PG 64-22 binder are 1.45 N and 1.31 N with standard deviations of 0.22 and 0.17 at 12°C and 16°C, respectively, as shown in **Figure 5-4(a)** and **5-4(b)**. The F_2 values of the RTFO aged 2% SBS modified PG 64-22 binder are 1.36 N and 1.02 N with standard deviations of 0.15 and 0.04 at 12°C and 16°C, respectively.

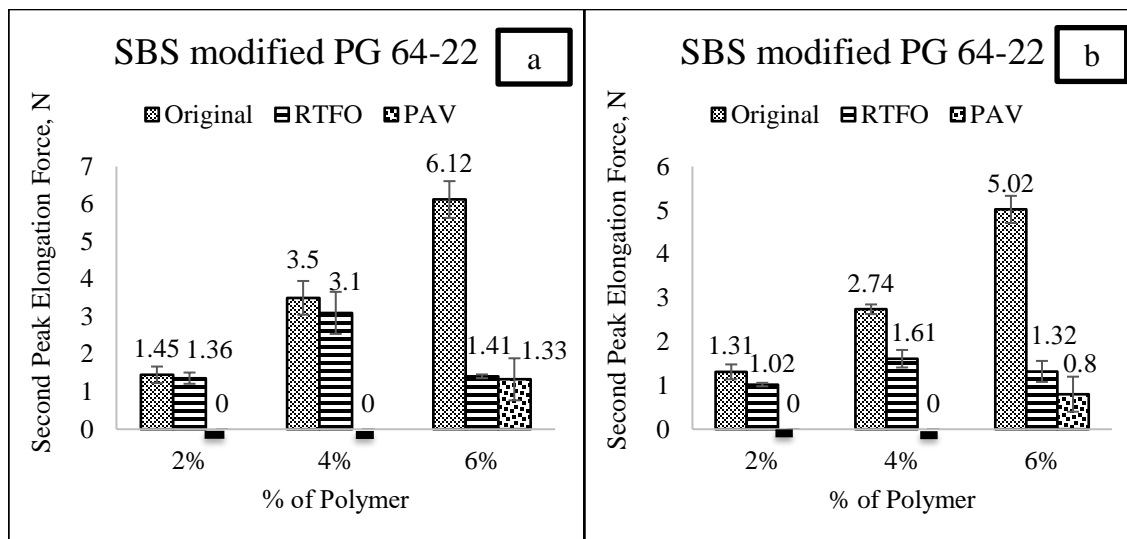


Figure 5-4: Second peak elongation force of different percent of polymer at (a) 12°C and (b) 16°C.

It is observed that the F_2 value decreases with the increment in temperature. No F_2 value is found from the SER test results of PAV aged 2% SBS modified PG 64-22. For the original 4% SBS modified PG 64-22, F_2 values are 3.50 N and 2.74 N, which have standard deviations of 0.45 and 0.11 at 12°C and 16°C, respectively. The F_2 values of the RTFO aged 4% SBS modified PG 64-22 are 3.10 N and 1.61 N along with standard deviations of 0.56 and 0.20 at 12°C and 16°C, respectively. As mentioned earlier, F_2 decreases with temperature increment for the original and short-term aged 4% SBS modified PG 64-22. In the case of both temperatures, F_2 reduces after RTFO aging, which is an indication that the polymer degrades due to aging. In the case of PAV aged binders, no F_2 data is obtained with SER at 12°C and 16°C. The sample breaks before reaching any F_2 .

F_2 values of the original 6% SBS modified PG 64-22 binder are 6.12 N and 5.02 N with standard deviations of 0.49 and 0.31, respectively. The values of F_2 for the RTFO aged PG 64-22 are 1.41 N and 1.32 N with standard deviations of 0.05 and 0.24,

respectively. It can be observed that F_2 decreases with an increment in temperature for the original and aged 6% SBS modified PG 64-22 asphalt binder. At both temperatures, F_2 reduces after RTFO aging and further reduces after PAV aging indicating polymer degrades due to aging.

5.3.4.2 Reduction of F_2/F_1 after RTFO and PAV Aging

F_2/F_1 values of different types of samples with different percentages of the polymer at different temperatures are shown in **Figure 5-5**. F_2/F_1 is a very distinctive parameter of the original and aged PMAB. As the polymer is degraded with aging, F_2/F_1 decreases. **Table 5-3** represents the F_2/F_1 values and percent reduction of F_2/F_1 values of RTFO and PAV aged binders.

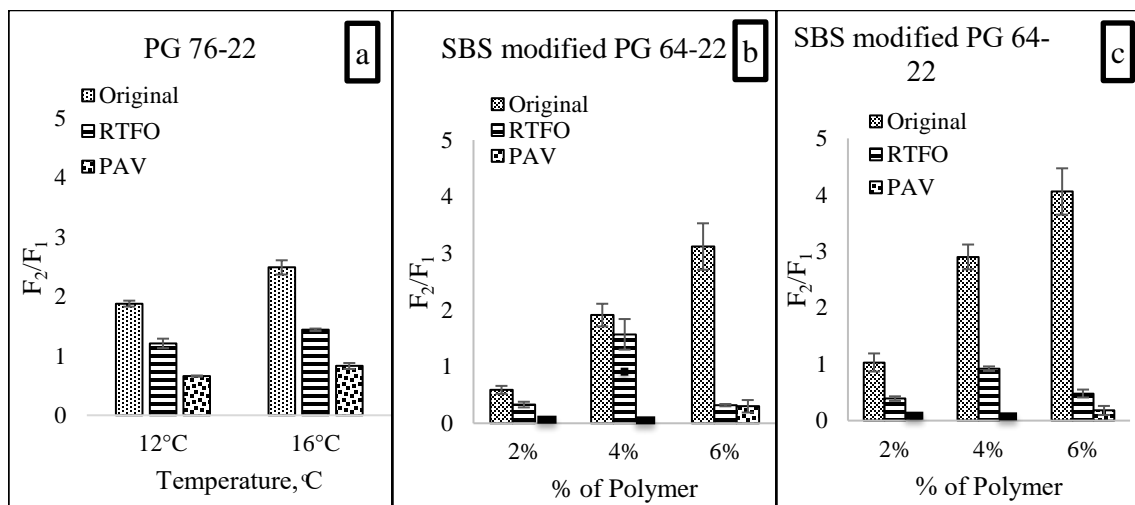


Figure 5-5: Second peak elongation force over first peak elongation force- (a) temperature curve for PG 76-22, (b) different percent of polymer at 12°C and (c) different percent of polymer at 16°C.

Clearly, from **Figure 5-5(a)**, we observe in the case of the PG 76-22 binder, RTFO aging reduces F_2/F_1 , and PAV aging further reduces F_2/F_1 . It is also obvious from the figures that F_2/F_1 increases with temperature increment for all the original, RTFO, and PAV

aged binders. As shown in **Figures 5-5(b)** and **5-5(c)**, the value of F_2/F_1 of the original 2% SBS modified PG 64-22 is higher at 16°C than at 12°C.

Table 5-3: Percent reduction of F_2/F_1 values of different types of binder at different temperature after RTFO and PAV aging.

Binder Type	Aging Type	Temp.	F_2/F_1	Standard Deviation	%Reduction
PG 76-22	Original	12°C	1.88	0.05	-
PG 76-22	RTFO	12°C	1.21	0.08	35.64%
PG 76-22	PAV	12°C	0.66	0.09	64.89%
PG 76-22	Original	16°C	2.49	0.12	-
PG 76-22	RTFO	16°C	1.44	0.02	42.17%
PG 76-22	PAV	16°C	0.83	0.09	66.67%
2% SBS modified PG 64-22	Original	12°C	0.59	0.07	-
2% SBS modified PG 64-22	Original	16°C	1.03	0.16	-
2% SBS modified PG 64-22	RTFO	12°C	0.33	0.05	44.07%
2% SBS modified PG 64-22	RTFO	16°C	0.39	0.04	62.14%
2% SBS modified PG 64-22	PAV	12°C	0	0	100%
2% SBS modified PG 64-22	PAV	16°C	0	0	100%
4% SBS modified PG 64-22	Original	12°C	1.91	0.20	-
4% SBS modified PG 64-22	Original	16°C	2.90	0.22	-
4% SBS modified PG 64-22	RTFO	12°C	1.57	0.27	17.80%
4% SBS modified PG 64-22	RTFO	16°C	0.92	0.03	68.28%
4% SBS modified PG 64-22	PAV	12°C	0	0	100%
4% SBS modified PG 64-22	PAV	16°C	0	0	100%
6% SBS modified PG 64-22	Original	12°C	3.12	0.41	-
6% SBS modified PG 64-22	Original	16°C	4.06	0.41	-
6% SBS modified PG 64-22	RTFO	12°C	0.32	0.02	89.74%
6% SBS modified PG 64-22	RTFO	16°C	0.48	0.07	88.20%
6% SBS modified PG 64-22	PAV	12°C	0.30	0.11	90.4%
6% SBS modified PG 64-22	PAV	16°C	0.11	0.08	97.3%

It is clearly observed from **Figures 5-5(b)** and **5-5(c)** that RTFO aging reduces F_2/F_1 in the case of 2% and 4% SBS modified asphalt binder. As there is no F_2 found for PAV aged 2% and 4% SBS modified asphalt binder, the ratio of F_2/F_1 can be assumed at zero. As found earlier, it is clear from **Figures 5-5(b)** and **5-5(c)** that RTFO aging reduces F_2/F_1 , and PAV aging further reduces F_2/F_1 in the case of 6% SBS modified PG 64-22. It is also obvious that SBS is degrading due to RTFO and PAV aging. Therefore, through this

study, it is recommended that this parameter be used to determine the aging susceptibility of SBS in an asphalt binder.

5.3.4.3 Understanding the F_2 Value of Stiffer Binder due to Aging by Increasing the Testing Temperature until Stiffness (F_1) of Aged Binder becomes the same as Unaged State

Figure 5-6 shows the elongation force-step time curve of 4% and 6% SBS modified PG 64-22 original, RTFO and PAV aged binder at different temperatures. **Figures 5-6(a)** and **5-6(c)** show how F_2 decreases after RTFO and PAV aging. Due to the high stiffness of the aged binder, F_1 increases. The sample breaks before elongation, which indicates that PAV aged PMAB cannot exhibit polymer characteristics at low temperature. Extensional deformation testing is done up to 28°C temperature to understand the reduction in the effect of polymer characteristics after PAV aging.

Figures 5-6(b) and **5-6(d)** indicate, in the case of PAV aged binder with the increment of temperature, that the binder's stiffness reduces. As a result, F_1 decreases, and the sample can elongate, showing the F_2 value. However, the F_2 value of the PAV aged sample is less than the F_2 value of the original and RTFO aged binder for the same F_1 value. When the RTFO aged binder undergoes PAV aging, F_2 reduces. Considering RTFO and PAV aged 6% SBS modified binder, a similar reduction is observed. **Table 5-4** represents the percent reduction of F_2 value at similar stiffness (F_1) value of different types of the sample after RTFO and PAV aging. It can be concluded that in the case of PAV aged binder, F_2 is not found due to the impact of F_1 value at a low temperature. At higher a temperature, the F_2 value is found, but the value is lower than the F_2 value of a similar stiff original and RTFO aged binder, which clearly indicates polymer degrades due to aging.

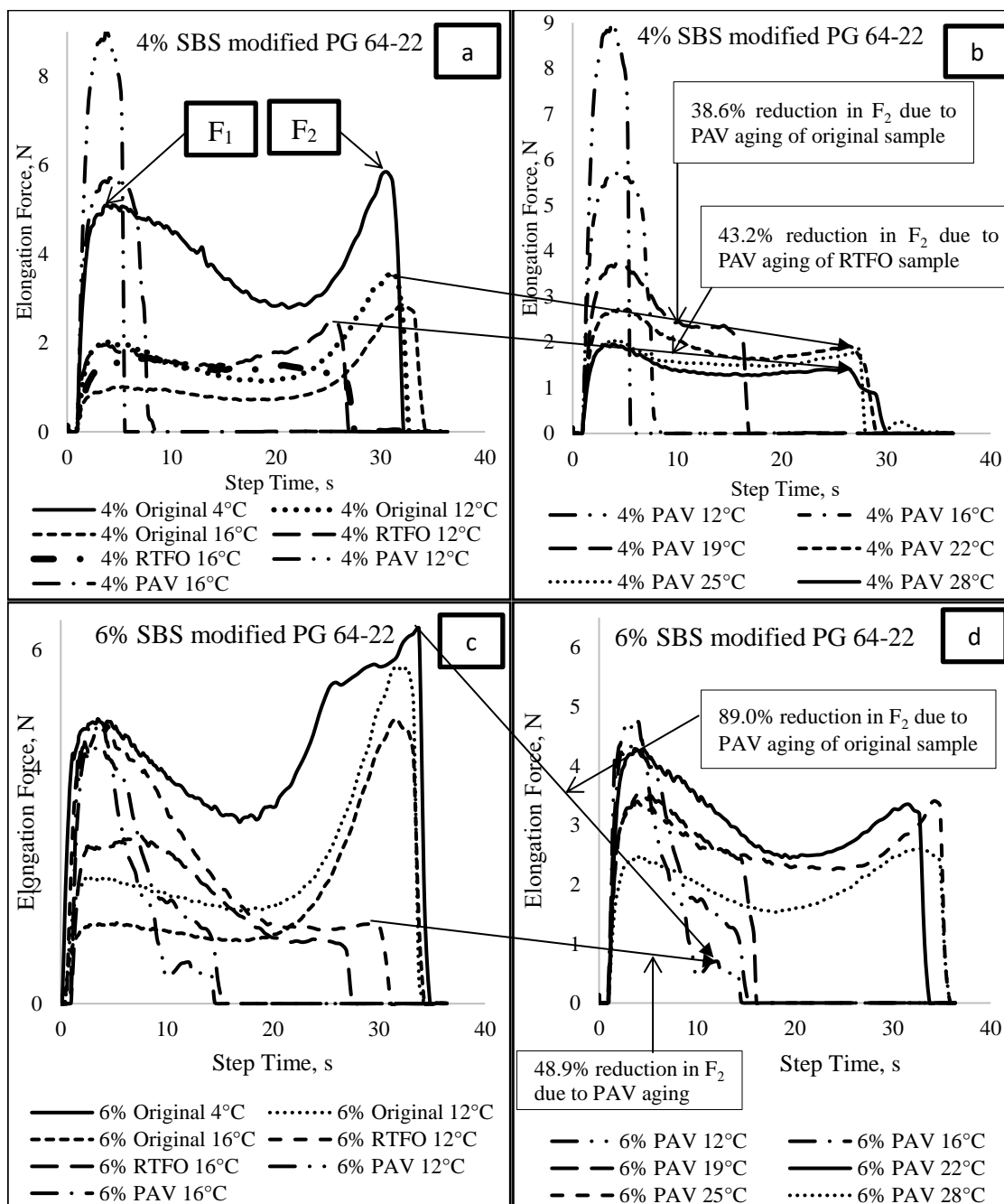


Figure 5-6: Elongation force-step time curve for (a) 4% SBS modified PG 64-22 (original, RTFO and PAV aged), (b) 4% SBS modified PG 64-22 (PAV aged), (c) 6% SBS modified PG 64-22 (original, RTFO and PAV aged), and (d) 6% SBS modified PG 64-22 (PAV aged).

Table 5-4: Percent reduction of F_2 value due to aging of different types of samples at similar stiffness, F_1 .

Binder Type	Aging Type	Similar Stiffness, F_1	Temp. at Similar Stiffness	F_2 Value	% Reduction
4% SBS modified PG 64-22	Original	2.02 N	12°C	3.60 N	38.6%
	PAV	2.05 N	25°C	2.21 N	
	RTFO	1.96 N	12°C	2.48 N	43.2%
	PAV	1.96 N	28°C	1.41 N	
6% SBS modified PG 64-22	Original	4.81 N	4°C	6.36 N	89.0%
	PAV	4.73 N	12°C	0.70 N	
	RTFO	4.66 N	12°C	1.37 N	48.9%
	PAV	4.73 N	12°C	0.70 N	

5.3.4.4 Degradation due to UV Aging

Figure 5-7 shows the second peak elongation force, F_2 of different types of UV, and oven aged samples at 16°C. RTFO aged 4% and 6% SBS modified PG 64-22 binders are UV aged to understand the effect of UV aging on SBS degradation. For better comparison, the same binders are kept in the normal oven for the same time duration at 70°C (as the UV chamber reaches 70°C during UV aging). For UV aged 4% and 6% SBS modified binders, no F_2 is found after 48 and 60 hours.

In the case of oven aged 4% (RTFO aged) SBS modified binder, F_2 is found to be equal to 2.51 N and 0.81 N with standard deviations of 0.26 and 0.41 after 48 hours and 60 hours of aging, respectively. Similarly, for the oven aged 6% (RTFO aged) SBS modified binder, F_2 is equal to 3.31 N and 2.22 N with standard deviations of 0.50 and 0.60 after 48 hours and 60 hours aging, respectively. UV aged samples do not even show any F_2 value at higher temperatures (up to 28°C). Therefore, it can be concluded that after UV aging of this duration, SBS is completely degraded.

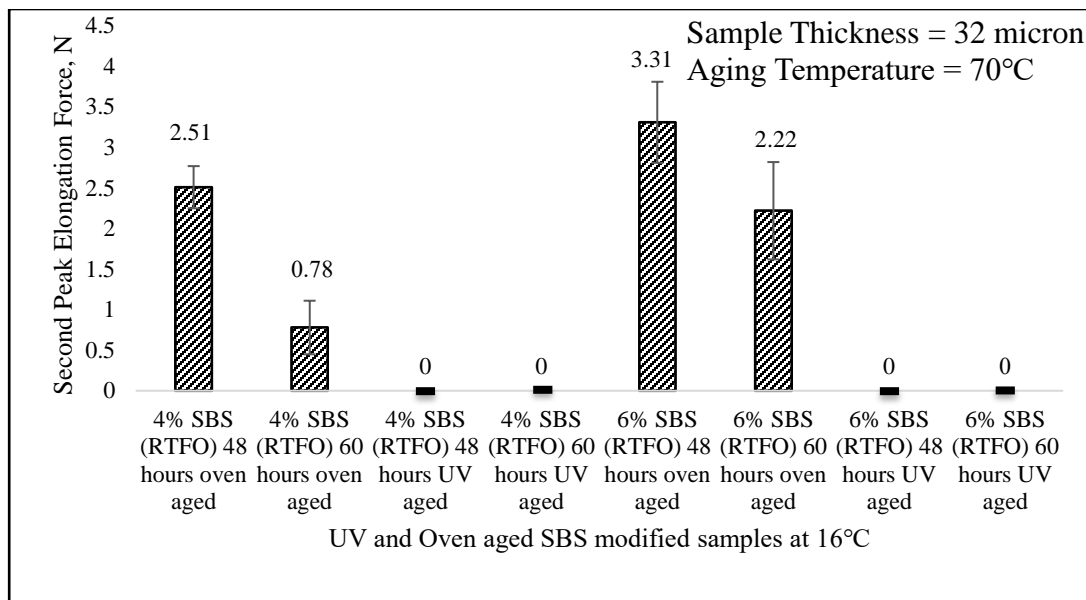


Figure 5-7: Second peak elongation force of different types of UV and oven aged binder.

5.4 Conclusions

The objective of this study is to investigate the degradation of the polymer due to RTFO, PAV, and UV aging. We can draw from the following specific conclusions:

- The maximum speed of the high shear mixer needs to be set at 4000 rpm at any set temperature at or below 200°C to control the temperature during mixing.
- F_1 is the stiffness of the base binder, and F_2 reflects polymer characteristics. F_2 is found after adding SBS with PG 64-22, and F_2 value increases with the increment of SBS percentages. For SBS modified PG 64-22, F_2 linearly increases at 1.16 N per percent of the polymer. Unmodified binders and PPA modified binders do not exhibit F_2 .
- The decrease in F_2 indicates the degradation of the polymer. It is observed that at all the temperatures, F_2 decreases after RTFO aging. After PAV aging due to

high a F_1 value, the samples break before reaching any F_2 , resulting in the F_2 value being equal to zero. By increasing the test temperature (up to 28°C), the F_2 value is found, although the value is less than the F_2 value of the similarly stiff original and RTFO aged binders. This confirms that polymer degrades due to aging.

- F_2/F_1 value is studied to normalize the stiffness effect. All the testing temperatures used in this study exhibit reduction in F_2/F_1 due to RTFO aging, and further reduction is observed due to PAV aging. RTFO aging reduces F_2/F_1 about 18% to 90%, and PAV aging reduces F_2/F_1 about 65% to 100% with respect to the original binder. Therefore, F_2/F_1 is recommended as a polymer degradation parameter due to aging.
- UV aging degrades the SBS polymer completely as no F_2 value is observed. At the same aging temperature and the same conditions as the other (sample thickness, duration, air supply) UV aging chambers, normal oven aged binder shows the F_2 value. Extensional testing at higher temperatures also did not show any F_2 value, confirming the complete degradation of SBS due to UV aging.

CHAPTER 6

A NOVEL EXTENSIONAL DEFORMATION TEST FOR EVALUATING SBS DEGRADATION DUE TO AGING OF ASPHALT MIXTURE*

6.1 Introduction

Modification of asphalt binder has become very popular to improve the asphalt binders' viscoelastic properties and subsequently reduce the distress in the asphalt pavement [36], [98], [99]. Among all the modifiers, thermoplastic elastomer SBS has gained more attention in pavement construction [13], [100], [101]. SBS modified asphalt binder improves the low-temperature cracking resistance [94], [102] and high-temperature rutting resistance, and it enhances the fatigue performance [36], [101]. Also, it reduces the impact of oxidative aging on the pavement in the long run compared to the unmodified binder [100], [103]. However, the aging degree has always been a distressing issue for SBS modified asphalt binder from the economic perspective [103]–[105].

Several researchers studied the aging characteristics of the SBS modified asphalt binder [104], [106], [107]. Asphaltenes in the base binder increased due to the aging and size exclusion chromatography showed the molecular size of the SBS polymer reduced

* This chapter or portions thereof has been published previously in the *International Airfield and Highway Pavements Conference 2021* under the title “Degradation of SBS Polymer During Laboratory Aging of Asphalt Binder”. The current version has been formatted for this dissertation.

[103]. Gel Permeation chromatography showed smaller asphalt molecules transform into a larger one, and the molecular weight of the SBS polymer reduced due to aging [108]. The SBS modifier's effectiveness was reduced due to aging, and the performance of the SBS modified asphalt pavement was affected severely [94], [108]. These reasons support the need to evaluate SBS polymer degradation for the better life of the pavement as aging continues.

Zhang *et al.* [94] investigated the aging evaluation technique of the SBS modified asphalt binder. Degradation of SBS polymer was demonstrated from different rheological behaviors such as zero shear viscosity, rutting factor, fatigue factor, and non-recoverable creep compliance. Three rheological indices were proposed to understand SBS polymer degradation. Fourier transform infrared (FT-IR) spectroscopy was used to understand the aging mechanism by several researchers [109], [110].

An advanced technology named atomic force microscopy-based infrared spectroscopy was applied to characterize the aged SBS modified asphalt binder [111]. Xu *et al.* [112] studied the microstructural, micromechanical, and rheological properties of the aged SBS modified asphalt binder. A correlation was established among the DSR, linear amplitude sweep test, attenuated total reflectance (ATR) FT-IR, and atomic force microscopic results for understanding the aging process. Xu *et al.* [113] established a partial least square model for predicting the physical and rheological properties of the aged SBS modified asphalt binder. X-ray photoelectron spectroscopy and proton nuclear magnetic resonance test results were analyzed to develop the predictive model. Principle component analysis was performed to eliminate the influence of the evaluation predictors.

Researchers studied the evaluation of the degradation of SBS polymer in SBS modified asphalt binder due to aging over the past years. However, there is no specific method for the evaluation of aging related degradation of SBS polymer in SBS modified asphalt binder. Recently, the introduced DSR-based extensional deformation test parameter can directly measure the SBS polymer degradation in SBS modified asphalt binder due to aging [1]. In this test, the SER fixture is inserted inside the DSR host system to control the environment effectively. This fixture can characterize the SBS modified asphalt binder's rheological behavior using only a few milligrams of the binder.

From the extensional deformation test, the elongation force curve is obtained with two peak forces. The first peak elongation force, F_1 , indicates the binder's stiffness, and the second peak elongation force, F_2 , indicates elastomeric polymer characteristics. A reduction in F_2 value indicates the SBS polymer degradation. In this study, asphalt mixture with an SBS modified binder was used to evaluate the degradation of SBS due to aging. Long-term mixture aging was performed in the laboratory, and the mixture-extracted binder was tested. Later, degradation of SBS polymer due to the extreme aging was evaluated from the extensional deformation test parameters.

6.1.1 Objectives

The main objective of this study was to investigate the degradation of SBS polymer due to laboratory aging of the asphalt mixture. The specific objectives were to:

1. Understand the temperature effect on SBS degradation,
2. Study the relation between the first peak elongation force and test temperatures, and

3. Evaluate the reduction in second peak elongation force after mixture aging.

6.2 Materials and Experimental Plan

6.2.1 SBS Modified Asphalt Binder

An unmodified PG 64-22 original binder was used in this study; 4% SBS polymer (21.5-24.1% PS content) was mixed with the PG 64-22 binder; 4% SBS polymer was selected as optimum polymer content for the PG 64-22 binder, according to Hossain *et al.* [35]. PG 64-22 binder was heated at 180°C for melting properly before mixing with the SBS polymer; 4% SBS of PG 64-22 binder was weighted and added to the melted PG 64-22 binder by a mechanical mixer for 15 minutes. A high shear mixer was used for 2 hours to shear the mix at a rotational speed of 4000 rpm. The mixing process was performed at 180°C.

6.2.2 Laboratory Aged Asphalt Mixture

Asphalt aggregate mixture of 3000 gm was prepared for short term and long-term lab aging. Samples were kept in the oven at 135°C to simulate the short-term aging during mixing, storage, placement, and construction. After four hours of short-term aging, some samples were kept at 85°C for five days following AASHTO R 30 to simulate long term (5 to 10 years) field aging. Again, to simulate the 5-Days aging at 85°C and reduce aging duration, some samples were kept at 135°C for one day [113]. The asphalt mixture before and during laboratory aging are shown in **Figure 1(a)** and **1(b)**, respectively. Asphalt binder from these asphalt mixtures was extracted following ASTM D2172 method using n-propyl bromide, as shown in **Figure 1(c)**.

6.2.3 Experimental Plan

Table 1 represents the materials and experimental plan, which were followed in this study.

6.2.4 Sample Preparation

In this study, the sample preparation method that was demonstrated by Hossain and Wasiuddin [1] was followed. Original and extracted SBS modified asphalt binders

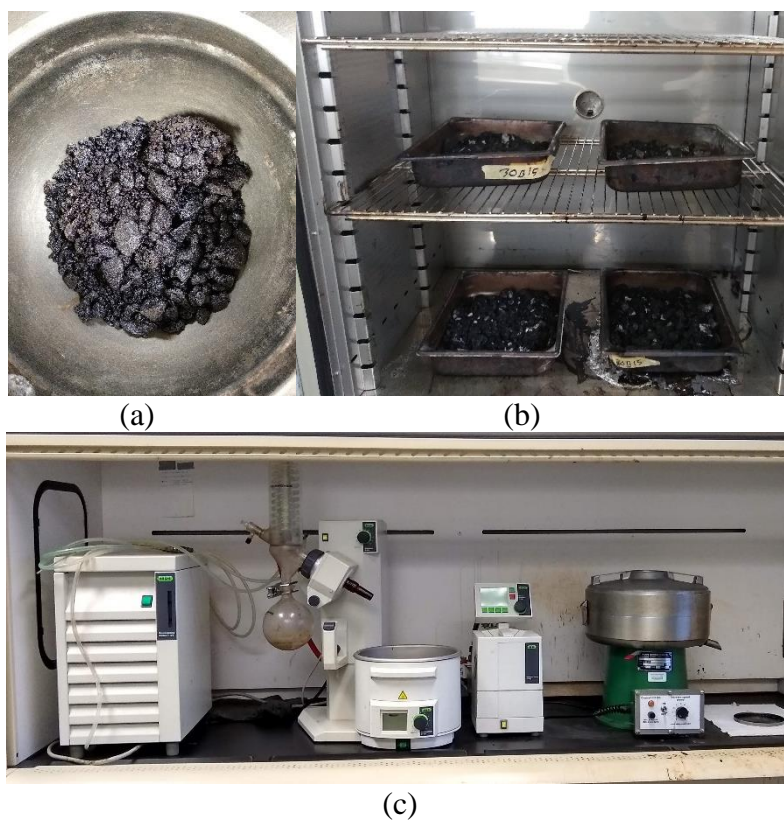


Figure 6-1: (a) Collection of mixture in a bowl before aging started, (b) Laboratory mixture aging at 85°C and 135°C, and (c) Asphalt binder extraction from loose mixture.

were heated at 163°C and 180°C, respectively, to collect the binder in a 25 mm DSR mold. When the binder reached room temperature, the binder was collected immediately from the mold and kept on a silicone mat within two stainless steel plates, which were 1.7 inches apart from each other, as shown in **Figure 2(a)**. A 2 in x 2 in silicone mat followed by a 2

in x 2 in glass plate was kept over the sample, as shown in **Figure 2(b)**. The reason for using a 2 in x 2 in silicone mat between the glass plate and the sample was to ensure that there was no direct contact between the sample and the glass plate.

Table 6-1: Summary of Materials and Experimental Plan.

Type	Specified Sample	Duration of Aging	Test Temperature	No. of Sample
4% SBS Modified PG 64-22 binder	Original	-	4°C, 12°C & 16°C	3 replicates for a specific test temperature
Laboratory aged mixture	Aging at 85°C temperature in forced draft oven	0 hour	4°C to 16°C at 4°C interval & 19°C to 28°C at 3°C interval	3 replicates for a specific test temperature
		4 hours		
		1 day		
		3 days		
		5 days		
	Aging at 135°C temperature in forced draft oven	0 hour	4°C to 16°C at 4°C interval & 19°C to 31°C at 3°C interval	3 replicates for a specific test temperature

Four 5-lb. loads were placed over the glass plate, and the glass plate spread the loads uniformly on the binder, as shown in **Figure 6-2(c)**. The whole system was done inside a force draft oven at 58°C for three hours. It took five hours in the oven to get the required thickness (0.72 mm) of the laboratory aged SBS modified mixture extracted binder. The required thickness of the sample was obtained after removing the loads, as shown in **Figure 6-2(d)**. For collecting the required SER sample, we used a freezer, a knife, and a caliper. Within two minutes of removing the sample from the freezer, the required sample was cut with a sharp knife immediately after measuring with the caliper. The sample dimension was 3 mm by 0.72 mm.

6.2.5 Test Procedure

A double-sided adhesive tap was used on both the SER's drums to attach the sample over the drums. Two clamps were used on the SER sample, and the drums were kept at 12.7 mm apart (**Figure 6-2e**). Using clamps were required; otherwise, the sample would come out of the drums when the tensile force was applied. In the Trios software, the soak

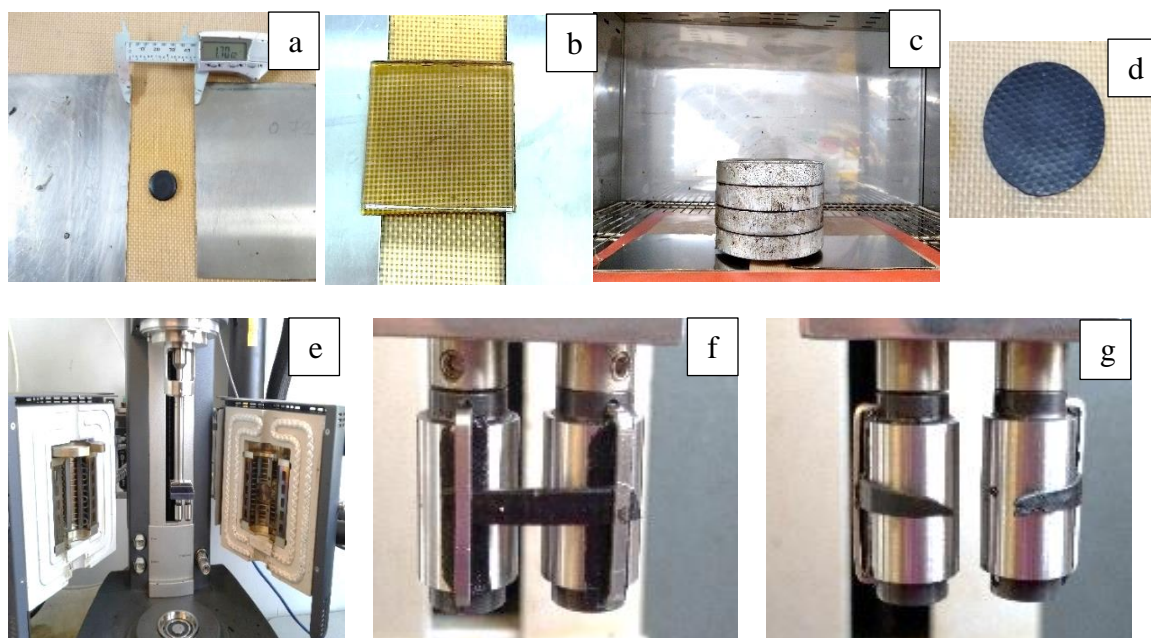


Figure 6-2: (a) Binder placed between two stainless steel plates, (b) A silicone mat and a glass plate over the sample, (c) Sample preparation in the oven, (d) Binder size after removing the loads, (e) SER inserted in DSR host system, (f) Sample shape before the test, and (g) Sample shape after the end of the test.

time was 600 s, the solid density was 1.0 g/cm^3 , the melt density was 0.95 g/cm^3 , the final strain was 3.70, and the extension rate was 0.1 1/s throughout all the test of this study. The temperature was changed from 4°C to 31°C for different original and aged samples. When the test was finished, the broken sample was removed from the drums. Then the drums were cleaned with paint thinner for loading another new sample. It took 12 minutes to

complete a test, and three tests were performed for every single binder. **Figure 6-2(f)** shows the sample before the test, and **Figure 6-2(g)** shows the sample after the end of the test.

6.3 Result and Discussion

6.3.1 Effect of Temperature on Elongation Force

Figures 6-3 and **6-4** represent the elongation force vs. step time curve at different test temperatures of two different binders extracted from two different mixtures. Two peak forces were obtained from these curves. The first peak elongation force, F_1 value, represents the binder's stiffness and the second peak elongation force, F_2 value, indicates elastomeric polymer characteristics.

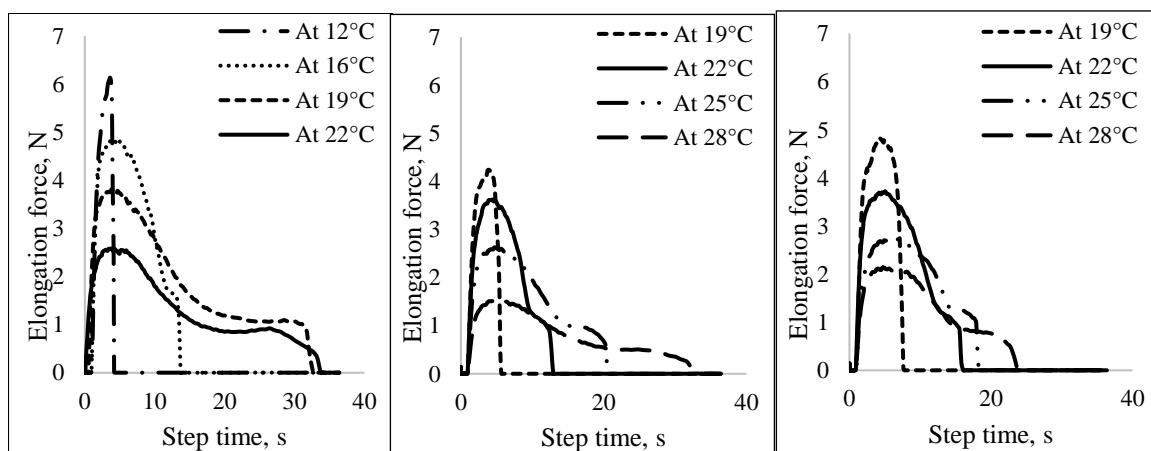


Figure 6-3: Elongation force and step time curve of mixture extracted binder (a) 1-Day aged, (b) 3-Days aged, and (c) 5-Days aged (aged at 85°C).

The binder's stiffness, F_1 value, was increased due to aging. At medium-low temperature, extensional deformation test samples could not have an F_2 value in the case of laboratory aged mixture extracted binders. Because before reaching the second peak, F_2 , the sample broke due to the binder's high stiffness. With the increment of the test temperatures, the F_1 value decreased, and the F_2 value was visible accordingly. Also, the

binder's stiffness significantly affected the elongation of the sample with time before fracture.

Figures 6-3(a), 6-3(b), and 6-3(c) represent the elongation force vs. the step time curve for mixture extracted SBS modified PG 64-22 binder aged at 85°C for one day, three days, and five days, respectively. It was observed from **Figure 6-3(a)** that immediately after the F_1 value was obtained, the sample fractured due to high stiffness at test temperature 12°C. F_2 value was observed with the increment of the test temperature to 16°C along with decreased F_1 value. Similar characteristics were observed at test temperatures 19°C and 22°C. **Figure 6-3(b)** and **6-3(c)** also showed that with the increment of test temperatures, F_1 values decreased, and F_2 values were observed at higher test temperatures. In the case of 3-Days aged binder, the first F_2 value was obtained at 22°C, and in the case of 5-Days aged binder, the first F_2 value was obtained at 25°C. The 5-Days aged binder was the stiffest binder at 85°C aging temperature, and the F_2 value was obtained at the highest test temperature.

Elongation force vs. step time curve of the mixture extracted SBS modified PG 64-22 binder aged at 135°C for 4 hours, 8 hours, and 12 hours are shown in **Figure 6-4(a), 6-4(b), and 6-4(c)**, respectively. With the increment of temperature, the second peak was easily found in 4-Hour and 8-Hour aged binders. However, in the case of the 12-Hour aged binder, the second peak was hardly found. The absence of the F_2 value was because the SBS polymer highly degraded after 12 hours of aging at 135°C aging temperature. At 25°C test temperature, the 12-Hour aged sample did not show much elongation compared to the 1-Day aged binder at 85°C.

Finally, it was obvious that with the increment of test temperature, the F_2 value was observed in the case of a laboratory aged mixture extracted binder, which revealed SBS polymer exists. The absence or reduction of F_2 value at a higher temperature in any SBS modified aged binder indicated SBS degradation. It could be concluded that the temperature had a significant effect on the binder's stiffness and polymer characteristics.

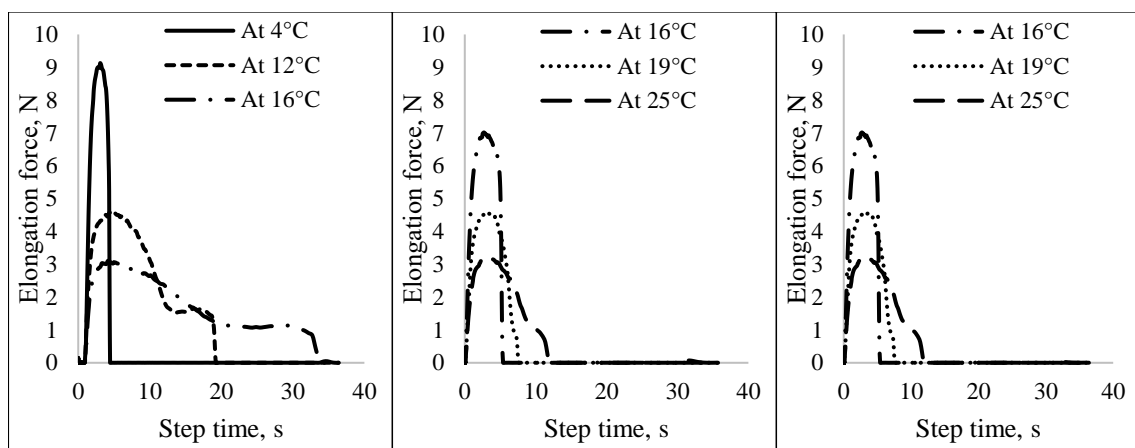


Figure 6-4: Elongation force and step time curve of mixture extracted binder (a) 4-Hours aged, (b) 8-Hour aged, and (c) 12-Hour aged (aged at 135°C).

6.3.2 Reduction in F_2 Value after Laboratory Aging at 85°C

In the case of a laboratory aged binder, the extensional deformation test parameter, F_2 value, could not identify the degradation of SBS polymer at a similar temperature. In that case, degradation due to aging could be found out from the reduction in F_2 value at the equal stiffness, F_1 value [1]. Tests were performed at three different temperatures for each binder to get an equal stiffness value for all different types of mixture extracted binders. Those three temperatures were selected based on the aging duration and aging temperature.

Figure 6-5 represents the relationship between temperature and stiffness of the mixture extracted binders aged for 0 hours, 4 hours, one day, three days, and five days. The mixture collected immediately after mixing is considered 0-Hour aged. To simulate RTFO

aging or short-term aging, the mixture was kept in the oven at 135°C for 4 hours and named a 4-Hour aged mixture. After 4 hours of aging, the mixture was placed in the oven at 85°C, and the aging duration for one day, three days, and five days were aptly named 1-Day, 3-Days, and 5-Days aged mixture, respectively.

According to AASHTO R 30 standard, 5-Days aging at 85°C represents long-term aging. Previous studies showed that 4 to 8 days of aging at 85°C simulate 7-15 years of field aging [114]–[116]. In this study, 1-Day and 3-Days aging were performed to understand laboratory aged binders' aging characteristics. Stiffness of 3-Days and 5-Days aged binders was almost equal at the same test temperatures, which indicated binder aging was slower at these aging durations. It was obvious from the figure that the first peak elongation force, the F_1 value, was highly correlated with the test temperature.

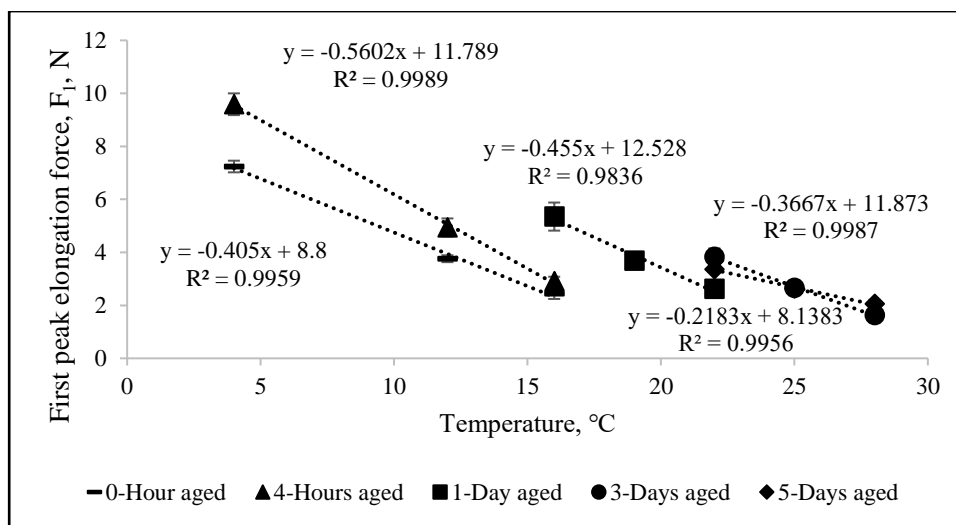


Figure 6-5: Relation between temperature and stiffness of the mixture extracted binder (aged at 85°C).

For evaluating the aging degradation of the laboratory-aged binders, the second peak force, F_2 , was calculated at equal stiffness. F_2 values for the laboratory-aged binders were calculated considering the highest F_1 value of the original SBS modified binder.

Lower F_1 values may underestimate the F_2 values of the laboratory-aged binders. Reduction in F_2 value indicated degradation of SBS polymer in SBS modified asphalt binder.

From the linear relationship, as shown in **Figure 6-5**, the required test temperatures were calculated as 1.1°C, 9.3°C, 11.1°C, 11.9°C, and 2.9°C for the laboratory-aged binders. Similarly, F_2 values were obtained at the required test temperatures. **Figure 6-6** represents the reduction in the F_2 value of the laboratory aged mixture extracted binder compared to the original modified binder. Reduction rate in F_2 value was calculated following **Equation (1)**. Immediately after mixing, the rate was 31%, and after five days, we observed a 65% reduction. The reduction rate of F_2 value decreased later with an increased aging duration.

$$\begin{aligned} & \textit{Reduction rate} \\ & = \frac{F_2 \textit{ for unaged binder} - F_2 \textit{ for aged binder}}{F_2 \textit{ for unaged binder}} * 100 \end{aligned} \quad \text{Eq. 6-1}$$

6.3.3 Reduction in F_2 Value after Extreme Aging at 135°C

Previous literature reported that one day aging at 135°C was the maximum aging level of asphalt mixture to simulate the long-term aging [113], [117]. Required test temperatures of the aged mixture extracted binders were selected by plotting the stiffness values at different temperatures, as shown in **Figure 6-7**. In this study, 0-Hour aged mixture extracted binder represented mixture collected immediately after binder aggregate mixing. Aging for 4 hours at 135°C was performed to simulate short-term aging and aging for one day was performed to simulate long-term aging. The 8-Hour and 12-Hour aging were performed to understand the aging mechanism of laboratory-aged mixture extracted binders.

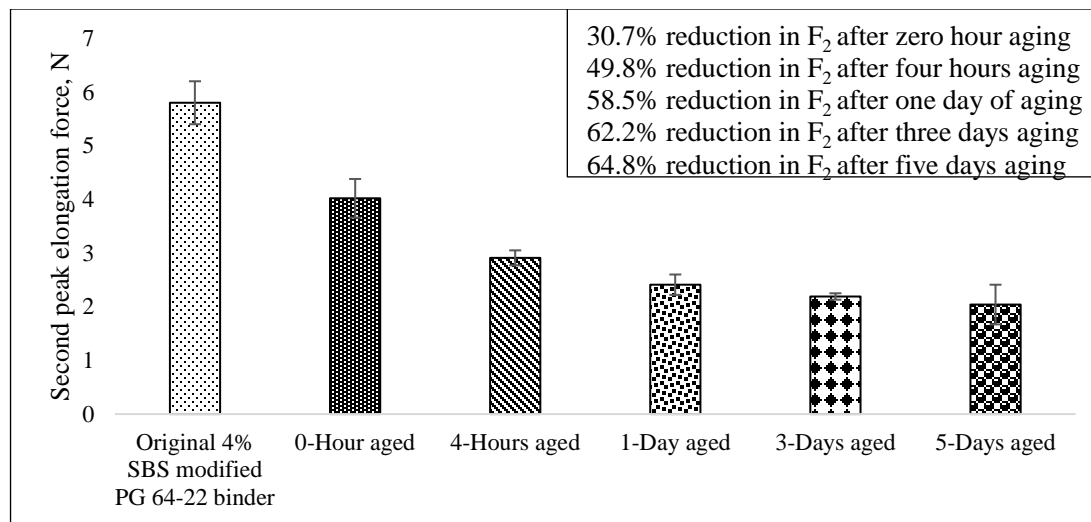


Figure 6-6: Reduction in F_2 value of the laboratory aged mixture extracted binder at equal stiffness (aged at 85°C).

From the straight-line equation, 1.1°C, 9.3°C, 12.3°C, 18.5°C, and 20.1°C test temperatures were selected at equal stiffness for 0-Hour, 4-Hour, 8-Hour, 12-Hour, and 1-Day aged mixture extracted binder, respectively. Similarly, the F_2 values of the 0-Hour, 4-Hour, 8-Hour, 12-Hour, and 1-Day aged mixture extracted binders were obtained at that test temperature. **Figure 6-8** shows the reduction in F_2 value at equal stiffness of 4% SBS modified PG 64-22 original binder and the laboratory-aged mixture extracted binders. The F_2 values of the laboratory-aged binders were evaluated following a similar procedure as the mixture extracted binder aged at 85°C. **Equation 6-1** was used for obtaining the reduction rate in the F_2 value. Here, 30.7%, 49.8%, 55.5%, 66.0%, and 100% reduction in F_2 value were obtained in the case of 0-Hour, 4-Hour, 8-Hour, 12-Hour, and 1-Day aged binders, respectively, compared to the original binder. There was no second peak force, F_2 , at a higher test temperature (31°C) for the 1-Day aged mixture extracted binder, which indicated complete SBS polymer degradation after one day aging at 135°C.

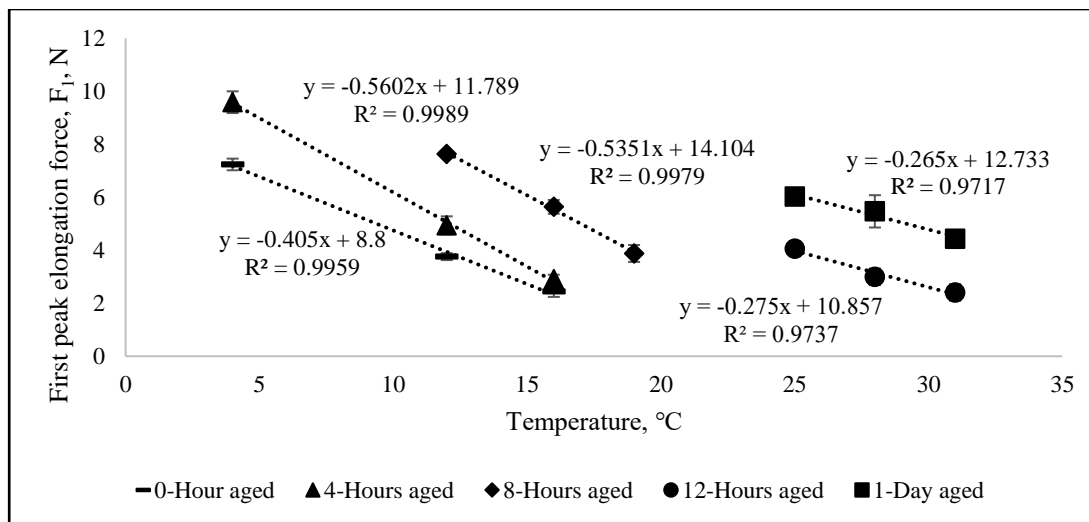


Figure 6-7: Relation between temperature and stiffness of the mixture extracted binder (aged at 135°C).

A similar decrease in F_2 value was observed in the mixture-extracted binder aged for 12 hours at 135°C, and the mixture-extracted binder aged for five days at 85°C. The reduction in F_2 value was faster than the reduction obtained from 85°C aging temperature. These reductions indicated that the degradation of SBS polymer occurred more in 4% SBS modified PG 64-22 binder mixture aging at 135°C than the mixture aging at 85°C. In conclusion, aging temperature was more significant than the aging duration in SBS polymer degradation.

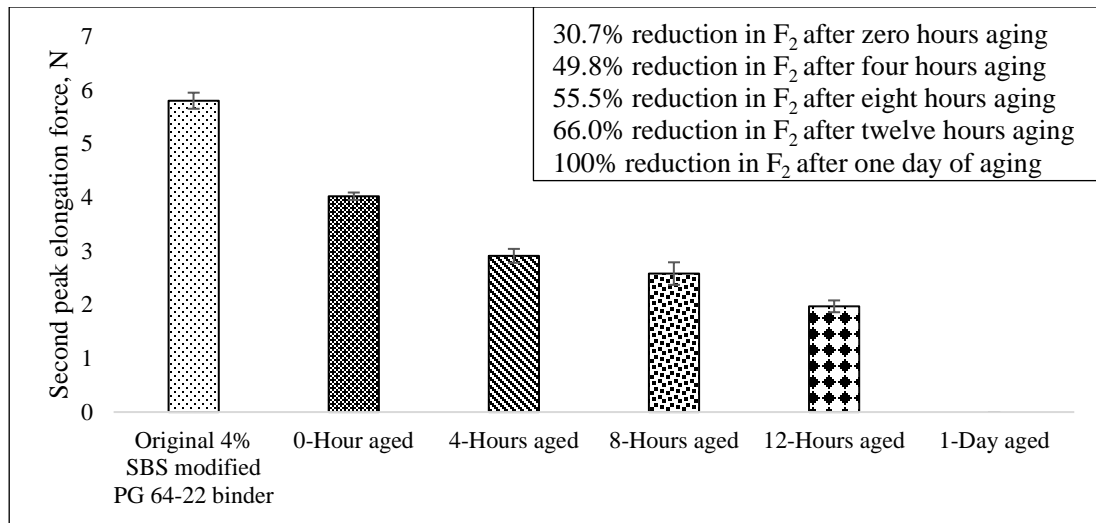


Figure 6-8: Reduction in F₂ value at similar stiffness of the SBS modified mixture extracted binder (aged at 135°C).

6.3.4 Statistical Analysis

In this study, Student's t-test for equal sample sizes and unequal variances was performed to understand the result's significance. **Table 6-2** represents the analysis result, and the Microsoft Excel software package was used to analyze the data. The null hypothesis was that the mean F₂ value of the original and mixture extracted aged binder was the same.

$$\text{Test statistics, } t_o = \frac{\bar{x}_1 - \bar{x}_2}{\sqrt{\left(\frac{s_1^2}{n_1} + \frac{s_2^2}{n_2}\right)}} \quad \text{Eq. 6-2}$$

$$\text{Degree of freedom, } \nu = \frac{\left(\frac{s_1^2}{n_1} + \frac{s_2^2}{n_2}\right)^2}{\frac{\left(\frac{s_1^2}{n_1}\right)^2}{n_1 - 1} + \frac{\left(\frac{s_2^2}{n_2}\right)^2}{n_2 - 1}} \quad \text{Eq. 6-3}$$

Table 6-2: Statistical Analysis of Laboratory aged Mixture Extracted Binder.

Binder type (mixture extracted SBS modified binder)	Test statistics, t_o	Degree of freedom, ϑ	$t_{\frac{\sigma}{2}, \vartheta} = t_{0.025, 2}$	Rejection criteria: $ t_o > t_{\frac{\sigma}{2}, \vartheta}$
Mixture extracted binder (0-Hour aged at 85°C)	18.63	$2.002 \approx 2$	= 4.303 (from standard T-table)	$18.63 > 4.303$
Mixture extracted binder (4-Hours aged at 85°C)	25.22	$2.007 \approx 2$		$25.22 > 4.303$
Mixture extracted binder (1-Day aged at 85°C)	24.26	$2.02 \approx 2$		$24.26 > 4.303$
Mixture extracted binder (3-Days aged at 85°C)	38.70	$2.002 \approx 2$		$38.70 > 4.303$
Mixture extracted binder (5-Days aged at 85°C)	16.31	$2.06 \approx 2$		$16.31 > 4.303$
Mixture extracted binder (8-Hours aged at 135°C)	21.61	$2.02 \approx 2$		$21.61 > 4.303$
Mixture extracted binder (12-Hours aged at 135°C)	35.66	$2.005 \approx 2$		$35.66 > 4.303$
Mixture extracted binder (1-Day aged at 135°C)	66.97	2		$66.97 > 4.303$

On the other hand, the alternate hypothesis was that the mean F_2 value of the original and mixture extracted aged binder was not the same. **Equations 6-2** and **6-3** were used to calculate the test statistics and degree of freedom. From **Table 6-2**, it was obvious that the null hypothesis could be rejected for all cases. It can be concluded that there was a significant difference between the mean F_2 value of the original and mixture-extracted aged binder.

6.4 Conclusion

In this study, the asphalt mixture with SBS modified binder was studied to evaluate SBS polymer degradation after laboratory aging. The following conclusions could be drawn from this study:

- Due to the high stiffness of the laboratory aged mixture extracted binder, F_2 value was not observed at low temperature from the extensional deformation test. With

the increment of temperature, the stiffness of the binder decreased as well as the F_2 value obtained.

- F_2 value of the binders was considered to obtain the degradation of SBS polymer in the laboratory aged mixture extracted binder. At the same stiffness (F_1) value, the required test temperature for evaluating the F_2 value was found from the linear relationship. Percent reduction in F_2 value of the laboratory-aged binder was calculated compared to the original binder.
- The most aged binder was found from the 1-Day laboratory aged mixture at 135°C, which showed a complete reduction in F_2 value at higher test temperature (31°C). Mixture aged for five days at 85°C showed a 65% reduction in F_2 value, which confirmed that the effect of aging temperature was more on the degradation of SBS than the aging duration.

CHAPTER 7

UNDERSTANDING OF OXIDATIVE AGING AND EVALUATION OF SBS DEGRADATION USING FT-IR SPECTRA*

7.1 Introduction

Aging reduces the long-term performance of the asphalt binder because aging makes the asphalt binder brittle and stiff. It is crucial to understand the aging mechanism to improve the service life of the asphalt pavement. Several researchers [92], [94], [118] studied the aging behavior and tried to find the relationship between the chemical and rheological properties of the aged asphalt binder. According to Li *et al.*, aging degraded the chemical, physical, and rheological performance of the neat asphalt binder [119]. Different modifiers are added to the asphalt binder for improving aging behavior. Among all the modifiers, SBS is the most used polymer for asphalt binder modification [120].

SBS is an elastomeric block copolymer that increases the elastic property of the asphalt binder. The physical and rheological properties of the base binder improve by the addition of SBS polymer [8]. SBS modified asphalt binder resists the low temperature cracking better than the unmodified binder [9]. SBS modified asphalt binder enhances the

* This chapter or portions thereof has been published previously in the RILEM International Symposium on Bituminous Materials, Lyon, France, December 2020 and International Conference on Transportation and Development, Washington, August 2020. The current version has been formatted for this dissertation.

base binder's complex modulus, resulting in high temperature rutting resistance, fatigue, and thermal cracking resistance of the pavement [7].

SBS modified asphalt binder is used to reduce pavement distress and increase the service life. However, the primary concern of using SBS modified asphalt binders in pavement construction is the degradation of SBS polymer due to aging [13], [34], [121]. Physical and rheological properties of aged SBS modified asphalt binder are different from the unaged binder because of the oxidation of the base binder and the degradation of SBS polymer [104]. On the other hand, the aged SBS modified asphalt binder shows better performance than the original aged base binder [31]. Due to the aging, the temperature susceptibility of SBS modified asphalt binder decreases, resulting in reduced low temperature cracking resistance of asphalt pavement [15].

Recently, the RT-IR spectrometer has become very popular in other modern techniques in asphalt binder research due to its abundant and accurate data obtained within a very short period with a tiny sample. Infrared (IR) spectrum region (14000cm^{-1} - 20cm^{-1}) is laid between the visible and the microwave region. The IR region is subdivided into three different regions: near, mid (4000 cm^{-1} - 500 cm^{-1}), and far IR region. Mid IR region is subdivided into two regions: group frequency region (4000 cm^{-1} - 1500 cm^{-1}) and fingerprint region (1500 cm^{-1} - 500 cm^{-1}). The absorption pattern in the fingerprint region is very characteristic, promising, and reproducible for material identification [60].

From FT-IR Spectrometer, wavenumbers at 4000 cm^{-1} - 500 cm^{-1} (mid IR region) can be obtained. Oxygen containing compounds (C=O and S=O), C=C, and C-H are observed at 1700 cm^{-1} , 1030 cm^{-1} , 1600 cm^{-1} , and 1460 cm^{-1} wavenumbers, respectively [122]. When SBS polymer is added to the asphalt binder, two peaks are found without any

overlapping. One is at 965 cm^{-1} , which is for polybutadiene content, and another is at 699 cm^{-1} , which is for polystyrene content [48]. C=C content in butadiene of SBS copolymer in SBS modified asphalt binder decreased after RTFO, PAV, and ultraviolet (UV) aging. As a result, butadiene content reduced after these three types of aging of SBS modified asphalt binder [15], [88], [123].

Recently, Hossain *et al.* [124] proposed a predictive model for determining SBS content in the SBS modified asphalt binder for field measurement. A universal curve was developed by linear regression analysis. It was observed from the FT-IR spectra that the peak of the polybutadiene functional group remained unchanged from the wavenumber 965 cm^{-1} after adding different types of binders from different sources, different SBS polymer, and a crosslinking agent (sulfur). According to the baseline correction method, peak height, and peak area at 965 cm^{-1} (polybutadiene functional group), they predicted the SBS content. Twenty-four curves were analyzed to propose the final equation for predicting the SBS content.

Currently, the rheological properties of the original and aged PG binders are mainly determined by the dynamic shear rheometer (DSR). FT-IR spectrometer can detect the carbonyl and sulfoxide content in the asphalt binders. Carbonyl content is an excellent measurement for aging in asphalt binder [118]. Liang *et al.* [121] obtained a linear relation between carbonyl and viscosity. A universal model was developed by Liu *et al.* to predict the carbonyl content after long-term aging behavior [92]. However, the chemical and rheological behavior of similarly stiff aged binders was not studied in the past. Also, there is a knowledge gap between the RTFO, PAV, UV, and oven aging at equal stiffness. Therefore, this study was initiated to understand the aging mechanism of asphalt binder at

similar stiffness by comparing the chemical and rheological behavior after four different types of aging (RTFO, PAV, UV, and forced draft oven). In addition, the degradation of SBS polymer due to aging was studied by analyzing the FT-IR spectrum.

7.1.1 Objectives

The main objectives of this study were to

1. Evaluate the characteristics of RTFO, PAV, UV, and forced draft oven aged unmodified binder using rheological and chemical tests,
2. Finding the relation between the rheological and chemical test results,
3. Determine the SBS content in SBS modified asphalt binder before and after RTFO and PAV aging using the proposed predictive model, and
4. Analyze the oxygen containing compounds of FT-IR spectrum for SBS modified binders before and after aging.

7.2 Methodology

7.2.1 Asphalt Binder

A neat unmodified PG 64-22 asphalt binder was selected to conduct the RTFO, PAV, UV, and forced draft oven aging.

7.2.2 UV and oven aging simulation test in the laboratory

In this study, UV and oven aging simulation was performed following Hossain and Wasiuddin [81]. Around 2 g of the binder was mixed in a small can with dichloromethane (DCM) to make enough liquid for the binder to spread on a 14.1 cm circular PAV plate uniformly. The UV chamber reached a constant temperature of 70°C after about 45 minutes. The PAV plate with the asphalt binder and DCM solvent was kept under the hood for drying. The dried PAV plate was placed inside the UV chamber when the UV chamber

had reached 70°C, as shown in **Figure 7-1(a)**. Similarly, a dried PAV plate was placed inside the forced draft oven at 70°C, as shown in **Figure 7-1(b)**. The thickness of the asphalt binder film was calculated to be 32 μm , and the intensity of the UV aging chamber was at 72 mW/m^2 .

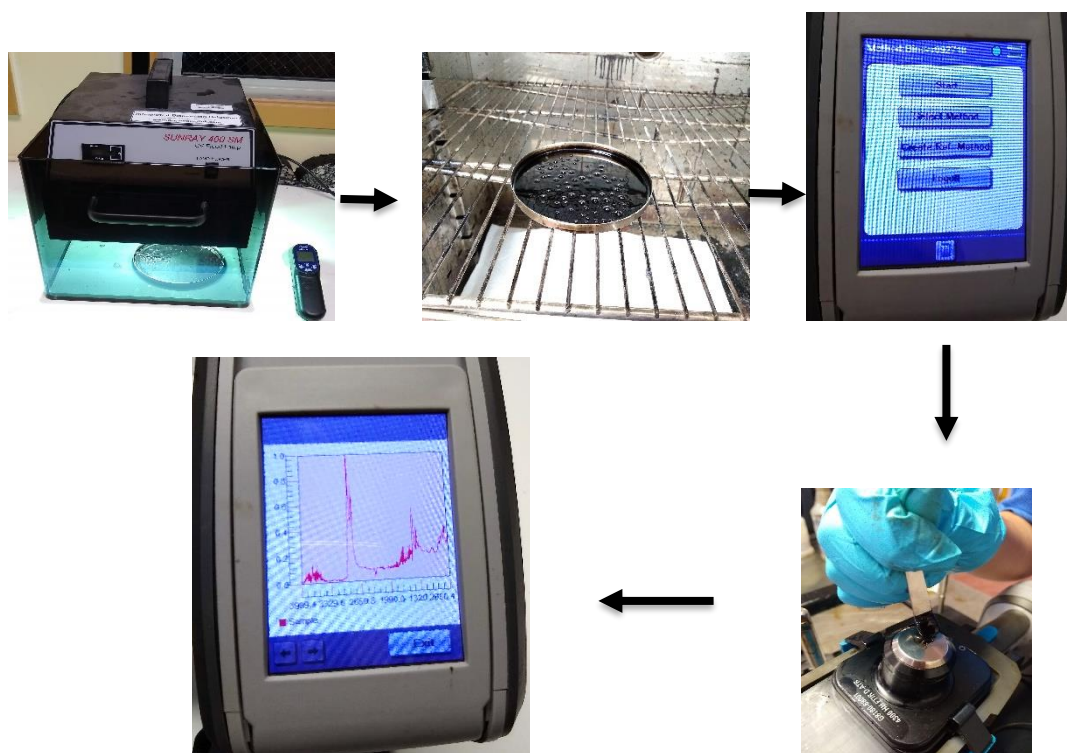


Figure 7-1: (a) UV aging of PG 64-22 binder, (b) Oven aging of PG 64-22 binder, (c) Sample placed over the FT-IRS for data collection, (d) Data collection using Microlab PC software, and (e) Spectrum after data collection.

7.2.3 Materials and Experimental Plan

In this study, different degrees of RTFO and PAV aging were performed to simulate extreme aging. RTFO aging was performed by following the AASHTO T240 standard. PAV aging was performed by following the AASHTO R28 standard except performing RTFO aging before placing the binder in the PAV chamber. Six SBS modified asphalt binders, namely PG 64-28, PG 64-34, PG 70-22, PG 70-28, and PG 76-22, were collected

from Nevada (NV), Mississippi (MS), and Washington (WA). Those binders were RTFO, and PAV aged according to AASHTO T240 and AASHTO R28, respectively. **Figure 7-2** represents the experimental flowchart of this study.

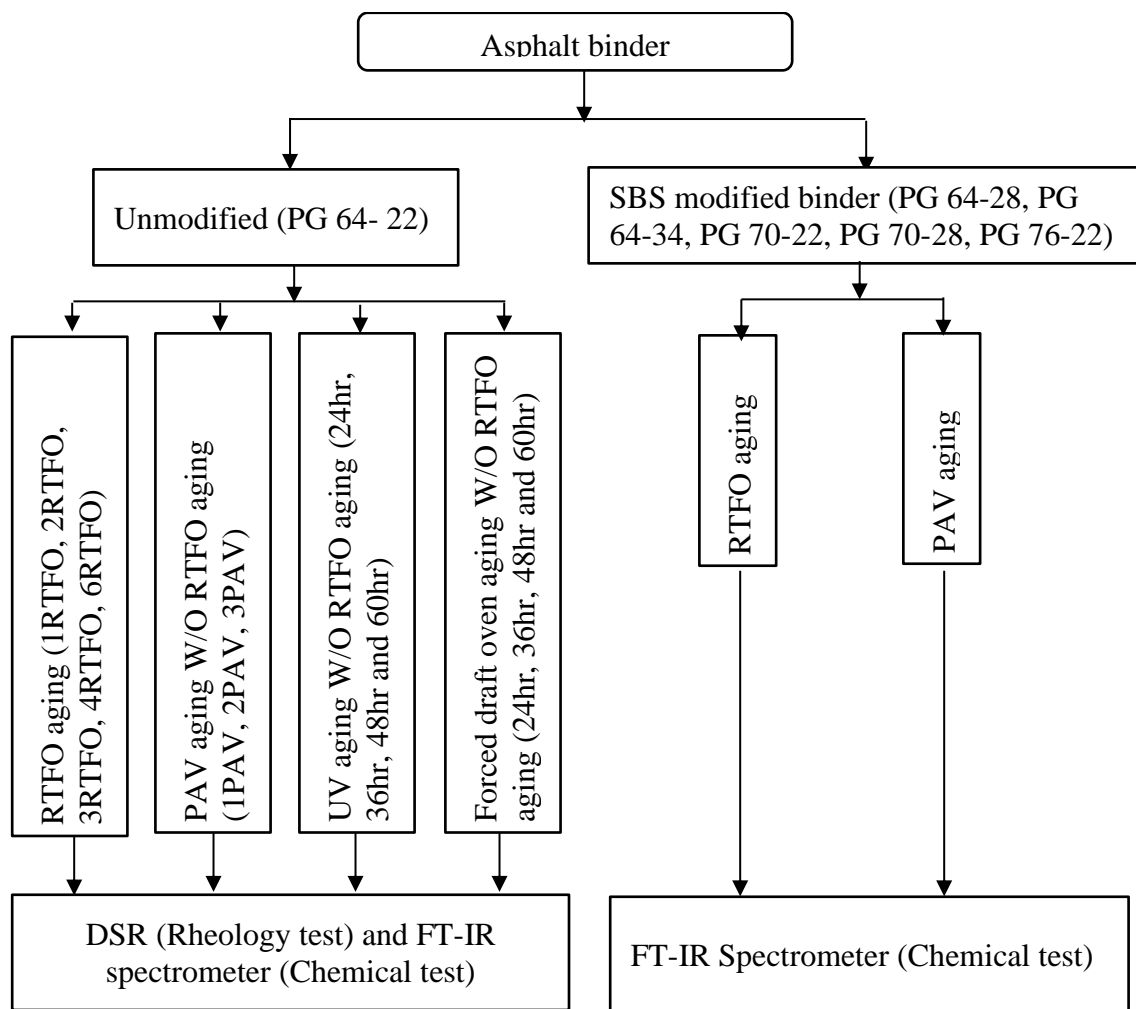


Figure 7-2: Experimental flowchart.

7.2.4 FT-IR Spectrometer Data Collection

In this study, a 4300 handheld FT-IR spectrometer with a diamond ATR (Attenuated total reflectance) sensor was used to obtain the spectrum. This type of ATR FT-IR spectrometer was considered because the collected spectrum remained unaffected by the amount of sample placed over the crystal (AASHTO T302). At first, for the FT-IR

spectrometer data collection, the asphalt binders were heated at 163°C to melt adequately. The FT-IR Spectrometer related to the laptop and Microlab PC software remained opened. After starting the software, cleaning of crystal and background checking were done. When it displayed “ensure contact with the sample,” we took a small amount of the binder at the tip of the spatula and kept over the crystal of the FT-IR spectrometer. After that, absorbance was collected by the FT-IR spectrometer from 4000 cm⁻¹ to 650 cm⁻¹ wavenumber region and a resolution of 4 cm⁻¹. A total of 10 spectra were collected for each of the binders. **Figures 7-1 (c), (d), and (e)** represent the data collection method using the FT-IR spectrometer.

7.2.5 FT-IR Spectrometer Data Analysis

Table 7-1 represents the FT-IR spectra analysis by different authors for understanding the aging of SBS modified asphalt binder before and after oxidative and UV aging. In this study, **Eqs. 7-3 and 7-4** were followed, which Hossain *et al.* [124] proposed to determine the SBS content before and after aging. For calculating the carbonyl index and sulfoxide index, **Equations 7-1 and 7-2** were followed, respectively.

Table 7-1: Literature on aging determination of SBS modified asphalt binders.

Author, year	FT-IRS data analysis for aging	
	Wavenumber	Index
Wu et al., [123]	1700cm ⁻¹ , 1030cm ⁻¹ and 968cm ⁻¹	Carbonyl, butadiene, and sulfoxide.
Xue et al., [125]	1700cm ⁻¹ and 1031cm ⁻¹	Carbonyl and sulfoxide.
Zhang et al., [88]	1603cm ⁻¹ , 1458cm ⁻¹ , 1375cm ⁻¹ , 1030cm ⁻¹ and 966cm ⁻¹	Carbonyl, butadiene, and sulfoxide.
Singh and Kumar, [122]	1700cm ⁻¹ , 1600cm ⁻¹ , 1460cm ⁻¹ , 1370cm ⁻¹ , 1240cm ⁻¹ , 1030cm ⁻¹ and 968cm ⁻¹	Aromaticity, Aliphatic, Carbonyl, sulfoxide, trans-butadiene, and trans- acetate.
Zhao et al., [15]	1700cm ⁻¹ , 1030cm ⁻¹ and 966cm ⁻¹	Carbonyl, butadiene, and sulfoxide

$$I_{C=O} = \frac{\text{Peak height at } 1695 \text{ cm}^{-1}}{\text{Peak height at } 1456 \text{ cm}^{-1}} \quad \text{Eq. 7-1}$$

$$I_{S=O} = \frac{\text{Peak height at } 1031 \text{ cm}^{-1}}{\text{Peak height at } 1456 \text{ cm}^{-1}} \quad \text{Eq. 7-2}$$

7.3 Result and Discussion

7.3.1 Analysis of Carbonyl and Sulfoxide Content

Figures 7-3 and **7-4** show the carbonyl (C=O) and sulfoxide (S=O) peak height indices of the original, RTFO, PAV, UV, and oven aged PG 64-22 binder. Due to oxidation, oxygen containing functional groups such as C=O and S=O increase in the asphalt binder. After 1RTFO, 2RTFO, 3RTFO, 4RTFO, and 6RTFO aging, the C=O index of PG 64-22 binder was increased by 23%, 36%, 54%, 65%, and 81%, respectively (**Figure 7-3**). In the case of 1PAV, 2PAV, and 3PAV aging, the C=O index was increased by 59%, 70%, and 72%, respectively (**Figure 7-3**). It was observed that after 40 hours of PAV aging, the change in the C=O index was not significant. UV and oven aged binder showed an increment of the C=O index up to 36 hrs of aging. After 36 hrs of aging, the C=O index was reduced in both cases of UV and oven aging.

As shown in **Figure 7-4**, the S=O index was increased by 1.27, 1.61, 1.91, 2.09, and 2.20 times of original binder in the case of 1RTFO, 2RTFO, 3RTFO, 4RTFO, and 6RTFO aging, respectively. In the case of 1PAV, 2PAV, and 3PAV aging, the S=O index was increased by 2.83, 3.38, and 3.96 times. In the case of UV aging, the S=O index was increased by 1.62, 1.73, 1.43, and 1.39 times after 24 h, 36 hrs, 48 hrs, and 60 hrs of aging. Again, after 24 hrs, 36 hrs, 48 hrs, and 60 hrs of oven aging, the S=O index was increased by 1.66, 2.07, 2.18, and 1.96 times. An increment of the functional groups (C=O and S=O

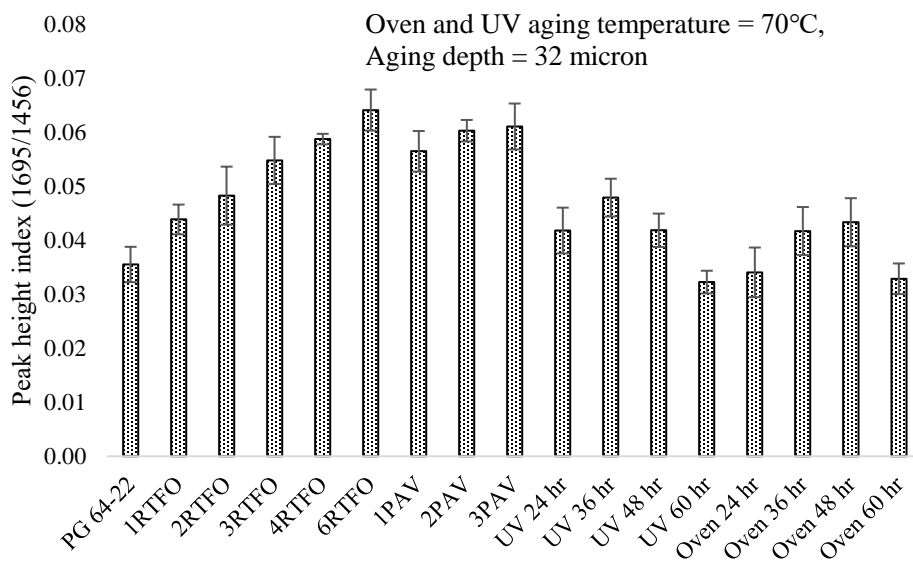


Figure 7-3: C=O peak height index ($1695\text{ cm}^{-1}/1456\text{ cm}^{-1}$) for PG 64-22 original and aged binder.

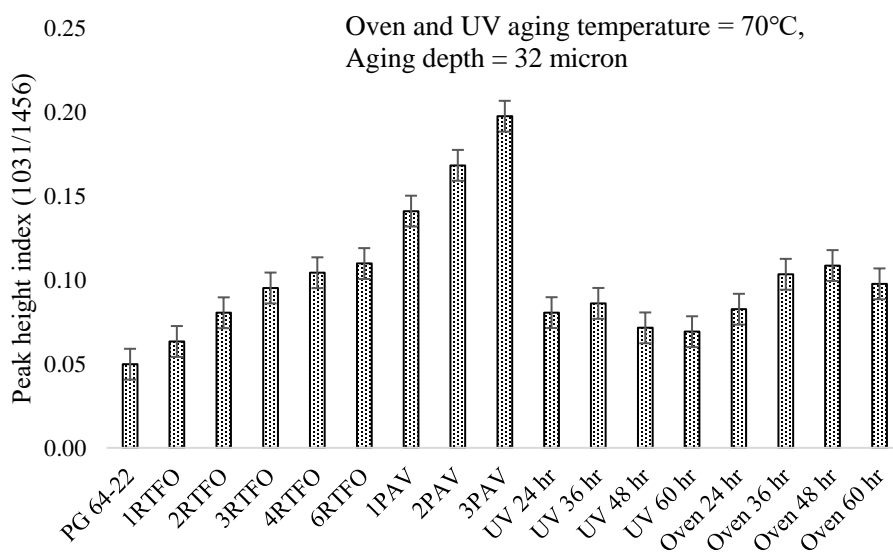


Figure 7-4: S=O peak height index ($1031\text{ cm}^{-1}/1456\text{ cm}^{-1}$) for PG 64-22 original and aged binder.

indices) can make the asphalt binder more viscous, leading to brittle and harder asphalt binder.

7.3.2 Carbonyl and Sulfoxide Indices of Aged Asphalt Binder at Similar Stiffness

From the DSR temperature sweep test, stiffness ($G^*/\sin\delta$) and phase angle (δ) values of different RTFO and PAV aged PG 64-22 binders were obtained. It was observed that 3RTFO and 1PAV, 4RTFO and 2PAV, and 6RTFO and 3PAV aged binders have similar stiffness and similar phase angle at 64°C, as shown in **Figure 7-5**. The base binder's stiffness increased by twelve times after 3RTFO and 1PAV, seven times after 4RTFO and 2PAV, and ten times after 6RTFO and 3PAV aging (**Figure 7-5a**). Again, the base binder's phase angle decreased by 11% after 3RTFO and 1PAV, 18% after 4RTFO and 2PAV, and 25% after 6RTFO and 3PAV aging (**Figure 7-5b**). Rutting depends on the binder's stiffness and phase angle. It can be concluded that extreme aging increased stiffness and reduced the phase angle of the base binder.

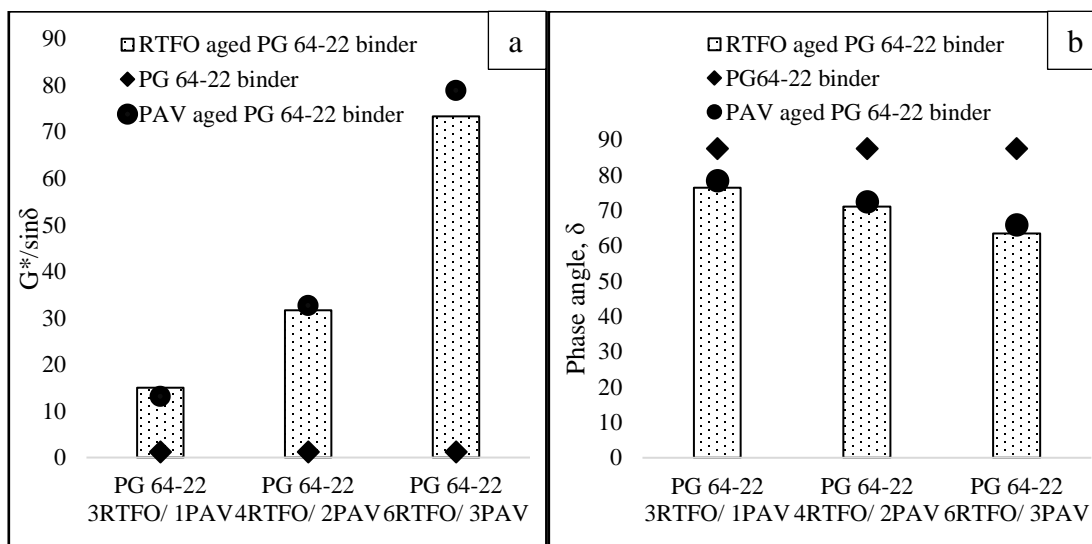


Figure 7-5: Relation between RTFO and PAV aged (W/O RTFO) PG 64-22 binder considering (a) Stiffness (b) Phase angle.

It can be observed from **Figure 7-6** that at similar stiffness and phase angle, the C=O index of RTFO and PAV aged binder was the same for two different types of indices

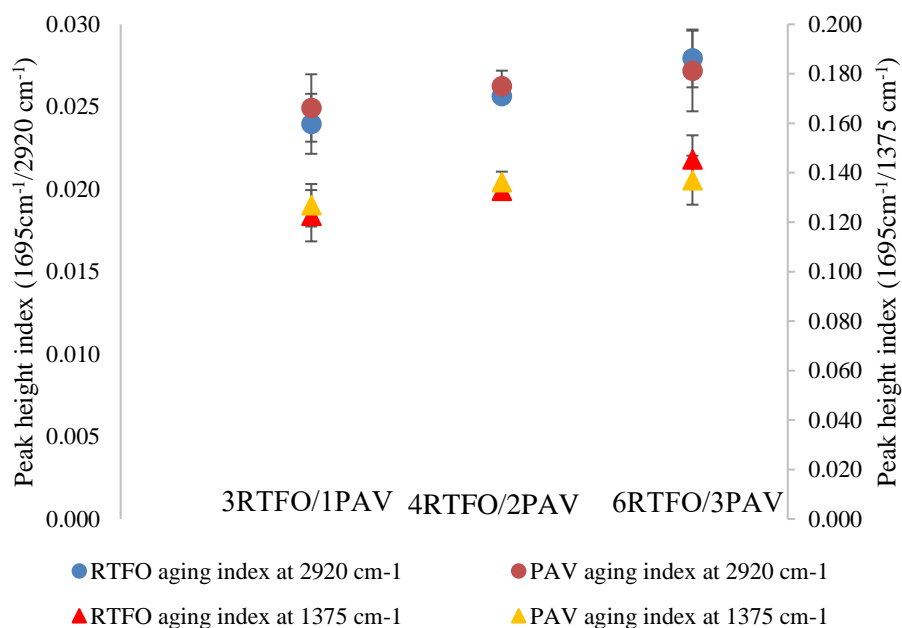


Figure 7-6: Comparison of C=O index of RTFO and PAV aged PG 64-22 binder at similar stiffness.

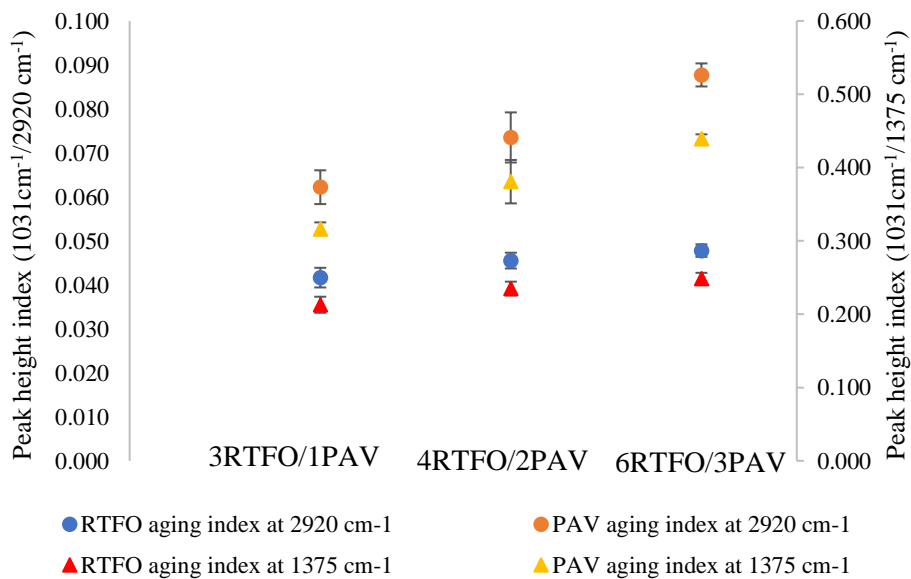


Figure 7-7: Comparison of S=O index of RTFO and PAV aged PG 64-22 binder at similar stiffness.

calculations. **Figure 7-7** represents two different types of S=O indices of RTFO and PAV aged binders at similar stiffness and phase angle. The S=O index of PAV aged samples

was higher than the S=O index of RTFO aged samples in the case of both index calculation. It can be concluded that, at similar stiffness of unmodified aged binder, the C=O index was similar. In contrast, the S=O index was not similar, which indicated the C=O index has a direct correlation with the stiffness of the binder.

7.3.3 Prediction of SBS Content in Asphalt Binder before and after Aging

In the previous study, a total of twenty-four curves were developed by analyzing the FT-IR spectra. Two analysis methods: peak area and peak height, were used in that study by considering all the contributing factors such as different PG binders, different sources of binders, different types of SBS polymer, and modification with a crosslinking agent (sulfur). In both methods, the baseline was drawn from 984 cm^{-1} to 924 cm^{-1} . Based on the peak height measurement, the final regression model was developed in that study at 965 cm^{-1} (the functional group of polybutadiene) with a correlation value of 0.97. The R^2 , RMSE, and MAE of the predicted model were 0.94, 0.0014, and 0.0010.

Using Cook's distance [68], the outliers were removed, which negatively affected the regression analysis. Using the equations, the percent error for predicting the SBS content in the laboratory prepared samples ranged from 0%-5%, and 5% in the field samples. The following two equations were used to predict the SBS content in SBS modified asphalt binder [124].

$$\text{With outlier: Peak height at } 965\text{ cm}^{-1} = 0.003814 * \text{SBS concentration} + 0.002419 \quad \text{Eq. 7-3}$$

$$\text{Without outlier: Peak height at } 965\text{ cm}^{-1} = 0.003809 * \text{SBS concentration} + 0.002413 \quad \text{Eq. 7-4}$$

Figure 7-8 represents the SBS content for the different types of modified binders before and after RTFO and PAV aging. All six binders showed a reduction in the SBS content after RTFO aging and further reduction after PAV aging. The SBS content in

Figure 7-8 was determined by using the **Equation 7-3**. The use of **Equation 7-4** also showed the same result as **Equation 7-3**. **Table 7-2** represents the percentage reduction

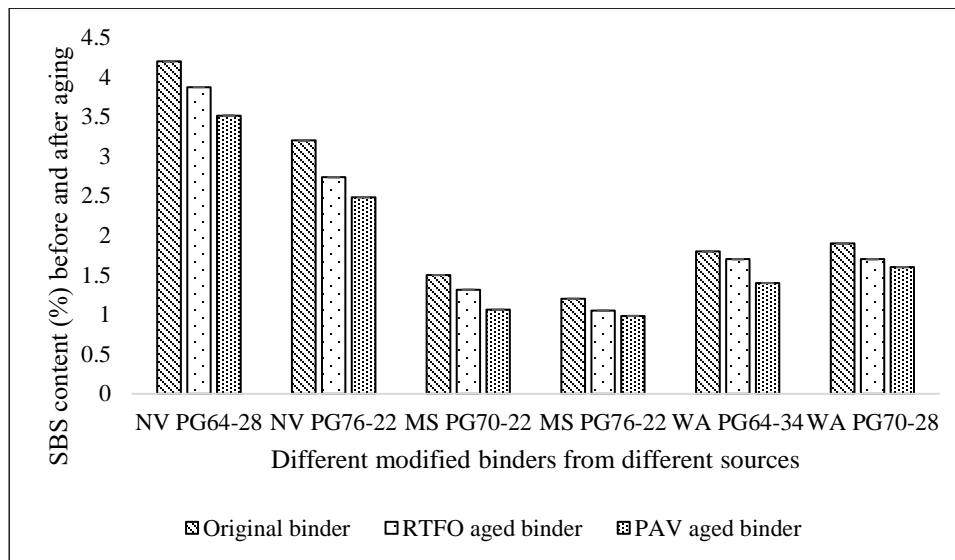


Figure 7-8: PB content of different types of modified binders from different sources after RTFO and PAV aging.

in SBS content after RTFO and PAV aging. It was found that 5.6 to 14.5% SBS content was reduced after RTFO aging. After PAV aging, 14.6-30% SBS content was reduced in all six modified binders. For predicting the SBS content, standard deviation (SD), coefficient of variation (CV), and 95% confidence interval (CI) were calculated. It was observed that the developed regression model predicted SBS concentration in the binders before and after aging varying with ± 0.02 to ± 0.11 concentration (%) accuracy at 95% CI. From the above results, it can be concluded that SBS polymer degraded after RTFO and PAV aging.

Table 7-2: Reduction in SBS content (%) after RTFO and PAV aging.

Binder	Source	Binder condition	SBS content (%)	%Reduction after aging	SD	CV	CI	95% upper CI	95% lower CI
PG 64-28	NV	Original	4.2		0.0003	1.37	0.02	4.2	4.2
		RTFO aged	3.9	7.46	0.0008	4.48	0.06	3.9	3.9
		PAV aged	3.5	16.06	0.0005	3.15	0.04	3.5	3.5
PG 76-22	NV	Original	3.2		0.0015	9.95	0.13	3.2	3.2
		RTFO aged	2.7	14.46	0.0009	7.01	0.11	2.7	2.7
		PAV aged	2.5	22.33	0.0007	6.26	0.09	2.5	2.5
PG 70-22	MS	Original	1.5		0.000	5.99	0.04	1.5	1.5
		RTFO aged	1.3	13.19	0.000	4.32	0.02	1.3	1.3
		PAV aged	1.1	29.91	0.000	6.35	0.03	1.1	1.1
PG 76-22	MS	Original	1.2		0.0003	3.83	0.02	1.2	1.2
		RTFO aged	1.1	8.88	0.0003	5.36	0.03	1.1	1.0
		PAV aged	1.0	14.59	0.0004	7.26	0.04	1.0	1.0
PG 64-34	WA	Original	1.8		0.000	4.253	0.05	1.8	1.8
		RTFO aged	1.7	5.56	0.000	2.019	0.02	1.7	1.7
		PAV aged	1.5	16.67	0.000	2.735	0.08	1.5	1.5
PG 70-28	WA	Original	1.9		0.000	3.313	0.03	1.9	1.9
		RTFO aged	1.7	10.53	0.001	3.867	0.11	1.7	1.7
		PAV aged	1.6	15.79	0.000	5.703	0.06	1.6	1.6

7.3.4 Carbonyl and Sulfoxide Indices of Aged SBS Modified Asphalt Binders

Aging does not produce any new functional group in unmodified or modified asphalt binder; it only changes the content in some functional groups [122]. **Figures 7-9** and **7-10** represent the carbonyl (C=O) and sulfoxide (S=O) content of different types of SBS modified asphalt binders from different sources before and after RTFO and PAV aging. It was clearly observed from the figures that C=O and S=O indices increased after

RTFO and PAV aging in all the six modified binders. In the case of RTFO aging, the C=O index was increased by 40%, 65%, 6%, 10%, 30%, and 13% for NV PG 64-28, NV PG 76-22, MS PG 70-22, MS PG 76-22, WA PG 64-34, and WA PG 70-28 SBS modified asphalt binder, respectively (compared to the original binder).

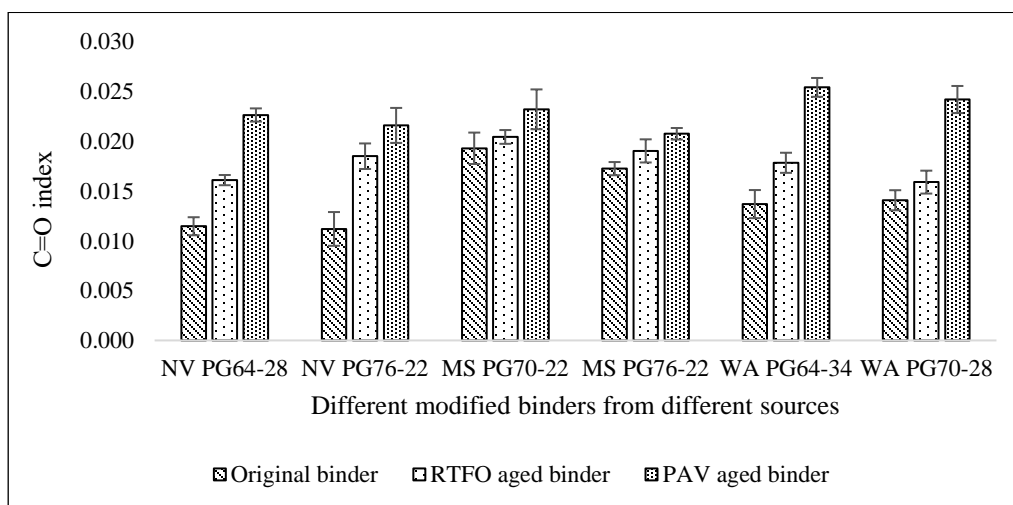


Figure 7-9: Carbonyl content of different modified binders from different sources before and after RTFO and PAV aging.

After PAV aging, the C=O index was increased by 97%, 93%, 20%, 20%, 86%, and 72% of the original binder in the case of NV PG 64-28, NV PG 76-22, MS PG 70-22, MS PG 76-22, WA PG 64-34, and WA PG 70-28 SBS modified asphalt binder, respectively. After RTFO aging, the S=O index was increased by 79%, 42%, 33%, 70%, 57%, and 30% in the case of NV PG 64-28, NV PG 76-22, MS PG 70-22, MS PG 76-22, WA PG 64-34, and WA PG 70-28 SBS modified asphalt binder respectively (compared to the original binder). After PAV aging, the S=O index was increased by 4.2 times, 2.5 times, 2.5 times, 3.1 times, 3 times, 3.1 times, and 2.6 times of original binder in the case of NV PG 64-28, NV PG 76-22, MS PG 70-22, MS PG 76-22, WA PG 64-34, and WA PG 70-28 SBS modified asphalt binder, respectively. The increment in C=O and S=O indices indicates the

increment in oxygen containing compounds. It can be concluded that the increment in the S=O index of SBS modified asphalt binder after RTFO and PAV aging was more than the increment in C=O index of aged SBS modified asphalt binder.

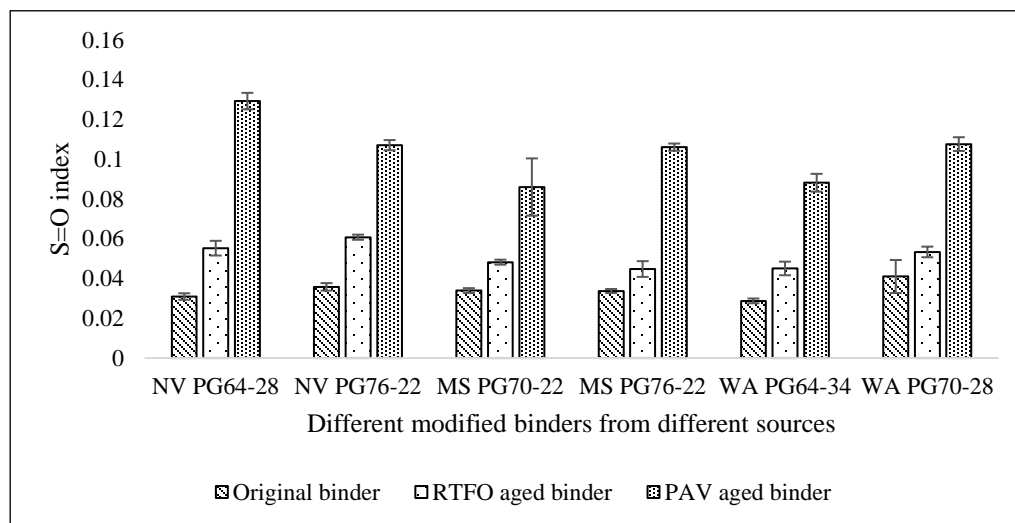


Figure 7-10: Sulfoxide content of different modified binders from different sources before and after RTFO and PAV aging.

7.4 Conclusions

A comparative study between original asphalt binder and four different types of aged (RTFO, PAV, UV, and forced draft oven) binders were performed to understand the rheological and chemical behaviors and determine the relationship between the rheological and chemical properties. For SBS modified asphalt binder, a model from the previous study was used to predict the SBS content before and after aging. The following conclusions can be drawn from this study:

- In the case of the original binder, oxygen containing functional groups increased after different degrees of RTFO and PAV aging. On the other hand, after UV and oven aging, these compounds increased up to a certain time and

decreased. Stiffness and phase angle values were similar in higher degrees of RTFO aging and higher degrees of PAV aging.

- The C=O content of the aged binders was the same at similar stiffness, which indicates C=O content correlates with the binder's stiffness. In contrast, at similar stiffness, the S=O content of the PAV aged binder was higher than the RTFO aged binder.
- In the previous study, Hossain *et al.* [124] proposed a model to predict the SBS content in SBS modified asphalt binder through linear regression analysis of FT-IR spectra. Hossain *et al.* observed that the polybutadiene functional group at wavenumber 965 cm^{-1} did not change with different PG binders, different sources of binders, different types of SBS polymer, and addition of crosslinking agent (sulfur).
- After RTFO and PAV aging, SBS content decreased, which indicated SBS polymer degraded after aging. After RTFO aging, 5.6-14.5% SBS content was decreased and after PAV aging 14.6-30% SBS content was decreased.
- In the case of SBS modified asphalt binder, oxygen containing compounds, carbonyl, and sulfoxide also increased after RTFO and PAV aging. The increment in the S=O index was higher than the increment in the C=O index.

CHAPTER 8

CONCLUSIONS AND RECOMMENDATIONS

8.1 Conclusions

The overall objectives of this study were to determine SBS polymer content in asphalt binder and evaluate the degradation of the polymer due to oxidative aging through mechanical and chemical analyses. The findings from each of the specific objectives were presented at the end of the corresponding chapter.

8.1.1 SBS Polymer Quantification by Mechanical Analysis

The major findings from this study are stated below:

- The novel extensional deformation test can identify different modifiers in asphalt binder and their effectiveness. The first peak elongation force, F_1 , is the binder's stiffness and the second peak elongation force, F_2 , is the modifier's stiffness. Styrene-butadiene-styrene (SBS), styrene-butadiene-rubber (SBR) latex, and crumb rubber (CR) modified binder showed F_2 value among the five modifiers. On the other hand, polyphosphoric acid (PPA), and high density polyethylene (HDPE) did not show any F_2 value.
- It was observed that the stiffness (F_1) values of the PPA and HDPE modified asphalt binders were higher than the stiffness values of the SBS, SBR latex, and CR modified binders. On the other hand, the SBS modified binder showed the highest

F_2 value among SBS, SBR latex, and CR modified binder, indicating it can elongate more before cracking than the other two types of the modifiers. Therefore, it can be concluded that SBS was more effective in the modification of asphalt binder than the SBR latex and CR. F_1 has no linear correlation with the percent of polymer and the F_2 value has a linear correlation with the percent of the polymer. Temperature sweep tests and multiple stress creep recovery tests indicated that the F_2 value proposed in this new test method was a better indicator of polymer content than the rutting parameter, $G^*/\sin\delta$, and the non-recoverable creep compliance, J_{nr} .

8.1.2 SBS Polymer Quantification by Chemical Analysis

The findings from this analysis are summarized below:

- In this study, an FT-IR spectrometer with a diamond attenuated total reflectance (ATR) sensor was used to investigate the effect of variation in performance grade (PG) binders, SBS polymers, and the addition of cross-linking agent on the peak absorbance height at 965 cm^{-1} , which is accountable for polybutadiene (PB) functional group. A prediction model was developed by the linear regression analysis after observing the negligible effect of the factors mentioned earlier. The regression model was developed based on the relation between the peak absorbance height and the SBS content. The regression model can be used to predict the SBS content in the asphalt binder with unknown SBS content. The whole process for SBS content prediction required 30 minutes in the in-situ condition.
- Another study performed developed a universal model for quantifying SBS polymer in the asphalt binder considering the polystyrene (PS) functional group at 699 cm^{-1} . The PS regression model was developed from the peak absorbance height

measurement. Eleven SBS modified asphalt binders were collected from three different refineries to validate the model. SBS content was predicted from those binders using the developed models, and the results were sent to the refinery to verify the actual SBS content. Finally, the PS model was selected based on the verification results. The model fit test, KS, also showed that the PS model was the best fit. Therefore, it was recommended that the handheld FT-IR spectrometer can be implemented as a quality control tool in the field for quantifying the SBS polymer in asphalt binder.

8.1.3 Evaluation of SBS Polymer Degradation by Mechanical Analysis

The major conclusions from this study are stated below:

- In this study, the novel extensional deformation method was used to evaluate the degradation of SBS polymer due to oxidative aging. The F_2 value obtained from the extensional deformation test indicates the SBS polymer characteristics. It was hypothesized that a decrease in the F_2 value indicates degradation of SBS polymer. It was observed that F_2 value decreased after rolling thin film oven (RTFO) aging and further decreased after pressure aging vessel (PAV) aging. Reduction in the F_2 value was observed for similarly stiff original, RTFO, and PAV aged binders. This reduction confirms that polymer degrades due to oxidative aging.
- A similar reduction was observed in F_2/F_1 value due to RTFO and PAV aging that was studied to normalize the stiffness effect. Therefore, F_2/F_1 value is recommended as a polymer degradation parameter due to aging. On the other hand, ultraviolet (UV) aged SBS modified asphalt binder did not show any F_2 value at

higher test temperatures, confirming the complete degradation of SBS polymer due to UV aging.

- Laboratory aging was performed for the asphalt mixture with SBS modified binder to evaluate the SBS polymer degradation. Due to the high stiffness of the laboratory aged mixture extracted binder, the F_2 value was not observed at low temperature from the extensional deformation test. With the increment in test temperature, the stiffness of the binder decreased as well as the F_2 value obtained. At the same stiffness (F_1) value, the required test temperature for evaluating the F_2 value was found from the linear relationship. Percent reduction in F_2 value of the laboratory aged binder was calculated compared to the original binder. The most aged binder was found from the 1-Day laboratory aged mixture at 135°C, which showed a complete reduction in F_2 value. On the other hand, the mixture aged for five days at 85°C showed a 65% reduction in F_2 value, which confirmed that the effect of aging temperature was more than the aging duration.

8.1.4 Evaluation of SBS Polymer Degradation by Chemical Analysis

The major conclusions from this study are:

- A comparative study between the original asphalt binder and four different types of aged binder was performed to understand the rheological and chemical behaviors and determine the relationship between the rheological and chemical properties. For SBS modified asphalt binder, a linear regression model from the previous study was used to predict the SBS content before and after aging. The oxygen containing functional groups increased after different degrees of RTFO and PAV aging. Stiffness and phase angle values were similar in higher degrees of RTFO and PAV

aging. At similar stiffness, the carbonyl content of the aged binders was the same, indicating carbonyl content correlates with the binder's stiffness. In contrast, at similar stiffness, the sulfoxide content of the PAV aged binders was higher than the RTFO aged binders, indicating no relation with binder's stiffness.

- In the case of SBS modified asphalt binder, SBS content reduced after RTFO aging, and further reduced after PAV aging, which indicated SBS polymer degraded after oxidative aging. The oxygen containing compounds, carbonyl, and sulfoxide also increased after RTFO and PAV aging. Furthermore, the increment in the sulfoxide content was higher than the increment in the carbonyl content.

8.2 Recommendations for Future Work

The most important recommendations from this study are stated below:

- The developed extensional deformation test should be proposed as a new method for identifying polymer and determining polymer content in the asphalt binder. The second peak force should be specified for all the same polymer modified PG binders (such as PG 76-22, PG 70-28, PG 64-34). However, the specifications or the pass/fail criteria for each type of binder must developed in future study before implementation.
- For determining the SBS polymer content in an unknown asphalt binder using SER, additional work needs to be performed to build a universal calibration curve. The universal calibration curve should be based on the equal stiffness temperature.
- Besides, low temperature cracking susceptibility of polymer modified asphalt binder can be studied using the novel extensional deformation test method. A model can be developed for polymer content determination considering the presence of

cross-linking agents and additives. Also, peak height and peak area measurements at second peak elongation force can be considered for developing the model.

- Recently, the linear amplitude sweep LAS test (AASHTO TP 101) has become very popular for measuring the fatigue performance of the binder as well as of the mixture. Asphalt pavement analyzer—APA (AASHTO T 340) and semi-circular bending—SCB (ASTM D 8044) tests are the commonly used asphalt pavement performance test method. Extensional deformation test parameters can be analyzed to correlate with the standard pavement performance test results.
- A mathematical model can be established in future studies to predict the polymer characteristics under extensional deformation. The ductility and stiffness of the asphalt binder and polymer can be studied, respectively. The effect of the temperature on extensional deformation can also be studied.
- Styrene-butadiene (S/B) ratio can affect the peak absorbance at 965 cm^{-1} wavenumber. In the future study, the S/B ratio should be considered for updating the developed model in this study. Additionally, two significant peaks (vinyl and cis) were observed in the FT-IR spectrum in three different SBS modified asphalt binders that were tested. Those peaks can be investigated to improve the model. SBS polymer structure depends on the polymerization technique. Therefore, SBS polymer should be collected from other sources than the two sources mentioned in this study. Comparison of the significant peaks (vinyl, cis and trans) should be investigated in future studies with the SBS polymer from different sources.

REFERENCES

- [1] 117th Congress Educational Kits, “https://www.asphalt pavement.org/uploads/documents/117th_Congress_Education_KitFINAL.pdf.”
- [2] D. Anderson, J. Youtcheff, and M. Zupanick, “Asphalt binders,” *Transportation in the New Millennium*, 2000.
- [3] L. H. Lewandowski, “Polymer modification of paving asphalt binders,” *Rubber Chemistry and Technology*, vol. 67, no. 3, pp. 447–480, 1994.
- [4] J.-S. Chen, M.-C. Liao, and H.-H. Tsai, “Evaluation and optimization of the engineering properties of polymer-modified asphalt,” *Practical Failure Analysis*, vol. 2, no. 3, pp. 75–83, 2002.
- [5] Y. Becker, M. P. Mendez, and Y. Rodriguez, “Polymer modified asphalt,” 2001.
- [6] J.-S. Chen, M.-C. Liao, and M.-S. Shiah, “Asphalt modified by styrene-butadiene-styrene triblock copolymer: Morphology and model,” *Journal of materials in civil engineering*, vol. 14, no. 3, pp. 224–229, 2002.
- [7] M. S. Cortizo, D. O. Larsen, H. Bianchetto, and J. L. Alessandrini, “Effect of the thermal degradation of SBS copolymers during the ageing of modified asphalts,” *Polymer Degradation and Stability*, vol. 86, no. 2, pp. 275–282, 2004.
- [8] A. Abdelaziz, C.-H. Ho, and M. Snyder, “Evaluating the influence of polymer modified asphalt binders on low temperature properties,” in *MATEC Web of Conferences*, 2018, vol. 163, p. 05012.
- [9] P. Lin, W. Huang, Y. Li, N. Tang, and F. Xiao, “Investigation of influence factors on low temperature properties of SBS modified asphalt,” *Construction and Building Materials*, vol. 154, pp. 609–622, 2017.
- [10] K. Al-Adham and H. A.-A. Wahhab, “Influence of temperature on Jnr values of polymer modified asphalt binders,” *International Journal of Pavement Research and Technology*, vol. 11, no. 6, pp. 603–610, 2018.

- [11] A. Adedeji, T. Grünfelder, F. S. Bates, C. W. Macosko, M. Stroup-Gardiner, and D. E. Newcomb, "Asphalt modified by SBS triblock copolymer: structures and properties," *Polymer Engineering & Science*, vol. 36, no. 12, pp. 1707–1723, 1996.
- [12] X. Lu and U. Isacsson, "Modification of road bitumens with thermoplastic polymers," *Polymer testing*, vol. 20, no. 1, pp. 77–86, 2000.
- [13] F. Zhang, J. Yu, and J. Han, "Effects of thermal oxidative ageing on dynamic viscosity, TG/DTG, DTA and FTIR of SBS-and SBS/sulfur-modified asphalts," *Construction and Building Materials*, vol. 25, no. 1, pp. 129–137, 2011.
- [14] Y. Zhao, F. Gu, J. Xu, and J. Jin, "Analysis of aging mechanism of SBS polymer modified asphalt based on Fourier transform infrared spectrum," *Journal of Wuhan University of Technology-Mater. Sci. Ed.*, vol. 25, no. 6, pp. 1047–1052, 2010.
- [15] G. Hao, W. Huang, J. Yuan, N. Tang, and F. Xiao, "Effect of aging on chemical and rheological properties of SBS modified asphalt with different compositions," *Construction and Building Materials*, vol. 156, pp. 902–910, 2017.
- [16] M. L. Sentmanat, "Miniature universal testing platform: from extensional melt rheology to solid-state deformation behavior," *Rheologica acta*, vol. 43, no. 6, pp. 657–669, 2004.
- [17] G. R. Morrison, J. K. Lee, and S. A. M. Hesp, "Chlorinated polyolefins for asphalt binder modification," *Journal of Applied Polymer Science*, vol. 54, no. 2, pp. 231–240, 1994.
- [18] S. Rahman Nafis and N. M. Wasiuddin, "Field Performance Analysis of Open Graded Friction Course: A Case Study in Shreveport, Louisiana," in *Airfield and Highway Pavements 2021*, pp. 293–305.
- [19] G. L. Baumgardner, J. F. Masson, J. R. Hardee, A. M. Menapace, and A. G. Williams, "Polyphosphoric acid modified asphalt: proposed mechanisms," *Journal of the Association of Asphalt Paving Technologists*, vol. 74, pp. 283–305, 2005.
- [20] Q. Ye and H. Fu, "Rheological properties of polyphosphoric acid modified asphalt binder," 2014.
- [21] A. Forbes, R. G. Haverkamp, T. Robertson, J. Bryant, and S. Bearsley, "Studies of the microstructure of polymer-modified bitumen emulsions using confocal laser scanning microscopy," *Journal of microscopy*, vol. 204, no. 3, pp. 252–257, 2001.
- [22] R. Hossain, M. R. Islam, and N. M. Wasiuddin, "A Comparative Study between Emulsion Residue Recovery Methods Based on Polymer Degradation," in *TRANSET 2020*, American Society of Civil Engineers Reston, VA, 2021, pp. 205–214.

- [23] K. Takamura and W. Heckmann, "Polymer network formation in the pavement using SBR latex modified asphalt emulsions," in *Studies in Surface Science and Catalysis*, vol. 132, Elsevier, 2001, pp. 271–274.
- [24] M. Shafii, J. Ahmad, and E. Shaffie, "Physical properties of asphalt emulsion modified with natural rubber latex," *World Journal of Engineering*, 2013.
- [25] Y. Chen, G. Tebaldi, R. Roque, and G. Lopp, "Effects of Polymer Modified Asphalt Emulsion (PMAE) on Pavement Reflective Cracking Performance," in *7th RILEM International Conference on Cracking in Pavements*, 2012, pp. 879–888.
- [26] H. Siswanto, "The effect of latex on permanent deformation of asphalt concrete wearing course," *Procedia engineering*, vol. 171, pp. 1390–1394, 2017.
- [27] C. S. Ruggles, "The efficient use of environmentally-friendly natural rubber latex in road construction-past, present and the future," *Rubber in Transport: Breda, The Netherlands*, 2004.
- [28] M. Anwar Parvez, M. Al-Mehthel, H. I. Al-Abdul Wahhab, and I. A. Hussein, "Utilization of sulfur and crumb rubber in asphalt modification," *Journal of Applied Polymer Science*, vol. 131, no. 7, 2014.
- [29] A. Pérez-Lepe, F. J. Martínez-Boza, and C. Gallegos, "Influence of polymer concentration on the microstructure and rheological properties of high-density polyethylene (HDPE)-modified bitumen," *Energy & fuels*, vol. 19, no. 3, pp. 1148–1152, 2005.
- [30] R. Hossain, W. M. Omer, and N. M. Wasiuddin, "Evaluation of degradation of polymer due to aging in asphalt binder using a novel and DSR-based extensional deformation test," in *Advances in Materials and Pavement Performance Prediction*, CRC Press, 2018, pp. 167–170.
- [31] H. Al-Abdul-Wahhab and G. Al-Amri, "Laboratory evaluation of reclaimed rubber asphaltic concrete mixes," *Journal of Materials in Civil Engineering*, vol. 3, no. 3, pp. 189–203, 1991.
- [32] P. Shirodkar, Y. Mehta, A. Nolan, K. Dahm, R. Dusseau, and L. McCarthy, "Characterization of creep and recovery curve of polymer modified binder," *Construction and Building Materials*, vol. 34, pp. 504–511, 2012.
- [33] Q. Zhang, W. Fan, T. Wang, and G. Nan, "Studies on the temperature performance of SBR modified asphalt emulsion," in *2011 International Conference on Electric Technology and Civil Engineering (ICETCE)*, 2011, pp. 730–733.
- [34] R. Hossain, S. Arafat, and N. M. Wasiuddin, "Identification and Evaluation of the Elastomeric, Plastomeric, and Chemical Modifiers in Asphalt Binders," in *Airfield and Highway Pavements 2019: Testing and Characterization of Pavement Materials*, American Society of Civil Engineers Reston, VA, 2019, pp. 255–265.

- [35] A. Behnood and J. Olek, "Rheological properties of asphalt binders modified with styrene-butadiene-styrene (SBS), ground tire rubber (GTR), or polyphosphoric acid (PPA)," *Construction and Building Materials*, vol. 151, pp. 464–478, 2017.
- [36] J. Li *et al.*, "Preparation and properties of sbs-g-gos-modified asphalt based on a thiol-ene click reaction in a bituminous environment," *Polymers*, vol. 10, no. 11, p. 1264, 2018.
- [37] A. Goli, H. Ziari, and A. Amini, "Influence of carbon nanotubes on performance properties and storage stability of SBS modified asphalt binders," *Journal of Materials in Civil Engineering*, vol. 29, no. 8, p. 04017070, 2017.
- [38] S. Luo, J. Tian, Z. Liu, Q. Lu, K. Zhong, and X. Yang, "Rapid determination of styrene-butadiene-styrene (SBS) content in modified asphalt based on Fourier transform infrared (FTIR) spectrometer and linear regression analysis," *Measurement*, vol. 151, p. 107204, 2020.
- [39] R. Hossain and N. M. Wasiuddin, "A Novel method for polymer content determination in asphalt binder and emulsion," *International Journal of Pavement Research and Technology*, vol. 12, no. 6, pp. 604–612, 2019.
- [40] S. D. Diefenderfer, "Detection of polymer modifiers in asphalt binder.," Virginia Transportation Research Council, 2006.
- [41] U. Isacson and X. Lu, "Properties of bitumens modified with elastomers and plastomers," 2000.
- [42] M. McCann, J. F. Rovani, and K. P. Thomas, "Detection of Polymers in Asphalt Binders," in *Transportation and Development Institute Congress 2011: Integrated Transportation and Development for a Better Tomorrow*, 2011, pp. 514–527.
- [43] W. H. Daly, I. Negulescu, and S. S. Balamurugan, "Implementation of GPC characterization of asphalt binders at Louisiana materials laboratory.," Louisiana. Dept. of Transportation and Development, 2013.
- [44] H. I. A.-A. Wahhab, I. M. Asi, F. M. Ali, and I. A. Al-Dubabi, "Prediction of asphalt rheological properties using HP-GPC," *Journal of materials in civil engineering*, vol. 11, no. 1, pp. 6–14, 1999.
- [45] A. Zofka, *Evaluating applications of field spectroscopy devices to fingerprint commonly used construction materials*. Transportation Research Board, 2013.
- [46] C. W. Curtis, D. I. Hanson, S. T. Chen, G.-J. Shieh, and M. Ling, "Quantitative determination of polymers in asphalt cements and hot-mix asphalt mixes," *Transportation research record*, no. 1488, 1995.

- [47] J. Masson, L. Pelletier, and P. Collins, "Rapid FTIR method for quantification of styrene-butadiene type copolymers in bitumen," *Journal of Applied Polymer Science*, vol. 79, no. 6, pp. 1034–1041, 2001.
- [48] M. Ling, C. W. Curtis, D. I. Hanson, and J. N. Hool, "Quantitative analysis of polymers and crumb rubber in hot-mix asphalts," *Transportation research record*, vol. 1586, no. 1, pp. 57–67, 1997.
- [49] Q. Lu, M. Gunaratne, and L. Guo, "Field Test Method to Determine Presence and Quantity of Modifiers in Liquid Asphalt," 2015.
- [50] D. Q. Sun, L. W. Zhang, and X. L. Zhang, "Quantification of SBS content in SBS polymer modified asphalt by FTIR," in *Advanced Materials Research*, 2011, vol. 287, pp. 953–960.
- [51] K. Hu, S. Han, Z. Liu, and D. Niu, "Determination of morphology characteristics of polymer-modified asphalt by a quantification parameters approach," *Road Materials and Pavement Design*, vol. 20, no. 6, pp. 1306–1321, 2019.
- [52] Q. Wang, S. Li, X. Wu, S. Wang, and C. Ouyang, "Weather aging resistance of different rubber modified asphalts," *Construction and Building Materials*, vol. 106, pp. 443–448, 2016.
- [53] M. R. S. Fernandes, M. M. C. Forte, and L. F. M. Leite, "Rheological evaluation of polymer-modified asphalt binders," *Materials research*, vol. 11, no. 3, pp. 381–386, 2008.
- [54] S. Nasrazadani, D. Mielke, T. Springfield, and N. Ramasamy, "Practical applications of FTIR to characterize paving materials," 2010.
- [55] A. Whelan, *Polymer technology dictionary*. Springer Science & Business Media, 2012.
- [56] A. Behnood and M. M. Gharehveran, "Morphology, rheology, and physical properties of polymer-modified asphalt binders," *European Polymer Journal*, vol. 112, pp. 766–791, 2019.
- [57] E. Birkel and L. Rodriguez-Saona, "Application of a portable handheld infrared spectrometer for quantitation of trans fat in edible oils," *Journal of the American Oil Chemists' Society*, vol. 88, no. 10, pp. 1477–1483, 2011.
- [58] R. Davis and L. J. Mauer, "Fourier transform infrared (FT-IR) spectroscopy: a rapid tool for detection and analysis of foodborne pathogenic bacteria," *Current research, technology and education topics in applied microbiology and microbial biotechnology*, vol. 2, pp. 1582–1594, 2010.
- [59] M. R. Derrick, D. Stulik, and J. M. Landry, *Infrared spectroscopy in conservation science*. Getty Publications, 2000.

- [60] S. B. Munteanu and C. Vasile, "Spectral and thermal characterization of styrene-butadiene copolymers with different architectures," *Journal of Optoelectronics and Advanced materials*, vol. 7, no. 6, p. 3135, 2005.
- [61] B. Hofko, M. Z. Alavi, H. Grothe, D. Jones, and J. Harvey, "Repeatability and sensitivity of FTIR ATR spectral analysis methods for bituminous binders," *Materials and Structures*, vol. 50, no. 3, pp. 1–15, 2017.
- [62] J.-S. Chen and C. C. Huang, "Fundamental characterization of SBS-modified asphalt mixed with sulfur," *Journal of applied polymer science*, vol. 103, no. 5, pp. 2817–2825, 2007.
- [63] W. Huang and N. Tang, "Characterizing SBS modified asphalt with sulfur using multiple stress creep recovery test," *Construction and Building Materials*, vol. 93, pp. 514–521, 2015.
- [64] T. Mandal, R. Sylla, H. U. Bahia, and S. Barmand, "Effect of cross-linking agents on the rheological properties of polymer-modified bitumen," *Road Materials and Pavement Design*, vol. 16, no. sup1, pp. 349–361, 2015.
- [65] V. O. Bulatović, V. Rek, and K. J. Marković, "Effect of polymer modifiers on the bitumen properties," *J Elastom Plast*, vol. 46, no. 5, pp. 448–469, 2014.
- [66] Z. C. Ye, D. Chen, C. Ling, and F. Y. Guan, "Quantifying SBS content in modified asphalt using fourier transform infrared spectroscopy," in *Advanced Materials Research*, 2015, vol. 1065, pp. 691–695.
- [67] R. D. Cook, "Influential observations in linear regression," *Journal of the American Statistical Association*, vol. 74, no. 365, pp. 169–174, 1979.
- [68] P. Bruce, A. Bruce, and P. Gedeck, *Practical Statistics for Data Scientists: 50+ Essential Concepts Using R and Python*. O'Reilly Media, 2020.
- [69] G. James, D. Witten, T. Hastie, and R. Tibshirani, *An introduction to statistical learning*, vol. 112. Springer, 2013.
- [70] D.-C. Huang, Y.-C. Lin, and R. C.-C. Tsiang, "Synthesis of SBS thermoplastic block copolymers in cyclohexane in the presence of diethylether used as a structure modifier," *Journal of Polymer Research*, vol. 2, no. 2, pp. 91–98, 1995.
- [71] L. Zani, F. Giustozzi, and J. Harvey, "Effect of storage stability on chemical and rheological properties of polymer-modified asphalt binders for road pavement construction," *Construction and building materials*, vol. 145, pp. 326–335, 2017.
- [72] M. Sugano, J. Kajita, M. Ochiai, N. Takagi, S. Iwai, and K. Hirano, "Mechanisms for chemical reactivity of two kinds of polymer modified asphalts during thermal degradation," *Chemical engineering journal*, vol. 176, pp. 231–236, 2011.

- [73] W. Zhang, Z. Jia, Y. Zhang, K. Hu, L. Ding, and F. Wang, "The effect of direct-to-plant styrene-butadiene-styrene block copolymer components on bitumen modification," *Polymers*, vol. 11, no. 1, p. 140, 2019.
- [74] N. S. Mashaan, A. H. Ali, M. R. Karim, and M. Abdelaziz, "Effect of crumb rubber concentration on the physical and rheological properties of rubberised bitumen binders," *International journal of the physical sciences*, vol. 6, no. 4, pp. 684–690, 2011.
- [75] A. Zofka, *Evaluating applications of field spectroscopy devices to fingerprint commonly used construction materials*. Transportation Research Board, 2013.
- [76] J. Button, "Methods to Determine Polymer Content of Modified Asphalt," 1991.
- [77] F. S. Choquet and E. J. Ista, "The determination of SBS, EVA and APP polymers in modified bitumens," in *Polymer Modified Asphalt Binders*, ASTM International, 1992.
- [78] J. B. Wei, J. C. Shull, Y.-J. Lee, and M. C. Hawley, "Characterization of asphalt binders based on chemical and physical properties," *International Journal of Polymer Analysis and Characterization*, vol. 3, no. 1, pp. 33–58, 1996.
- [79] Y. Wang, D. Chong, and Y. Wen, "Quality verification of polymer-modified asphalt binder used in hot-mix asphalt pavement construction," *Construction and Building Materials*, vol. 150, pp. 157–166, 2017.
- [80] K. Wang, Y. Yuan, S. Han, and Y. Yang, "Application of FTIR spectroscopy with solvent-cast film and PLS regression for the quantification of SBS content in modified asphalt," *International Journal of Pavement Engineering*, vol. 20, no. 11, pp. 1336–1341, 2019.
- [81] R. Hossain and N. M. Wasiuddin, "Evaluation of Degradation of SBS Modified Asphalt Binder Because of RTFO, PAV, and UV Aging using a Novel Extensional Deformation Test," *Transportation Research Record*, vol. 2673, no. 6, pp. 447–457, 2019.
- [82] M. Tazreiter, P. Christian, R. Schennach, T. Grießer, and A. M. Coclite, "Simple method for the quantitative analysis of thin copolymer films on substrates by infrared spectroscopy using direct calibration," *Analytical Methods*, vol. 9, no. 36, pp. 5266–5273, 2017.
- [83] F. J. Massey Jr, "The Kolmogorov-Smirnov test for goodness of fit," *Journal of the American statistical Association*, vol. 46, no. 253, pp. 68–78, 1951.
- [84] N. L. Johnson, "Continuous univariate distributions," 1970.

- [85] H. U. Bahia, D. I. Hanson, M. Zeng, H. Zhai, M. A. Khatri, and R. M. Anderson, *Characterization of modified asphalt binders in superpave mix design*, no. Project 9-10 FY'96. 2001.
- [86] W. H. Daly, *Relationship between chemical makeup of binders and engineering performance*, no. Project 20-015 (Topic 47-13). 2017.
- [87] M. D. I. Domingos and A. L. Faxina, "Creep-recovery behavior of asphalt binders modified with SBS and PPA," *Journal of materials in civil engineering*, vol. 26, no. 4, pp. 781–783, 2014.
- [88] D. Zhang, H. Zhang, and C. Shi, "Investigation of aging performance of SBS modified asphalt with various aging methods," *Construction and Building Materials*, vol. 145, pp. 445–451, 2017.
- [89] N. Dehouche, M. Kaci, and K. A. Mokhtar, "Influence of thermo-oxidative aging on chemical composition and physical properties of polymer modified bitumens," *Construction and Building Materials*, vol. 26, no. 1, pp. 350–356, 2012.
- [90] C. Yan, W. Huang, and N. Tang, "Evaluation of the temperature effect on Rolling Thin Film Oven aging for polymer modified asphalt," *Construction and Building Materials*, vol. 137, pp. 485–493, 2017.
- [91] D. Ge, K. Yan, L. You, and Z. Wang, "Modification mechanism of asphalt modified with Sasobit and Polyphosphoric acid (PPA)," *Construction and Building Materials*, vol. 143, pp. 419–428, 2017.
- [92] F. Liu, Z. Zhou, and Y. Wang, "Predict the rheological properties of aged asphalt binders using a universal kinetic model," *Construction and Building Materials*, vol. 195, pp. 283–291, 2019.
- [93] P. Liang, M. Liang, W. Fan, Y. Zhang, C. Qian, and S. Ren, "Improving thermo-rheological behavior and compatibility of SBR modified asphalt by addition of polyphosphoric acid (PPA)," *Construction and Building Materials*, vol. 139, pp. 183–192, 2017.
- [94] H. Zhang, Z. Chen, G. Xu, and C. Shi, "Evaluation of aging behaviors of asphalt binders through different rheological indices," *Fuel*, vol. 221, pp. 78–88, 2018.
- [95] W. Zeng, S. Wu, Y. Xiao, Z. Chen, and Y. Sun, "Low temperature properties of UV aged asphalts containing layered double hydroxides modifier," *Journal of applied biomaterials & functional materials*, vol. 14, no. 1_suppl, pp. 73–76, 2016.
- [96] W. Zeng *et al.*, "Research on Ultra Violet (UV) aging depth of asphalts," *Construction and Building Materials*, vol. 160, pp. 620–627, 2018.

- [97] E. Pullicino, W. Zou, M. Gresil, and C. Soutis, "The effect of shear mixing speed and time on the mechanical properties of GNP/epoxy composites," *Applied Composite Materials*, vol. 24, no. 2, pp. 301–311, 2017.
- [98] F. M. Nejad, A. R. Azarhoosh, G. H. Hamed, and M. J. Azarhoosh, "Influence of using nonmaterial to reduce the moisture susceptibility of hot mix asphalt," *Construction and Building Materials*, vol. 31, pp. 384–388, 2012.
- [99] F. Dong, X. Yu, S. Liu, and J. Wei, "Rheological behaviors and microstructure of SBS/CR composite modified hard asphalt," *Construction and Building Materials*, vol. 115, pp. 285–293, 2016.
- [100] J. Zhu, B. Birgisson, and N. Kringos, "Polymer modification of bitumen: Advances and challenges," *European Polymer Journal*, vol. 54, pp. 18–38, 2014.
- [101] N. Attoh-Okine, P. Cook, E. Martey, T. Boyce, and A. Alshali, "Asphalt rheology and strengthening through polymer binders," Rutgers University. Center for Advanced Infrastructure & Transportation, 2016.
- [102] U. Isacsson and H. Zeng, "Relationships between bitumen chemistry and low temperature behaviour of asphalt," *Construction and Building Materials*, vol. 11, no. 2, pp. 83–91, 1997.
- [103] Y. Ruan, R. R. Davison, and C. J. Glover, "Oxidation and viscosity hardening of polymer-modified asphalts," *Energy & fuels*, vol. 17, no. 4, pp. 991–998, 2003.
- [104] X. Lu and U. Isacsson, "Chemical and rheological evaluation of ageing properties of SBS polymer modified bitumens," *Fuel*, vol. 77, no. 9–10, pp. 961–972, 1998.
- [105] W. J. Woo, J. M. Hilbrich, and C. J. Glover, "Loss of polymer-modified binder durability with oxidative aging: base binder stiffening versus polymer degradation," *Transportation research record*, vol. 1998, no. 1, pp. 38–46, 2007.
- [106] Y. Wang, L. Sun, and Y. Qin, "Aging mechanism of SBS modified asphalt based on chemical reaction kinetics," *Construction and Building Materials*, vol. 91, pp. 47–56, 2015.
- [107] H. Yu *et al.*, "Impact of ultraviolet radiation on the aging properties of SBS-modified asphalt binders," *Polymers*, vol. 11, no. 7, p. 1111, 2019.
- [108] Y. Gao, F. Gu, and Y. Zhao, "Thermal oxidative aging characterization of SBS modified asphalt," *Journal of Wuhan University of Technology-Mater. Sci. Ed.*, vol. 28, no. 1, pp. 88–91, 2013.
- [109] R. Wang, M. Yue, Y. Xiong, and J. Yue, "Experimental study on mechanism, aging, rheology and fatigue performance of carbon nanomaterial/SBS-modified asphalt binders," *Construction and Building Materials*, vol. 268, p. 121189, 2021.

- [110] R. Hossain and N. M. Wasiuddin, "An FT-IRS Approach for the Evaluation of SBS Degradation in SBS Modified Asphalt Binder," in *International Conference on Transportation and Development 2020*, 2020, pp. 260–270.
- [111] C. Xing, L. Liu, and M. Li, "Chemical composition and aging characteristics of linear SBS modified asphalt binders," *Energy & Fuels*, vol. 34, no. 4, pp. 4194–4200, 2020.
- [112] M. Xu, Y. Zhang, P. Zhao, and C. Liu, "Study on aging behavior and prediction of SBS modified asphalt with various contents based on PCA and PLS analysis," *Construction and Building Materials*, vol. 265, p. 120732, 2020.
- [113] C. Chen, F. Yin, P. Turner, R. C. West, and N. Tran, "Selecting a laboratory loose mix aging protocol for the NCAT top-down cracking experiment," *Transportation Research Record*, vol. 2672, no. 28, pp. 359–371, 2018.
- [114] C. A. Bell, A. J. Wieder, and M. J. Fellin, *Laboratory aging of asphalt-aggregate mixtures: Field validation*, no. SHRP-A-390. 1994.
- [115] S. Brown and T. v Scholz, "Development of laboratory protocols for the ageing of asphalt mixtures," 2000.
- [116] W. N. Houston, M. W. Mirza, C. E. Zapata, and S. Raghavendra, "Environmental effects in pavement mix and structural design systems," *NCHRP, Project*, pp. 9–23, 2005.
- [117] O. Sirin, M. Ohiduzzaman, E. Kassem, and D. K. Paul, "Comprehensive evaluation of long-term aging of asphalt mixtures in hot climatic condition," *Road Materials and Pavement Design*, vol. 21, no. 4, pp. 927–949, 2020.
- [118] K. L. Martin, R. R. Davison, C. J. Glover, and J. A. Bullin, "Asphalt aging in Texas roads and test sections," *Transportation Research Record*, no. 1269, 1990.
- [119] Y. Li *et al.*, "Aging degradation of asphalt binder by narrow-band UV radiations with a range of dominant wavelengths," *Construction and Building Materials*, vol. 220, pp. 637–650, 2019.
- [120] Y. Liang, R. Wu, J. T. Harvey, D. Jones, and M. Z. Alavi, "Investigation into the oxidative aging of asphalt binders," *Transportation Research Record*, vol. 2673, no. 6, pp. 368–378, 2019.
- [121] R. Hossain and N. M. Wasiuddin, "Degradation of SBS Polymer during Laboratory Aging of Asphalt Mixture," in *Airfield and Highway Pavements 2021*, pp. 135–146.
- [122] B. Singh and P. Kumar, "Effect of polymer modification on the ageing properties of asphalt binders: Chemical and morphological investigation," *Construction and Building Materials*, vol. 205, pp. 633–641, 2019.

- [123] S. Wu, L. Pang, L. Mo, Y. Chen, and G. Zhu, "Influence of aging on the evolution of structure, morphology and rheology of base and SBS modified bitumen," *Construction and Building Materials*, vol. 23, no. 2, pp. 1005–1010, 2009.
- [124] R. Hossain, L. Noor, N. M. Wasiuddin, and L. N. Mohammad, "Field Implementation of Handheld FT-IR Spectrometer for Quantifying SBS Content in Polymer Modified Asphalt Binder," 2020.
- [125] Y. Xue, Z. Hu, C. Wang, and Y. Xiao, "Evaluation of dissolved organic carbon released from aged asphalt binder in aqueous solution," *Construction and Building Materials*, vol. 218, pp. 465–476, 2019.